Low-cost point-of-care diagnostic devices for low resource settings

Blanca Leticia Fernández Carballo

http://hdl.handle.net/10803/401780

DOCTORAL THESIS

Title	Low-cost point-of-care diagnostic devices for low resource settings
Presented by	Blanca Leticia Fernández Carballo
Centre	IQS School of Engineering
Department	Bioengineering
Directed by	Dr. Salvador Borrós Gómez Dr. Alexis F. Sauer-Budge Dr. Albert Florensa Giménez

Summary

Point-of-care (POC) testing has great potential for the management and diagnosis of disease. POC devices allow for testing close to the patient permitting rapid diagnosis, prompt treatment initiation, and when needed, quick referral to other health-care units. They have the potential to be lower-cost, more robust, and more user-friendly than traditional medical devices. For these reasons, POC diagnostic tests are a promising approach for the developing world, where there is also the most urgent need for new health technologies. In this context, this thesis is focused in the development of POC *in vitro* diagnostic tests for global health.

Considering that the resources for developing POC devices for low-resource settings are limited, during Chapter 2 we focused on setting health research priorities to aid test developers setting their targets to increase the impact of the technology. The criteria for prioritization considered were very broad and took into account the impact of a new test on the burden of disease, the availability and expense of disease treatments, the technological investment to develop a new device, and the bioethical principles.

Chapter 3 describes the development of a medical device that can be easily manufactured in limited resources laboratories: paper diagnostic chemical dipsticks to detect biomarkers present in biological fluids produced with domestic inkjet printers and simple ink preparation recipes. This fabrication technique for diagnostic strips was tested for the detection of iodine deficiency, a severe global health problem worldwide. In this chapter we present successful experiments for chemical inks preparation, printing on paper, detection of iodine in the concentrations present in the urine, and guidelines for new ink development to target other disease biomarkers. This simple and versatile manufacturing process for diagnostic tests would allow hospitals and laboratories with limited infrastructure to design diagnostics for relevant diseases in a format and quantity adapted to each community needs.

Unfortunately, not all diseases can be diagnosed using simple chemical dipstick assays and more complex diagnostic devices are required. Chapter 4 is focused on the development of a low-cost, real-time, point-of-care PCR and RT-PCR systems for quantitative detection of DNA and RNA-based pathogens. Our systems

are based on continuous-flow PCR which maintains fixed temperatures zones and pushes the PCR solution between heated areas allowing for faster heat transfer and as a result, faster PCRs. Both PCR and RT-PCR systems were built around disposable microfluidic chips designed to be economically produced industrially by roll-to-roll embossing methods. The optical system allows for pathogen detection *via* real-time fluorescence measurements. To demonstrate the function of the chips, two infectious bacteria and one viral target were selected: *Chlamydia trachomatis*, *Escherichia coli* O157:H7, and Ebola virus. For the three pathogens, different flow velocities were tested, the limit of detection of the system was determined, and PCR efficiencies were calculated. Our successful results, and the versatility of our system, make it promising for the detection of other DNA and RNA-based pathogens such as Zika or chikungunya, which constitute global health threats worldwide.

The two *in vitro* diagnostic tests presented in this thesis are good examples of promising POC diagnostic devices appropriate for global health.

Resumen

Los test de tipo 'point-of-care' (POC) presentan un gran potencial para el manejo y el diagnóstico de enfermedades. Los dispositivos POC permiten la realización de pruebas clínicas cerca del paciente, permitiendo así un diagnóstico rápido, una pronta iniciación de tratamientos, y en caso necesario, una derivación rápida a otros centros médicos. Estos dispositivos tienen además el potencial de ser más económicos, más robustos, y más fáciles de usar que los dispositivos médicos tradicionales. Por estos motivos, los dispositivos médicos de tipo POC se consideran prometedores para los países en vías de desarrollo, los cuales son también los que necesitan de forma más urgente nuevas tecnologías médicas. En este contexto, esta tesis se centra en el desarrollo de dispositivos médicos de diagnóstico *in vitro* de tipo POC para salud global.

Teniendo en cuenta que los recursos para el desarrollo de dispositivos POC para países con bajos recursos son limitados, el Capítulo 2 se enfoca en el desarrollo de prioridades de investigación en salud. Mediante el establecimiento de estas prioridades se pretende facilitar la selección de objetivos a fabricantes de dispositivos médicos, así como incrementar el impacto de las nuevas tecnologías desarrolladas. Los criterios de priorización considerados son muy amplios e incluyen el impacto de un nuevo test en la incidencia de una enfermedad, la disponibilidad y precio de los tratamientos de las enfermedades, la inversión tecnológica para el desarrollo de un nuevo dispositivo, y los principios bioéticos.

El Capítulo 3 describe el desarrollo de un dispositivo médico sencillo que puede ser fabricado fácilmente en laboratorios con escasos recursos: tiras reactivas de diagnóstico de papel para la detección de biomarcadores presentes en fluidos biológicos fabricados con impresoras de chorro de tinta domésticas y con recetas sencillas para la preparación de las tintas. Esta técnica de fabricación de tiras reactivas de diagnóstico fue probada para la detección de deficiencia de yodo, un problema severo de salud global en el mundo. En este capítulo se presentan experimentos de preparación de tintas químicas, impresión en papel, detección de yodo en las concentraciones presentes en la orina, y directrices para el desarrollo de nuevas tintas para la detección de otros biomarcadores de enfermedades. Este simple y versátil proceso de fabricación de tests de diagnóstico permitiría a

hospitales y laboratorios con pocos recursos diseñar sus propios diagnósticos para enfermedades relevantes, en una forma y cantidad adaptada a las necesidades de cada comunidad.

Desafortunadamente, no todas las enfermedades pueden diagnosticarse usando sencillas tiras reactivas de diagnóstico, y frecuentemente se necesitan dispositivos más complejos. El Capítulo 4 está enfocado en el desarrollo de dispositivos de PCR y RT-PCR de bajo coste, de tiempo-real, y de tipo POC que permiten detectar cuantitativamente patógenos basados en DNA y RNA respectivamente. Nuestro sistema se basa en PCR de flujo continuo, el cual mantiene zonas de temperatura fijas y empuja la solución de PCR entre las áreas calefactadas, permitiendo así una transferencia de calor más rápida y consecuentemente, PCRs más veloces. Ambos sistemas de PCR y RT-PCR fueron fabricados en base a un chip microfluídico desechable diseñado para ser producido a bajo coste industrialmente mediante métodos de 'roll-to-roll'. El sistema óptico permite la detección de patógenos en tiempo real mediante medidas de fluorescencia. Para demostrar la función del chip, dos bacterias infecciosas y un virus fueron seleccionados: *Chlamydia trachomatis*, *Escherichia coli* O157:H7, y Ebola virus. Para los tres patógenos, se probaron diferentes velocidades de flujo, se determinó el límite de detección del sistema, y se calcularon las eficiencias de las PCRs. El éxito de los resultados obtenidos y la versatilidad del sistema, hace que estos dispositivos se consideren prometedores para el diagnóstico de otros patógenos como Zika o chikungunya, que constituyen amenazas mundiales a la salud pública.

Ambos dispositivos de diagnóstico *in vitro* presentados en esta tesis son buenos ejemplos de dispositivos de diagnóstico prometedores apropiados para salud global.

Resum

Els test de tipus 'point-of-care' (POC) presenten un gran potencial per al maneig i el diagnòstic de malalties. Els dispositius POC permeten la realització de proves clíniques prop del pacient, permetent així un diagnòstic ràpid, una prompta iniciació de tractaments, i en cas necessari, una derivació àgil a altres centres mèdics. Aquests dispositius tenen a més el potencial de ser més econòmics, més robustos, i més fàcils d'usar que els dispositius mèdics tradicionals. Per aquests motius, els dispositius mèdics de tipus POC es consideren prometedors per als països en vies de desenvolupament, els quals són també els que necessiten de forma més urgent noves tecnologies mèdiques. En aquest context, aquesta tesi se centra en el desenvolupament de dispositius mèdics de diagnòstic *in vitro* de tipus POC per salut global.

Tenint en compte que els recursos per al desenvolupament i explotació de dispositius POC per a països amb baixos recursos són limitats, el Capítol 2 s'enfoca en el desenvolupament de prioritats d'investigació en salut. Mitjançant l'establiment d'aquestes prioritats es pretén facilitar la selecció d'objectius a fabricants d'instruments mèdics, així com incrementar l'impacte de les noves tecnologies desenvolupades. Els criteris de priorització considerats són molt amplis i inclouen l'impacte d'un nou test en la incidència d'una malaltia, la disponibilitat i preu dels tractaments de les malalties, la inversió tecnològica per al desenvolupament d'un nou dispositiu, i els principis bioètics.

El tercer capítol descriu el desenvolupament d'un dispositiu mèdic senzill que pot ser fabricat fàcilment en laboratoris amb escassos recursos: tires reactives de diagnòstic de paper per a la detecció de biomarcadors presents en fluids biològics fabricats amb impressores de raig de tinta domèstiques i amb receptes senzilles per la preparació de les tintes. Aquesta tècnica de fabricació de tires reactives de diagnòstic va ser provada per a la detecció de deficiència de iode, un problema sever de salut global al món. En aquest capítol es presenten experiments de preparació de tintes químiques, impressió en paper, detecció de iode en les concentracions presents en l'orina, i consells per al desenvolupament de noves tintes per a la detecció d'altres biomarcadors de malalties. Aquest simple i versàtil procés de fabricació de tests de diagnòstic permetria a hospitals i laboratoris amb pocs

recursos dissenyar els seus propis diagnòstics per a malalties rellevants, i en la forma i quantitat adaptada a les necessitats de cada comunitat.

Desafortunadament, no totes les malalties es poden diagnosticar usant senzilles tires reactives de diagnòstic, i freqüentment es necessiten dispositius més complexos. El capítol 4 està enfocat en el desenvolupament de dispositius de PCR i RT-PCR de baix cost, a temps real, i de tipus POC que permeten detectar quantitativament patògens basats en DNA i RNA respectivament. El nostre sistema es basa en la utilització de la tècnica de PCR de flux continu. Aquest, manté zones de temperatura fixes i empeny la solució de PCR entre les àrees calefactades, permetent així una transferència de calor més ràpida i conseqüentment, una PCR més veloç. Tots dos sistemes de PCR i RT-PCR van ser fabricats a partir d'un xip microfluídic d'un sol ús dissenyat per a ser produït a baix cost industrialment mitjançant mètodes de 'roll-to-roll'. El sistema òptic permet la detecció de patògens en temps real mitjançant mesures de fluorescència. Per demostrar la funció del xip, es van seleccionar dos bacteris infecciosos i un virus: *Chlamydia trachomatis*, *Escherichia coli* O157:H7, i virus de l'Ebola. Per als tres patògens, es van provar diferents velocitats de flux, es va determinar el límit de detecció del sistema, i es van calcular les eficiències de les PCRs. L'èxit dels resultats obtinguts i la versatilitat del sistema, fa que aquests dispositius es considerin prometedors per al diagnòstic d'altres patògens com Zika o chikungunya, que constitueixen amenaces mundials a la salut pública.

Tots dos dispositius de diagnòstic *in vitro* presentats en aquesta tesi són bons exemples de dispositius de diagnòstic prometedors apropiats per a salut global.

Acknowledgments

I would like to express my deepest gratitude to my PhD directors: Dr. Salvador Borrós, Dr. Alexis Sauer-Budge, and Dr. Albert Florensa. I would like to thank first Dr. Salvador Borrós for his trust, the great guidance, and encouragement. He has been very supportive throughout my PhD thesis, from the design to the writing phase, especially when the experiments did not work as we were expecting. He gave me the freedom to shape my thesis according to my interests and I am not sure if I could ever express how grateful I feel for this. I would like to express my sincere gratitude to Dr. Alexis Sauer-Budge. She has always been very supportive, and provided me with exceptional guidance. She has always welcomed me in my several stays at Fraunhofer CMI, and her knowledge and expertise were invaluable to find solutions to my research problems. Her leadership and commitment was very inspiring for me. I would like to thank Dr. Albert Florensa, who shares my interest in global development, for his enthusiastic support of my research, his very positive comments, and meaningful discussions.

I am very grateful to Dr. Christine McBeth for her support, for being available at any time for asking experimental questions, and for providing great advice especially in the molecular biology field. She always had positive comments and encouraging words when I had difficulties with my experiments. I would also like to thank Ian McGuiness, who was very supporting in numerous ways regarding mechanical engineering difficulties. Thanks to Dr. Maxim Kalashnikov for his help in the design of the optical detection system for the nucleic acid platform and for valuable comments and discussions. I also want to thank Dr. Marco Stella for teaching me how to use the roll-to-roll plasma machine and for his kindness answering all my questions about it. I would like to thank Albert Comellas for his enormous help preparing and printing chemical inks. I am very glad I had the chance to work with him during his bachelor thesis, he had great ideas, and we learnt many things together.

Thanks to all the staff and interns at Fraunhofer CMI. Especially I would like to thank Dr. Andre Sharon, for allowing me to be part of Fraunhofer CMI several times; Doug Foss, for his assistance solving problems; Dr. Sudong Shu, for his help writing computer programs; Jochen, Nicole and Kewal with whom I shared the

project and we worked as a team for a couple of months. I had a great time at Fraunhofer CMI and I am very grateful to everyone in the team.

I would like to thank everyone in GEMAT, in particular Sejin, Pere, Víctor, Miguel Ángel, María Sánchez, Anna Mas, Nathaly, Primiano, Óscar, Sara, Robert, Elena, Joan, Indrid, Mariana, Germán, Anna Cascante, Nuria, Marina, Gemma, Cris, Ignasi, Alberto, and Pau. With them I spent a very important part of my thesis, working long hours in the lab and sharing a lot of jokes and laughs. I also want to thank the groups of Tissue Engineering and Biochemistry, especially Mireia, Lourdes, Alex, Estela, Cris, Caterina, and Tere; we all became very good friends and shared many lunches, weekends, trips, and beers.

I want to thank my husband, Franco, for his enormous support both academically and emotionally. He helped me with my experiments, he assisted me writing data analysis software, and he supported me during the period of writing my thesis, including extra help with LaTeX. And equally important, he was always there to cheer me up when I was frustrated with my experiments and helped me seeing things from a different perspective. I am grateful to my parents, Blanca and Corsino, to my brother Álvaro, and my grandparents, Arturo, Fina, and Ditas, for their constant support and encouragement along the way. I would like to thank my family-in-law, Celia, Daniel, Peter, and Andreas, for their kindness.

Contents

List of Figures

17

List of Tables

19

Abbreviations

% (v/v)	Percentage volume/volume
% (w/v)	Percentage weight/volume
%(w/w)	Percentage weight/weight
ΔRn	Ratio of fluorescence emission intensity of the reporter dye to the fluorescence emission intensity of the passive reference dye
AAS	Atomic absorption spectrometry
ASSURED	Affordable, Sensitive, Specific, User-friendly, Rapid and Robust, Equipment-free, and Delivered to end-users
BSA	Bovine serum albumin
CAD	Computer-aided design
CATT	Card agglutination trypanosomiasis test
CCD	Charge-coupled device
CMI	Center for Manufacturing Innovation
COC	Cyclic olefin copolymer
COP	Cyclic olefin polymer
CSF	Cerebrospinal fluid
C_T	Cycle threshold
C. trachomatis	*Chlamydia trachomatis*
DALYs	Disease burden - Days Adjusted Life Years
DAT	Direct agglutination test
DNA	Deoxyribonucleic acid
DOD	Drop-on-demand
EBOV	Ebola virus
E. coli	*Escherichia coli*
ELISA	Enzyme-linked immunosorbent assay
EVD	Ebola virus disease
FAM	Fluorescein amidite
FITC	Fluorescein isothiocyanate
HIV	Human Immunodeficiency virus
ICP-MS	Inductively coupled plasma mass spectrometry
ICP-OES	Inductively coupled plasma optical emission spectrometry

IDD	Iodine deficiency disorders
IDT	Integrated DNA Technologies
INAA	Neutron activation analysis
IQ	Intelligence quotation
LED	Light-emitting diode
LIF	Laser-induced fluorescence
LMICs	Low- and middle-income countries
LOAC	Lab-on-a-chip
LOD	Limit of detection
ML^2	Multilayer MicroLab
mPADS	Microfluidic paper-based analytical devices
m/z	Mass-to-charge ratio
NAT	Nucleic acid-based test
NIH	United States National Institute of Health
OCA	O-carboxyanhydride
PBS	Phosphate-buffered saline
PC	Polycarbonate
PCR	Polymerase chain reaction
PDMS	Polydimethylsiloxane
PEG	Polyethylene glycol
PET	Polyethylene terephthalate
PMMA	Poly(methyl)methacrylate
POC	Point-of-care
POCT	Point-of-care test
qPCR	Quantitative polymerase chain reaction
RdRp	RNA-dependent RNA polymerase
RNA	Ribonucleic acid
RT	Reverse transcription
RT-PCR	Reverse transcription polymerase chain reaction
RT-qPCR	Reverse transcription quantitative polymerase chain reaction
S-K	Sandell-Kolfhoff
sccm	Standard cubic centimeters-per-minute
TBE	Tris/Borate/EDTA buffer
Tg	Glass transition temperature
TMB	3,3',5,5'-tetramethybenzidine
TOF-SIMS	Time-of-flight secondary ion mass spectrometry
TSH	Thyroid stimulating hormone
UV	Ultraviolet
WHO	World Health Organization

Chapter 1

Motivation and Aims

1.1 Motivation

Rapid and accurate diagnosis, in high- and low-income countries alike, is crucial to deliver proper health care and improve the health of individuals and populations.[1] Diagnostic medical devices play a key role for proper and successful diagnosis. They are essential for identifying the presence and cause of a disease, selecting an appropriate treatment, limiting the spread of a diseases in a population, avoiding waste of resources in ineffective treatments, monitoring the evolution of a disease or intervention, and determining drug resistances.[1,2]

In the early days of medicine, diagnosis was performed in the patients homes through physician house visits, during which clinical decisions were immediately made. As medical discoveries were made and new technologies were developed, care then shifted to hospitals. Laboratory testing for diagnostic purposes was performed in centralized laboratories with accurate and automated equipment that allowed analysis of large number of samples accurately and at a relatively low-cost.[3] This health provider-centered model, also known as 'conventional diagnostics' is currently dominant around the world.[3]

The main drawback of conventional diagnostic laboratory-based is the long turn-around time (days) from sample collection until the diagnosis is communicated to the patient, mostly when testing is performed in remote areas.[4] Samples collected at rural clinics need to be transported to centralized laboratories, which are usually located a significant distance away in large cities. At central labora-

tories, samples are processed in a batch manner, and then the diagnoses need to be transmitted correctly to the health-care provider who should afterwards communicate it to the patient and manage clinical decisions.[5] This long process line makes challenging successful extension of centralized testing to remote settings.[6] The long confirmatory diagnostic turn-arounds, and the fact that patients in rural settings, who live far away from the clinic, are less prone to come back in a timely manner for second medical appointments or confirmatory diagnosis, lead many physicians to manage diseases during the first clinical encounter without waiting for confirmatory diagnosis.[5,6] Infectious diseases especially are routinely managed with antibacterial therapy without confirmation of the causative pathogen or its antibiotic-resistances, which lead to the overuse of antibiotics driving the increase of antibiotic-resistant pathogens.[5–9] Additionally, late diagnosis of infectious diseases contributes to the spread the infection since precautions cannot be taken.[10] In the case of non-communicable diseases, poor assessment of health status and infrequent monitoring of risks factors usually implies worse disease management.[10] These examples of disease mismanagement support the vital need for fast and accurate disease diagnostic procedures.

In this context, during the last few decades, Point-Of-Care-Tests (POCT) have arisen as rapid and accurate diagnostic devices, with the potential to combine the accuracy and sensitivity of centralized laboratory equipment while being patient-centered and allowing a more rapid management of clinical decisions.[3,4] According to Ehrmeyer et al. POCT can be defined as 'patient specimens assayed at or near the patient with the assumption that test results will be available instantly or in a very short timeframe to assist caregivers with immediate diagnosis and/or clinical intervention'.[11] Although there is a large diversity of definitions of POC testing, and no universal one, the characteristics that most definitions have in common include testing close to the patient site and a short time-to-result to allow rapid diagnosis and management of clinical decisions in the same clinical encounter.[4,5,12–14]

The ability to diagnose and make clinical decisions in the same clinical encounter is undoubtedly the most significant characteristic of POC tests. Indeed, it constitutes the main difference respect to traditional diagnostics.[4] Figure 1.1

shows the comparison of the process time line for conventional laboratory-based diagnostics and POCT.
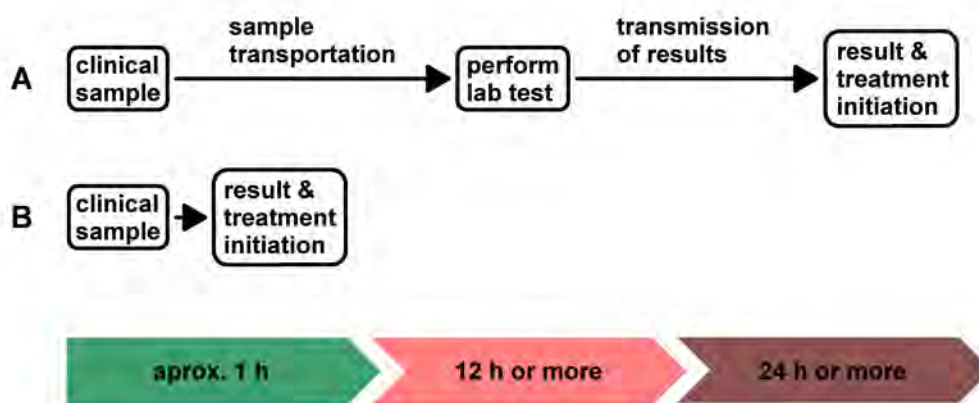
Figure 1.1: Comparison of the process time line from taking a clinical sample until treatment initiation. A: Using conventional laboratory-based diagnostics: which usually require several days from sample collection to treatment initiation. B: Using POC diagnostic tests: which usually take less than 1 h from sample collection to treatment initiation.[13]

Other important features of POCT are the high potential to be more simple and cost effective than traditional medical devices.[10,15] POC devices are less expensive than equipment in centralized laboratories that perform an equivalent function. Although the cost per test is usually lower in centralized laboratories (due to the sample multiplexing), when considering the overall costs of sample shipping and handling from rural or remote clinics and reporting the results back is often comparable to the cost of a POCT.[10] Other characteristics, such as user-friendly, equipment-free and delivered to end user are also achievable for POC diagnostic test.[3,15]

All these POCT features make them promising for places where timing is critical (e.g. emergency room), where laboratory facilities are nonexistent (e.g. military or extraterrestrial), and where resources are low (e.g. developing countries).[16] Diagnostics for global health are seen as the most promising users of POC and where there is the most urgent need for new health technologies.[1]

Along this line, although low- and middle-income countries account for approximately 90 % of the global disease burden[a], they lack essential medical devices and almost all their available diagnostic devices were designed to be used in high-income settings and are inappropriately complex and/or costly when considered for international health[b] applications.[2,20] When these medical devices arrive to a new setting with poor infrastructure often lacking stable sources of electricity or clean water, they very frequently malfunction, are not properly exploited, or stay unused, reducing and/or eliminating their intended benefit and impact.[20] To maximize health benefits, diagnostic medical devices need to be appropriate for the context or environment of intended use.[1,16,20]

Moreover, the international health community is increasingly appreciating the pressing need for new health technologies, and especially new technologies for health diagnostics.[1] In a survey performed by internationally eminent scientists with expertise in global health, the top-ranking overall priority was 'modified molecular technologies for affordable, simple diagnosis of infectious diseases'.[21] Another study conducted by Bill and Melinda Gates Foundation and the United States National Institutes of Health (NIH) identified 14 'Grand Challenges for Global Health', two of the 14 global health priorities involved diagnostics and technologies to measure the health status of individual and populations (i.e. 'develop technologies that allow assessment of individuals for multiple conditions or pathogens at point-of-care', and 'develop technologies that permit quantitative assessment of population health status').[22]

Similarly, international organizations and an increasing number of studies request new appropriate and accessible diagnostics devices designed for the unique characteristics of developing countries.[1,2] In 2006, the World Health Organization (WHO) Sexually Transmitted Diseases Diagnostics Initiative has coined the term 'ASSURED tests' to describe the ideal features for diagnostic devices for developing countries. ASSURED accounts for Affordable, Sensitive (few false-negatives),

---

[a]Disease burden is defined as the impact of a health problem as measured by financial cost, mortality, morbidity, or other indicators. It is here quantified in terms disability-adjusted life years (DALYs). Disability-adjusted life years (DALYs) is calculated as the sum of years of potential life lost due to premature death and the years of productive live lost due to disability.[17]

[b]International health is defined by Merson, Black, and Mills as 'the application of the principles of public health to problems and challenges that affect low and middle-income countries and to the complex array of global and local forces that influence them'.[18,19]

Specific (few false-positives), User-friendly, Rapid and Robust, Equipment-free and Delivered to those who need it (end-users).[23,24]

POC diagnostics have the potential to fill the gap and fulfil most of the AS-SURED criteria. However, nowadays the ASSURED criteria is considered too restrictive, and fulfilling all ASSURED features might not be required for a successful POCT. The desirable features for a POCT are highly dependent on the specifics of the context of use. Five distinct contexts of use for POC use are generally considered: homes, communities, clinics, peripheral laboratories, hospitals. The relative importance of each context varies from country to country and within countries, where there may be significant differences in rural versus urban areas, and/or public versus private sectors.[4] For example, in most developing countries with high percentage of people living in rural areas, POCT targeted to communities and clinics may have a higher impact.[4]

When designing diagnostic medical devices, it is beneficial for scientists and engineers to be aware of the final targeted context of use of the device in the early device development stages since there are different design constraints.[1] For example, within developing countries, different design criteria apply to diagnostic devices used at reference laboratories, hospitals, rural health clinics, or at home and also the purpose of the test may vary from referral, to monitoring, and treatment.[1,4] In Table 1.1, the main design constraints of the different context of use within low-resource countries are summarized.[1]

Test developers who aim to design high impact POC diagnostic tests for international health should take into account the disease prevalence and should focus on those diseases which are in most need of diagnostic devices.[16] It is remarkable the large difference in the prevalence of the different types of diseases in high-, middle-, and low-income countries as shown in Figure 1.2.[25] While communicable diseases, maternal and perinatal conditions, and nutritional deficiencies constitute more than 55 % of the disease burden in developing countries; in high-income countries, these diseases represent less than 6 % of the disease burden.[25] New POC diagnostic devices should focus on priority diseases in the intended place of use.

During the last decades, there has been abundant research in the area of POC diagnostics for international health; however, readily available devices in

Table 1.1: Design constraints for POC devices in different settings of developing countries.[1,4]

Design constraints	Hospital	Ref. laboratory	Clinic
Settings constraints			
Lack of stable electricity	U	U	S
Lack of well-equipped health infrastructure	S	S	I
Lack of skilled personnel (end-users)	U	S	S
Large temperature fluctuations	S	S	I
Device constraints			
Low cost of fixed instrument	U	S	I
Low cost of disposables	S	I	I
Rapid analysis	U	U	I
High sensitivity and specificity	I	I	I
Portability	U	S	S

I: Important, S: Somewhat important, and U: Unimportant.
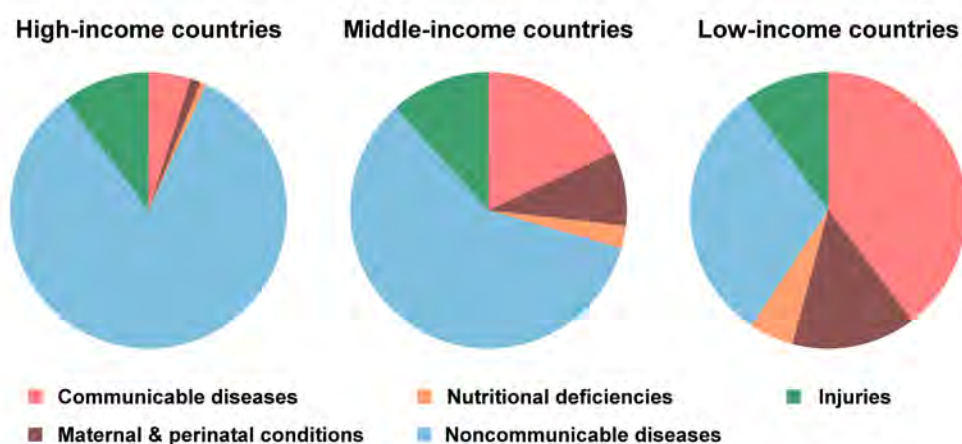
Figure 1.2: Distribution of disease burden (DALYs) in high-, middle-, and low-income countries. Data from 2012.[25]

the market are scarce.[3,26,27] Even when the design is adequate for the context, many promising POC devices fail when it comes to the implementation and/or production steps.[3] Devices designed and produced in developing countries have more chances to succeed and be implemented since, among other reasons, they are well adapted to the local conditions, can be maintained and repaired by the local population, and count with availability of spare parts.[20] However, in general, only simple devices can be produced successfully at a low-cost in settings with scarce infrastructure. Complex devices, such as nucleic acid or cells assays, require machines from industrialized countries for large-scale production in order to keep the price of the device and disposables low. Many new promising devices are stuck in the 'R&D' phase indefinitely because the device cannot be easily translated to the industrial scale.

A 'holistic approach' to POC device design is one in which considerable attention is given to the context, the end-users, the prevalent diseases, the end goal of production and implementation of the device and which fulfills the bioethical principles — beneficence, autonomy, justice, and no maleficence.

1.2   Aims

Given the need for fast and accurate diagnostics for international health purposes and the importance of the holistic approach in the design of diagnostic devices, the aim of this thesis was to apply such holistic approach to the development of POC diagnostic devices appropriate for low-resource countries.

- Develop prioritization criteria for POC device development.

- Develop POC devices of different complexity that fulfill the holistic approach to POC devices design that can be applied to prevalent diseases in developing countries and are appropriate to be used at health clinics in the context of low-resource countries.

- Characterize the POC diagnostic devices developed with diseases of high prevalence in developing countries.

31

1.3 Thesis Structure

According to these aims, the thesis is structured as follows.

In Chapter 2, several prioritization criteria for the development of POC diagnostic devices are described in detail. These criteria take into account the burden of disease, disease treatments, the technologies of the devices, and the bioethical principles. At the end of the chapter, POC devices in high need are described.

Chapter 3 is focused on the development of simple POC chemical tests in a dipstick format that can be fully manufactured in developing countries. The assay target are metabolites from body fluids and uses simple chemical reactions. The characterization of the POC device developed is also presented in this chapter.

Chapter 4 is focused on the development of a more complex nucleic-acid based device to overcome the limitations of chemical dipsticks and immunoassays and allowing the diagnosis of diseases that cannot be detected with simpler assay formats. This complex POC test was designed to be fabricated in industrialized countries with mass production systems in order to keep low the price of the device and disposables. The POC device characterization is also presented in this chapter.

Chapter 5 summarizes the conclusions of this thesis.

Bibliography

1. Chin, C. D., Linder, V. & Sia, S. K. Lab-on-a-chip devices for global health: past studies and future opportunities. *Lab on a chip* **7,** 41–57. ISSN: 1473-0197 (2007).

2. Hay Burgess, D. C., Wasserman, J. & Dahl, C. a. Global health diagnostics. *Nature* **444 Suppl,** 1–2. ISSN: 1476-4687 (2006).

3. St John, A. & Price, C. P. Existing and Emerging Technologies for Point-of-Care Testing. *The Clinical biochemist. Reviews* **35,** 155–67. ISSN: 0159-8090 (2014).

4. Pai, N. P., Vadnais, C., Denkinger, C., Engel, N. & Pai, M. Point-of-Care Testing for Infectious Diseases: Diversity, Complexity, and Barriers in Low-And Middle-Income Countries. *PLoS medicine* **9,** e1001306. ISSN: 1549-1676 (2012).

5. Bissonnette, L & Bergeron, M. Diagnosing infectionscurrent and anticipated technologies for point-of-care diagnostics and home-based testing. *Clinical Microbiology and Infection* **16,** 1044–1053. ISSN: 1198743X (2010).

6. Peeling, R. W. & Mabey, D. Point-of-care tests for diagnosing infections in the developing world. *Clinical microbiology and infection* **16,** 1062–9. ISSN: 1469-0691 (2010).

7. World Health Organization. *Antimicrobial resistance* 2016. <http://www.who.int/mediacentre/factsheets/fs194/en/> (2016).

8. Ventola, C. L. The antibiotic resistance crisis: part 1: causes and threats. *P & T : a peer-reviewed journal for formulary management* **40,** 277–83. ISSN: 1052-1372 (2015).

9. Dittrich, S. *et al.* Target Product Profile for a Diagnostic Assay to Differentiate between Bacterial and Non-Bacterial Infections and Reduce Antimicrobial Overuse in Resource-Limited Settings: An Expert Consensus. *PloS one* **11,** e0161721. ISSN: 1932-6203 (2016).

10. Mohd Hanafiah, K., Garcia, M. & Anderson, D. Point-of-care testing and the control of infectious diseases. *Biomarkers in medicine* **7,** 333–47. ISSN: 1752-0371 (2013).

11. Ehrmeyer, S. S. & Laessig, R. H. Point-of-care testing, medical error, and patient safety: a 2007 assessment. *Clinical chemistry and laboratory medicine* **45,** 766–73. ISSN: 1434-6621 (2007).

12. Price, C. P. Regular review: Point of care testing. *BMJ* **322,** 1285–1288. ISSN: 09598138 (2001).

13. Bissonnette, L. & Bergeron, M. G. Infectious Disease Management through Point-of-Care Personalized Medicine Molecular Diagnostic Technologies. *Journal of Personalized Medicine* **2,** 50–70. ISSN: 2075-4426 (2012).

14. Engel, N. *et al.* Point-of-care testing in India : missed opportunities to realize the true potential of point-of-care testing programs. *BMC Health Services Research* **15,** DOI 10.1186/s12913–015–1223–3. ISSN: 1472-6963 (2015).

15. Drancourt, M., Michel-lepage, A. & Boyer, S. The Point-of-Care Laboratory in Clinical Microbiology. *Clinical Microbiology Reviews* **29,** 429–447. ISSN: 10986618 (2016).

16. *Point-of-Care Diagnostics on a Chip* (eds Issadore, D. & Westervelt, R. M.) ISBN: 978-3-642-29267-5. doi:10.1007/978-3-642-29268-2 (Berlin, Heidelberg, 2013).

17. Murray, C. J. Quantifying the burden of disease: the technical basis for disability-adjusted life years. *Bulletin of the World Health Organization* **72,** 429–45. ISSN: 0042-9686 (1994).

18. Merson, M. H., Black, R. E. & Mills, A. J. *Global health Diseases: Programs, Systems, and Policies* Thrid. ISBN: 0763785598 (Jones & Bartlett Learning, Burlington, 2012).

19. Koplan, J. P. *et al.* Towards a common definition of global health. *The Lancet* **373,** 1993–1995. ISSN: 01406736 (2009).

20. World Health Organization. *Medical devices: Managing the mismatch* ISBN: 978 92 4 156404 5 (Geneva, 2010).

21. Daar, A. S. *et al.* Top ten biotechnologies for improving health in developing countries. *Nature genetics* **32,** 229–32. ISSN: 1061-4036 (2002).

22. Varmus, H *et al.* Grand Challenges in Global Health. *Science* **302,** 398–9. ISSN: 1095-9203 (2003).

23. Peeling, R. W., Holmes, K. K., Mabey, D & Ronald, A. Rapid tests for sexually transmitted infections (STIs): the way forward. *Sexually transmitted infections* **82 Suppl 5,** v1–v6. ISSN: 1368-4973 (2006).

24. Mabey, D., Peeling, R. W., Ustianowski, A. & Perkins, M. D. Diagnostics for the developing world. *Nature reviews. Microbiology* **2,** 231–40. ISSN: 1740-1526 (2004).

25. World Health Organization. *Cause-specific mortality estimates for 2000-2012* 2014. <http://www.who.int/healthinfo/global_burden_disease/estimates/en/index1.html> (2016).

26. Sia, S. K. & Kricka, L. J. Microfluidics and point-of-care testing. *Lab on a chip* **8,** 1982–3. ISSN: 1473-0197 (2008).

27. Yetisen, A. K., Akram, M. S. & Lowe, C. R. Paper-based microfluidic point-of-care diagnostic devices. *Lab on a chip* **13,** 2210–51. ISSN: 1473-0189 (2013).

Chapter 2

Prioritization criteria for the development of diagnostic medical devices

During the Motivation and Aims Chapter, the urgent need for diagnostic medical devices was described and the characteristics of ideal POC devices for limited-resource settings were analyzed. However, since the resources available for designing and developing new POC devices are limited, there is a clear need for prioritization.[1] In this chapter, several criteria for the prioritization of diagnostic medical devices are described in detail to aid in setting health research priorities and assure optimal health intervention outputs for the available budget. The criteria for prioritization are very broad and take into account the burden of disease, disease treatments, the technologies of the devices and bioethical principles. A summary of the different criteria is shown in Table 2.1 followed by a detailed description of each criterion.

Table 2.1: Criteria for diagnostic POC medical devices prioritization.

Disease burden
1. Reducing the global disease burden
2. Expected impact of a new test on disease burden
3. Feasibility of global or local disease elimination

Treatment
4. Availability, expense and toxicity of treatment

Device
5. Feasibility of developing an appropriate test
6. Availability of tests in the market and their limitations
7. Resources and infrastructure required for POC device production

Bioethics
8. Fulfillment of the bioethical principles

2.1 Disease burden-related prioritization criteria

Reducing the global disease burden is the first criterion of prioritization according to Mabey et al.[1] As a measure to estimate the importance of a disease, Disease-Adjusted Life Years (DALYs) are used, which are defined as the sum of years of potential life lost due to premature death and the years of productive live lost due to disability.[2] DALYs account for the years of life lost due to premature mortality as well as disability (in order to take into account those diseases that cause significant ill health but few direct deaths).[2,3] The relative burden of disease that most affect low-income countries is detailed in Table 2.2, where the DALYs for diseases, conditions and injuries as grouped by the World Health Organization (WHO) are shown. Data are presented for global, low-, middle- and high-income groups as organized by the World Bank Group. Diseases are clustered in 3 groups. Group 1, communicable, maternal, perinatal and nutritional conditions; group 2, non-communicable diseases; and group 3, injuries.[4]

Table 2.2: DALYs for diseases, conditions and injuries. Countries classified according to the World Bank Income Groups. Data from 2012.[4]

Cause category	Global		Low income		Middle income		High income	
	DALYs	% total	DALYs	% total	DALYs	% total	DALYs	% total
All Causes	38780	100	59979	100	37434	100	30046	100
1. Communicable, maternal, perinatal and nutritional conditions	13084	33.7	35611	59.4	12114	32.4	2046	6.8
Infectious and parasitic diseases	6112	15.8	18112	30.2	5419	14.5	903	3
Respiratory infections	2179	5.6	5655	9.4	2001	5.3	584	1.9
Maternal conditions	284	0.7	987	1.6	233	0.6	18	0.1
Neonatal conditions	3349	8.6	7735	12.9	3383	9	348	1.2
Nutritional deficiencies	1160	3	3121	5.2	1077	2.9	194	0.6
2. Noncommunicable diseases	21378	55.1	18365	30.6	20964	56	24929	83
3. Injuries	4318	11.1	6003	10	4357	11.6	3071	10.2

DALYs expressed per 100,000 population

As can be observed from Table 2.2, Group 1 of diseases represents a more important burden of diseases in low-income countries than in high-income ones. Those diseases have a greater potential for being eliminated when resources are available.

The biggest percentage of DALYS within Group 1 corresponds to infectious diseases.[4] As expected, infectious diseases represent a large burden of disease in developing countries (39.6 % total DALYs in low-income countries compared to 4.9 % total DALYs in high-income countries).[4] Figure 2.1 shows the DALYS lost due to different infectious diseases, as a proportion of the total caused by infection for low-income countries. It is remarkable that only 3 diseases, the trifecta of tuberculosis, HIV/AIDS, and malaria, represent 36.9 % of the disease burden caused by infection and 12.6 % of the total disease burden in developing countries.[4]
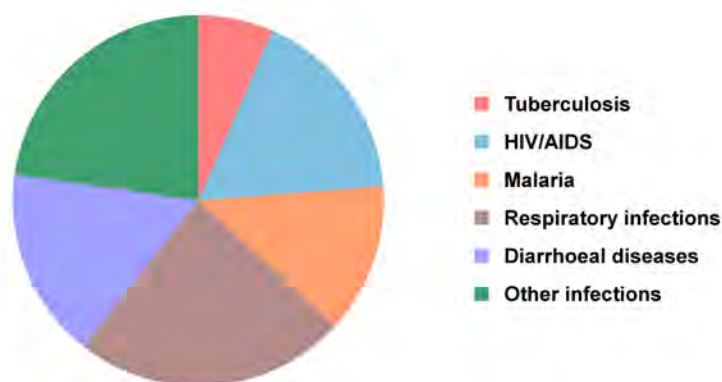
Figure 2.1: DALYs lost due to different infectious diseases as a proportion of the total caused by infection in low-income countries. Data from 2012.[4]

Other highly prevalent infectious diseases are respiratory infections, and diarrheal diseases, which account for 23.7 % and 16.7 % of the DALYs caused by infection in low-income countries respectively.[4] These diseases are also the most important causes of death of post-neonatal children under the age of five globally.[4] Most of child deaths were concentrated in developing regions, with African and South Asian countries the most affected.[4,5] Sexually-transmitted infections, other than HIV/AIDS (such as hepatitis B and C, *Chlamydia trachomatis*, gonorrhea, and syphilis), are also responsible for a significant disease burden.[3]

It is remarkable that most of the infectious diseases that are common in the developing world are treatable, and access to drugs has improved significantly over the past decade with the arrival of drug-access campaigns, mass treatment programs, and public resources.[1] However, the lack for accurate and rapid diagnostics remains a major obstacle for disease control. If appropriate diagnostic tests were available, the burden of infectious diseases in the developing world could be considerably reduced.[1]

The next subgroup within Group 1 of diseases are maternal and neonatal conditions. They significantly contribute to the DALYs of developing countries (14.5 %).[4] It is noteworthy that most of the deaths for children under 5 occur within the first month of life. Prematurity, intrapartum-related complications (including birth asphyxia), neonatal sepsis and infections, and congenital abnormalities are among the most important causes of neonatal death.[4]

Nutritional deficiencies represent an important part of the DALYs of low- and middle-income countries (5.2 % and 2.6 % respectively); with Sub-Saharan Africa being the most affected area.[3,4] Malnutrition is the single most important contributing cause to the disease burden.[3,6] Malnourished children are more prone to suffer and/or die from other diseases. Anemia, vitamin A, and iodine deficiency are the most common or severe micronutrient deficiencies worldwide.[7] Usually treatments are simple and available, however better diagnostics are needed to improve epidemiological surveillance and help to attract international aid.[7,8] In Table 2.3 the leading causes of DALYs for children under 5 are shown, as it can be observed, nutritional deficiencies are responsible for 8,802 DALYs per 100,000 population in developing countries, while in developed countries they account for 500 DALYs for the same amount of population (more than a 17 factor difference).[4]

Table 2.3: Ten leading causes of DALYs for children under five years of age. Countries classified according to the World Bank Income Groups. Data from 2012.[4]

	Low-income			Middle-income			High-income		
Rank	Causes	% total	DALYs	Causes	% total	DALYs	Causes	% total	DALYs
1	Neonatal conditions	30.9	52,285	Neonatal conditions	38.5	35,316	Neonatal conditions	35.6	4,992
2	Respiratory infections	15.8	26,802	Respiratory infections	14	12,877	Congenital anomalies	23.2	3,249
3	Diarrheal diseases	10	17,424	Diarrheal diseases	9	8,519	Unintentional injuries	6	845
4	Malaria	10.2	17,204	Congenital anomalies	7.2	6,577	Endocrine, blood, immune disorders	5.6	791
5	Nutritional deficiencies	5.2	8,802	Malaria	5.6	5,138	Respiratory infections	4.9	689
6	Unintentional injuries	5.2	8,769	Unintentional injuries	5	4,552	Diarrheal diseases	4.4	623
7	Congenital anomalies	4.5	7,680	Nutritional deficiencies	4.9	4,509	Nutritional deficiencies	3.6	500
8	Childhood-cluster diseases	4	6,790	Childhood-cluster diseases	2.8	2,596	Malignant neoplasms	2.6	361
9	Meningitis	2.4	4,114	Meningitis	1.9	1,764	Neurological conditions	1.7	244
10	HIV/AIDS	2.1	3,627	HIV/AIDS	1.2	1,078	Respiratory diseases	1.7	232

DALYs expressed per 100,000 population

Non-communicable diseases represent an important 30 % of the disease burden within low-income countries; however, unlike communicable diseases, non-communicable diseases are usually underestimated.[3,4] Cardiovascular diseases, cancer, mental and behavioral disorders, and musculoskeletal diseases are the conditions that contribute the most to the disease burden as can be observed in Figure 2.2.[4] As life expectancy and quality of life increase in developing regions, the burden of disease will gradually shift to non-communicable diseases, resembling more and more the disease burden of high-income countries.[3] This shift is intensified due to the increase of diets rich in sugars and saturated fats, contributing to the increase of obesity and diabetes in low- and middle-income countries.[3] Although diagnostics for non-communicable diseases are already available in developed countries, appropriate diagnostics adapted to the specific conditions encountered in low-resource settings are needed to face the increase of these conditions.[3]
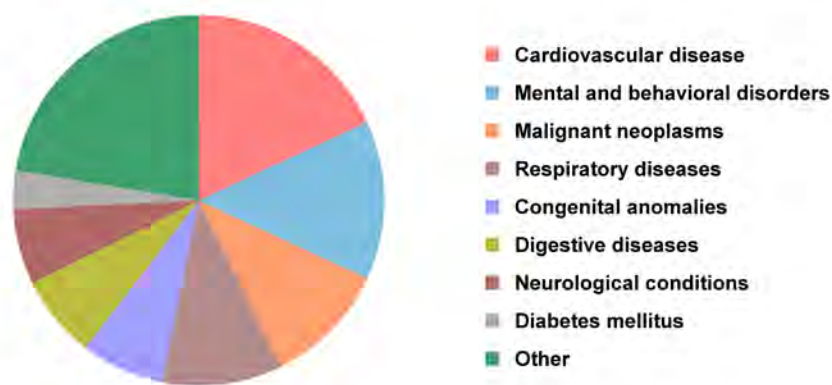
Figure 2.2: DALYs lost due to different non-communicable diseases as a proportion of the total caused by infection in low-income countries. Data from 2012.[4]

A population subgroup very vulnerable which deserves attention are children under the age of 5. In 2012, 6.6 million children died before reaching their fifth birthday; almost all (99 %) of these deaths occurred in low- and middle-income countries.[9] Diseases that affect children are the ones that contribute more to the increase of DALYs since they have a higher potential to result in the loss of many years of potentially healthy and productive life.[2] Table 2.3 summarizes the ten leading causes of DALYs for children under the age of 5 in low-, middle-, and high-income countries and the percentage of each cause is provided as well as the

DALYs per 100,000 population.[4] It is observed that neonatal conditions are the first contributing factor to DALYs for low-, middle-, and high-income settings and in all the cases they contribute between 30–40 % of the total disease burden; however, when comparing DALYs in a population of 100,000 habitants, they are more than 10 times higher in low-income countries compared to high-income ones.[4] In developing countries respiratory infections, diarrheal diseases, malaria, and nutritional deficiencies are among the most important contributing factors to DALYs.[4]

Summarizing this first prioritization criteria, Group 1 diseases, the traditional diseases of the poor, still constitute the most important difference on the disease burden between low- and high-income countries. More efforts should be directed towards the diagnosis of communicable, maternal and neonatal conditions, and nutritional deficiencies. Having said this, non-communicable diseases should not be forgotten, which are expected to increase as the quality of life improves in developing regions.

The **expected impact of a new test on disease burden** is considered the second criterion for prioritization by Mabey et al.[1] Diseases that can be clinically identified through its symptoms are in less need for POC diagnostics, since they can be syndromically treated. Diseases which have few, if any, symptoms but can lead to devastating consequences are diseases for which diagnostic devices can have a very high impact.[1] Gonorrhea and chlamydial infections are often asymptomatic, and when untreated they can lead to pelvic inflammatory disease, ectopic pregnancy or infertility.[10] Syphilis is also often asymptomatic during pregnancy but significantly increases the risks of stillbirth, spontaneous abortion, prematurity, clinical manifestations of congenital syphilis, infant death, and late sequelae.[11] Nutritional deficiencies are also a good example of conditions that can be asymptomatic. Malnourished people and specially children are weaker, grow poorly, and are more susceptible to infectious diseases.[6] These diseases and conditions are examples of diseases which may only be detected by screening and treating populations at risk, for which POC diagnostics are very likely to have a high impact.[1,10]

Additionally, it is remarkable that although some diseases that can be detected through its symptoms, it is important to perform periodic identification of pathogens responsible of the diseases. For example, for syndromic diseases such as pneumonia and diarrhea, it is recommended to periodically identify changes in disease spectrum and antimicrobial susceptibility to avoid the rise of antibiotic resistances.[1] This prioritization criterion highlights the need of new POC diagnostic devices for diseases such as chlamydial, gonorrhea and syphilis infections.

Feasibility of global or local disease elimination is the third criterion that should be considered regarding diseases for POC development prioritization.[1] Some infectious diseases are expected to be soon eliminated, either globally or regionally. Polio, guinea worm, leprosy, trachoma, onchocerciasis, syphilis, South American trypanomiasis or lymphatic filariasis are some of them.[1,12] Although these diseases are targeted for elimination, there is still a high need for diagnostics devices for surveillance to avoid resistant strains to re-emerge.[1] Although the disease burden of many of these diseases is low, when deciding priorities for POC device development, the benefits of disease elimination should be taken into account.[1] This prioritization criterion highlights the need of new POC devices for diseases targeted for elimination.

2.2 Treatment-related prioritization criteria

Availability, expense and toxicity of treatment (criterion 4) is another important criterion for prioritization. Diseases that require expensive and toxic treatments require a confirmatory diagnosis before the treatment can be initiated since they never justify a presumptive treatment.[1] For these diseases there is urgent need for specific and sensitive diagnostic devices. Visceral leishmaniosis and African trypanosomiasis, are examples of these types of diseases in urgent need for appropriate diagnostics.[1,13]

In the case of diseases with high morbidity and mortality and widely available inexpensive treatments, it might seem more cost effective to first treat all presumptive cases in endemic areas without confirmatory diagnosis. However, this

practice might lead to the increase of resistant strains and the subsequent need of new drugs, which at the end might be more costly.[1,14] Malaria treatment with chloroquine is an example of this practice, chloroquine treatment has been recommended for all children with fever in malaria-endemic areas.[1,15] However new resistant strains are now common and the alternative treatments are more expensive. Looking at this practice retrospectively, it would probably had been more cost-effective to only treat confirmed cases and avoid or at least slow down the rise of new resistant strains.[14,16,17]

It is remarkable that most of the infectious diseases that are common in the developing world are treatable, and access to drugs has improved significantly over the past decade with the arrival of drug-access campaigns, mass treatment programs and public resources.[1] However, the lack for accurate and rapid diagnostics remains a major obstacle for disease control.[1]

2.3 Device-related prioritization criteria

Other important criterion for prioritization is related with the diagnostic test itself: **feasibility of developing an appropriate test** (criterion 5). Priority should be given to those tests that are easier and/or cheaper to develop using existing technology, or that are already in the market but have not been adequately evaluated and are likely to function successfully.[1] Neglected tropical diseases are a good example of diseases that should be prioritized according to this criterion.[1] Currently, the methods for diagnosing these diseases are invasive and inadequate mostly due to the low research priority given to these diseases.[3] The WHO considers that there are powerful, easy and inexpensive interventions to prevent and cure 9 of the 13 neglected tropical diseases (which includes lymphatic filariasis, dengue, Chagas disease, leishmaniosis, onchocerciasis, schistosomiasis, trypanosomiasis, trachoma, and guinea worm).[18]

In order to facilitate a better understanding of the advantages, challenges and limitations of the wide variety of POC in the in research and commercial, a brief description of the main types of POC diagnostics is provided. The complexity and value of a diagnostic device depends on the device principle and the disease

46

biomarker. Biomarkers are present in biological fluids and are defined as "characteristic that is objectively measured and evaluated as an indicator of normal biological processes, pathogenic processes, or pharmacologic responses to a therapeutic intervention"[19,20] and can be classified as: metabolites and small molecules, proteins, nucleic acids, and cells.[21] According to the principle of the device, POC tests are based on electrochemical/chemical, antibody/antigen, nucleic acids, and cell reactions. Next a brief description of the main diagnostic types will be provided in order to understand their advantages and limitations for POC purposes.

POC devices that use electrochemical methods are probably the simplest. They allow measuring a wide range of blood, urine or other bodily fluids parameters including electrolytes, gases, metabolites, pH, lipids, vitamins, therapeutic drugs, drugs of abuse, hormones, inflammatory markers and cytokines, or coagulation proteins.[21,22] The main disadvantage of electrochemical assays when used for POC purposes is the high cost of electrodes, which need to be integrated onto disposable cartridges, considerably increasing the cost per test.[21,23] When qualitative or semi-quantitative detection is enough, paper dipsticks based on chemical reactions are an attractive option for POC since they are very inexpensive and simple to use and interpret.[24–26] Urinary sticks to detect metabolic products in urine are probably the best known chemical dipsticks. They usually contain impregnated reagents such that when a bodily fluid sample with the analyte of interest is applied, it reacts with the reagents producing a color change that allow estimating the concentration of analyte in the sample. In many cases the color change can be read by the naked eye or a small reading device can be used to reduce the potential operator error.[26,27] Some diseases with high prevalence in developing countries, such as malnutrition and micronutrient deficiencies can be diagnosed using electrochemical detection.[28] Unfortunately, very often other detection methods are required.

Immunoassays, the most common protein assays for POC diagnostics, are based on the interaction between antigens and antibodies to detect target proteins from pathogens or the host immune reaction. Immunoassays have been successfully used to detect a wide variety of pathogen types (viruses, bacteria, and parasites), and non-communicable diseases.[21] Enzyme-linked immunosorbent assay (ELISA), is the most common immunoassay.[21] However, conventional ELISAs are inappro-

priate for POC use due to high costs of the equipment and the requirement of trained personnel. There has been intensive research to miniaturize and reduce the costs of traditional equipment by using microfluidics.[3,21] The main challenges that are being addressed are focused on signal detection, fluid control, and fluid actuation and delivery.[3,21]

Undoubtedly, the best established immunoassay format for POC is the lateral flow immunoassay.[29] Lateral flow assays have a complex biological design but the resulting tests are user-friendly, rapid and relatively inexpensive, making them ideal for use at POC. Lateral flow assays usually provide binary results (yes/no), although they can also be semi-quantitative and a few of them are even quantitative. The most common lateral flow assay is for pregnancy detection, which were developed in the 1980s.[29,30] The main limitations of LFA concern two major areas: reproducibility and sensitivity.[31] Unfortunately, there are considerable variations between strip-to-strip and the sensitivity of lateral flow immunoassays is often insufficient to detect many diseases.[31] Although much research is being conducted to overcome the limitations of lateral flow immunoassays, the growing demand for sensitivity in many disease applications is driving attention to nucleic acid-based tests.

Nucleic acid-based assays are very promising due to its high sensitivity and selectivity.[32] However, they are more complex and historically costly and as a result mostly used in hospitals and centralized laboratories.[21] Currently there is a great interest in miniaturizing classic nucleic acid equipment, reducing its costs, and integrating the main functionalities (sample preparation, nucleic acid amplification, and detection) into a POC device.[21,32,33] To date, few POC nucleic acid tests are marketed. A nucleic acid amplification method is usually required to obtain enough nucleic acids for identification and quantification since the amount of nucleic acids from a raw or purified sample is usually too low for immediate detection.[21,32] Typically, an enzymatic reaction is carried out to copy a specific target sequence *in vitro*.[32] Polymerase chain reaction (PCR), invented in 1986,[34] is the most common amplification method. PCR is the preferred nucleic acid amplification assay due to its simplicity, easy methodology, extensively validated standard operating procedure and availability of reagents and equipment. Another

advantage of nucleic acid test is its versatility. Generally, nucleic acid tests developed can be used for different biomarkers of disease with few modifications in assay, only modifying the primers and probes.[35] This easy translation of nucleic acid assays contrast with immunoassays, which often require more intensive work testing antibody/antigen when translating a successful lateral flow immunoassay to target another disease biomarker. Generally, once a POC nucleic acid device is developed, the cost of adapting that device to target other disease biomarkers is usually significantly lower than adapting an immunoassay or cell-based device to the detection of other diseases.

Lastly, devices that can detect cells are also of great interest. Counting and identifying target cells in blood or other samples is promising for POC devices since conventional methods (e.g. flow cytometry) are expensive and bulky.[21,36] Full blood cell counts are useful for the diagnosis and monitoring of diseases such as anemia or HIV/AIDS (HIV/AIDS is monitored by counting CD4+ lymphocytes).[21] Currently there are few POC cell-based devices commercialized due to the high complexity and as a result cost, although their presence in the market is increasing.[27]

All the POC devices types -electrochemical, immunoassay, nucleic acid, cell-based– are all predicted to have a great impact; however, as previously described, prioritization should be considered. It is remarkable, that for groups of similar diseases and even for a single disease in many cases, several classes of assays are required for an accurate and complete diagnosis.[3]

Another criterion for POC device development prioritization, which is closely related to the previous criteria, takes into account the **availability of tests in the market and their sensitivity and specificity** (criterion 6). In the appendix, a detailed table (Table A.1) with the current methods used for the detection of different diseases is provided. Many diseases still rely on cultures and microscopy for their diagnosis and lack marketed rapid tests for their diagnosis.[1] Prioritization should be given to the diagnosis of diseases which lack rapid in the market and to those which sensitivity and/or specificity is low. As an example of diseases for which the available diagnostic test have low quality are *Chlamydia trachomatis*

49

and tuberculosis; being microscopy and/or cultures the gold standard.[20]

Another criterion for prioritization takes into account the **resources and infrastructure required for POC device production** (criterion 7). Priority should be given to those devices that can be locally produced in developing countries. Medical devices designed and manufactured in the place of use are well adapted to the local conditions and can be maintained and repaired by locals and count with local availability of all spare parts.[37] Malfunctioning devices due to an inappropriate design to the local conditions is unfortunately a very frequent problem in developing countries.[37] First, almost all medical devices are designed in developed countries to be used in high-resource settings. Industry in high-resource settings has limited interest in developing new diagnostics for the developing world since they promise a low return of investment.[37,38] Additionally, the high number of medical devices donations, which very often do not match the recipients need, contributes to this problem. Some low-income countries receive nearly 80 % of their health-care equipment in the form of donations; however, only 10–30 % of donated equipment becomes functional.[37,39] Other factor that contributes to increase the number of device malfunction is the lack of information and training regarding selection methods of appropriate medical devices in developing countries.[37]

Simple devices, such as paper dipsticks based on chemical/biochemical reactions, have a greater potential for production in resource-limited settings than more complex devices. More complex devices, such as lateral flow immunoassays and nucleic acid assays, require expensive and delicate reagents. In order to produce low-cost assays, well equipped infrastructure with capability for industrial scale production is required to reduce the production costs.

2.4   Bioethics-related prioritization criteria

Last but not least, another criterion for prioritization of POCT development, often forgotten, is the **fulfillment of the bioethical principles** (criterion 8), which should be considered in a holistic approach for POC device development.

As explained along this chapter, there are many challenges providing health care for diverse people in multicultural societies. Some of the challenges include allocating health resources, establishing research priorities for technical innovation, timing for medical treatment, etc. Bioethics were developed to provide broad guidelines that could be used to aid in decision making in controversial areas of biology, medicine, and life-sciences that can be accepted by people of different cultures, religions, and values.[40] Four principles are usually considered: autonomy, non-maleficence, beneficence, and justice.[41] These principles are not considered absolutes due to the diversity of situations, but serve as powerful tools to guide health-related actions. All the principles should be supported; however, when there are conflicts between two or more of them, a balance of the principles should be established by determining which carries more weight in the particular case.[40]

The principle of autonomy means that the user or patient has autonomy of thought, intention, and action regarding health care procedures.[40] The opinions, convictions, personal values and beliefs, rights of all users should be respected and full information should be provided regarding all risks, benefits of the procedure and likelihood of success in order to make a fully informed decision; special attention should be given to vulnerable populations such as the elderly, sick, and children.[40] This principle is not very relevant for resource allocation for health technologies research, but it is important for clinical experiments once the medical devices are developed.

The principle of non-maleficence requires of the provider not to create harm intentionally to the user, patient, and/or society. Providing a proper standard of care that avoids or minimizes the risk of harm is held by the commonly held moral convictions and the laws of society.[40]

The principle of beneficence requires that the health intervention, health technology, or health action provide a benefit the user and/or patient.[40] It is remarkable, that both the provider and user in an autonomous way should consider the action beneficial; when only the provider opinion is considered, then the action is considered paternalist and disregards autonomy.[40] This is an important difference between beneficence and non-maleficence. While beneficence is more subjective and depends on what provider and the user consider good, non-maleficence is

more absolute and depends merely on the provider.[40] The goal of providing benefit can be applied to individual users or patients and the society as a whole. For example, appropriate and rapid diagnosis for a patient would be an example of individual benefit while prevention of disease through vaccines, epidemiological surveillance, or international health research would benefit the society as a whole. New diagnostic medical devices should provide a benefit, such as improved sensitivity and specificity, be more rapid, lower cost, etc. with strict quality control. Additionally, appropriate training to health providers should be available to ensure that the patient is benefitted and not harmed through the use of the assay.

The principle of justice is usually defined as a form of fairness among all groups in society: benefits/burdens should be fairly distributed. This principle is usually forgotten in bioethics and it is only applied when problems cannot be solved considering only the other principles.[40] However, the principle of justice is the most relevant bioethical principle applied during this thesis and it is the only one that gives a vision of the society as a whole. The focus of this thesis –development of POC diagnostic devices appropriate for low-income settings– is the result of a fair and responsible conception of diagnostic devices in the society and the social relations between individuals, groups and public and private entities. People in developing countries have less resources and less access to appropriate diagnostic medical devices, and focusing on those who have the least follows the justice principle.

A remarkable example of unfair funds distribution is the 10/90 gap.[42] The 10/90 gap is a term adopted by the Global Forum for Health Research to draw attention to the finding by the Commission on Health Research for Development in 1990, that less than 10 % of worldwide resources for health research were put towards health in Developing Countries, where over 90 % of all preventable deaths worldwide occurred.[42] Nowadays, although progress has been made, we are still far from correcting this imbalance. The prioritization criteria for POC device development presented during this chapter hopes to aid for a fairer and more just allocation of the scarce resources and research funds.

During the next chapters, the prioritization criteria will be applied to the development of medical devices appropriate for low-resource settings.

As briefly described in the Motivation and Aims Chapter, during Chapter 3 a simple diagnostic chemical dipstick assay was developed. This assay responds to several prioritization criteria. First, chemical dipsticks are very simple diagnostic assays and they do not require new technologies for their development thereby responding to the feasibility of developing an appropriate test prioritization criterion (criterion 5). Secondly, inexpensive and limited infrastructure is required for the design and production of these simple diagnostic devices allowing to be fully produced in resource limited settings thus obeying the prioritization criterion 7, which takes into account the resources and infrastructure required for POC device production. The assay developed was applied to the diagnosis of a nutritional iodine deficiency. Thereby, the third prioritization criteria fulfilled by this technology is criterion 1, which tackles the reduction of the global disease burden. As previously described, nutritional deficiencies are the single most important contributing cause to the disease burden worldwide.[3,6] Since nutritional deficiencies in many cases do not have specific symptoms, but rather they contribute to debilitate individuals and make them more prone to suffer from other diseases, low-cost and appropriate diagnostic devices are expected to have a high impact on disease burden (criterion 2). Additionally, this diagnostic assay also responds to the prioritization criterion 6, to the best of our knowledge, there are no diagnostic dipsticks for iodine status determination in the market nowadays. Furthermore, considering that most people that suffer from iodine deficiencies live in developing countries, developing an appropriate test for those who have fewer economical resources considers and applies the bioethical principles of autonomy, non-maleficence, beneficence and specially the justice principle (prioritization criteria 8).

However, not all diseases can be diagnosed using chemical dipstick assays. Unfortunately for the identification of other diseases and conditions, more complex antigen/antibody and/or nucleic acid detection methods are required. Chapter 4 focuses on the development of a more complex nucleic-acid based device to overcome the limitations of chemical dipsticks and immunoassays and allowing diag-

nosis of diseases that cannot be detected with simpler assay formats. This assay responds to several prioritization criteria.

Although there are some nucleic acid-based POC devices in the market, it is likely that for the development of a new device, some kind of technological invention is needed to improve the current state of the technology. Once the technology is developed, it can be easily applied to several diseases and conditions. Flexibility is an attractive characteristic of nucleic acids -opposed to lateral flow immunoassays– and contributes to increase the feasibility of developing an appropriate nucleic acid-based test (criterion 5). The diagnostic device that has been developed during this thesis was applied to the detection of infectious diseases; specifically, diarrheagenic *Escherichia coli* O157:H7, *Chlamydia trachomatis* and Ebola Zaire virus. These infectious diseases are more prevalent in developing countries. A POC nucleic acid device to target these pathogens would contribute to decrease the current disease burden (criterion 1). The expected impact of a new test (criterion 2) is dependent on the specific pathogen. Thus, a new test for often asymptomatic chlamydial infections is expected to have a great impact. As previously mentioned, even for syndromic diseases, such as diarrheal or febrile diseases, identifying the causative pathogen may be of high importance. Importantly, it would help to distinguish viral versus bacterial infections and thus enabling appropriate treatment, reducing antibiotic resistances and avoiding the need for new treatments for antibiotic-resistant strains. This is an important point for prioritization criteria 4, which considers the availability, expense and toxicity of treatment. In the specific case of Ebola Zaire disease, although there is no effective and confirmed treatment yet, the measures that need to be adopted in case of infection –isolation, personal protective equipment, and materials– are very costly and a confirmatory diagnosis would be highly desirable before following them. Nowadays few nucleic acid-based POCTs are available in the market; their development should be prioritized according to criterion 6 which considers the availability of tests in the market and their limitations. Additionally, in a globalized world infectious disease are easily spread and their diagnosis not only benefit the communities where those infections are endemic, but they also have global benefits (criterion 8). Furthermore, infectious diseases, similarly to nutritional deficiencies, are more

prevalent in developing countries and devices targeted to the people who have less economic resources attends to the justice principle (criterion 8) and should be prioritized.

Bibliography

1. Mabey, D., Peeling, R. W., Ustianowski, A. & Perkins, M. D. Diagnostics for the developing world. *Nature reviews. Microbiology* **2,** 231–40. ISSN: 1740-1526 (2004).

2. Murray, C. J. Quantifying the burden of disease: the technical basis for disability-adjusted life years. *Bulletin of the World Health Organization* **72,** 429–45. ISSN: 0042-9686 (1994).

3. Chin, C. D., Linder, V. & Sia, S. K. Lab-on-a-chip devices for global health: past studies and future opportunities. *Lab on a chip* **7,** 41–57. ISSN: 1473-0197 (2007).

4. World Health Organization. *Disease burden estimates for 2000-2012* 2014. <http://www.who.int/healthinfo/global_burden_disease/estimates/en/index2.html> (2016).

5. UNICEF & World Health Organization. *Diarrhoea: why children are still dying and what can be done* tech. rep. (2009).

6. World Bank. *Global Burden of Disease and Risk Factors* (eds Lopez, A. D., Mathers, C. D., Ezzati, M., Jamison, D. T. & Murray, C. J.) ISBN: 0821362623 (Washington, 2006).

7. Flour Fortification Initiative *et al. Investing in the future: A united call to action on vitamin and mineral deficiencies* tech. rep. (Ontario, 2009).

8. Food and Agriculture Organization & CAB International. *Combating micronutrient deficiencies: food-based approaches* (eds Thompson, B. & Amoroso, L.) ISBN: 9781845937140. doi:10.1079/9781845937140.0000 (Wallingford, 2010).

9. World Health Organization. *The top 10 causes of death* <http://www.who.int/mediacentre/factsheets/fs310/en/index2.html> (2016).

10. Brunham, R. C., Gottlieb, S. L. & Paavonen, J. Pelvic inflammatory disease. *New England Journal of Medicine* **372,** 2039–2048. ISSN: 13573039 (2015).

11. Lago, E. G. Current Perspectives on Prevention of Mother-to-Child Transmission of Syphilis. *Cureus* **8.** ISSN: 2168-8184. doi:10.7759/cureus.525 (2016).

12. Remme, J. H. F. *et al. Tropical Diseases Targeted for Elimination: Chagas Disease, Lymphatic Filariasis, Onchocerciasis, and Leprosy* ISBN: 0821361791 (2006).

13. Goupil, L. S. & McKerrow, J. H. Introduction: Drug Discovery and Development for Neglected Diseases. *Chemical Reviews* **114,** 11131–11137. ISSN: 0009-2665 (2014).

14. Kapasi, A. J., Dittrich, S., Gonzalez, I. J. & Rodwell, T. C. Host biomarkers for distinguishing bacterial from non-bacterial causes of acute febrile illness: A comprehensive review. *PLoS ONE* **11,** 1–29. ISSN: 19326203 (2016).

15. World Health Organization Child and Adolescent Health and Development Division. *Integrated Management of Childhood Illness Information Pack* tech. rep. (Geneva, 1998).

16. Ventola, C. L. The antibiotic resistance crisis: part 1: causes and threats. *P & T : a peer-reviewed journal for formulary management* **40,** 277–83. ISSN: 1052-1372 (2015).

17. World Health Organization. *Antimicrobial resistance* 2016. <http://www.who.int/mediacentre/factsheets/fs194/en/> (2016).

18. World Health Organization. *Global plan to combat neglected tropical diseases 2008 - 2015* tech. rep. (Geneva, 2007).

19. Biomarkers Definitions Working Group. Biomarkers and surrogate endpoints: preferred definitions and conceptual framework. *Clinical pharmacology and therapeutics* **69,** 89–95. ISSN: 0009-9236 (2001).

20. Mohd Hanafiah, K., Garcia, M. & Anderson, D. Point-of-care testing and the control of infectious diseases. *Biomarkers in medicine* **7,** 333–47. ISSN: 1752-0371 (2013).

21. *Point-of-Care Diagnostics on a Chip* (eds Issadore, D. & Westervelt, R. M.) ISBN: 978-3-642-29267-5. doi:10.1007/978-3-642-29268-2 (Berlin, Heidelberg, 2013).

22. Schleicher, E. The clinical chemistry laboratory: Current status, problems and diagnostic prospects. *Analytical and Bioanalytical Chemistry* **384,** 124–131. ISSN: 16182642 (2006).

23. Myers, F. B. & Lee, L. P. Innovations in optical microfluidic technologies for point-of-care diagnostics. *Lab on a chip* **8,** 2015–2031. ISSN: 1473-0197 (2008).

24. Comer, J. P. Semiquantitative Specific Test Paper for Glucose in Urine. *Analytical Chemistry* **28,** 1748–1750. ISSN: 0003-2700 (1956).

25. Free, A. H., Adams, E. C., Kercher, M. L., Free, H. M. & Cook, M. H. Simple specific test for urine glucose. *Clinical chemistry* **3,** 163–8. ISSN: 0009-9147 (1957).

26. Then, W. L. & Garnier, G. Paper diagnostics in biomedicine. *Reviews in Analytical Chemistry* **32,** 269–294. ISSN: 2191-0189 (2013).

27. St John, A. & Price, C. P. Existing and Emerging Technologies for Point-of-Care Testing. *The Clinical biochemist. Reviews* **35,** 155–67. ISSN: 0159-8090 (2014).

28. Li, S., Kiehne, J., Sinoway, L. I., Cameron, C. E. & Huang, T. J. Microfluidic opportunities in the field of nutrition. *Lab on a Chip* **13,** 3993. ISSN: 1473-0197 (2013).

29. Yetisen, A. K., Akram, M. S. & Lowe, C. R. Paper-based microfluidic point-of-care diagnostic devices. *Lab on a chip* **13,** 2210–51. ISSN: 1473-0189 (2013).

30. Hawkes, R, Niday, E & Gordon, J. A dot-immunobinding assay for monoclonal and other antibodies. *Analytical biochemistry* **119,** 142–7. ISSN: 0003-2697 (1982).

31. Farrell, B. O. *Lateral Flow Immunoassays Systems: evolution from the current state of the art to the next generation of highly sensitive, quantitative rapid assays* 89–107. ISBN: 9780080970370. doi:10.1016/B978-0-08-097037-0.00078-6 (Elsevier Ltd, 2013).

32. Lee, T. M. H. & Hsing, I. M. DNA-based bioanalytical microsystems for hand-held device applications. *Analytica Chimica Acta* **556,** 26–37. ISSN: 00032670 (2006).

33. Chen, L., Manz, A. & Day, P. J. R. Total nucleic acid analysis integrated on microfluidic devices. *Lab on a Chip* **7,** 1413. ISSN: 1473-0197 (2007).

34. Mullis, K. *et al.* Specific enzymatic amplification of DNA in vitro: the polymerase chain reaction. 1986. *Biotechnology (Reading, Mass.)* **24,** 17–27. ISSN: 0740-7378 (1992).

35. Park, J. W. *Development and Validation of Novel Molecular Techniques to Elucidate Mechanisms of Endocrine Disruption* (Michigan State University. Department of Zoology-Environmental Toxicology, 2008).

36. Gubala, V., Harris, L. F., Ricco, A. J., Tan, M. X. & Williams, D. E. Point of care diagnostics: status and future. *Analytical chemistry* **84,** 487–515. ISSN: 1520-6882 (2012).

37. World Health Organization. *Medical devices: Managing the mismatch* ISBN: 978 92 4 156404 5 (Geneva, 2010).

38. Hay Burgess, D. C., Wasserman, J. & Dahl, C. a. Global health diagnostics. *Nature* **444 Suppl,** 1–2. ISSN: 1476-4687 (2006).

39. Dyro, J. F. in *Clinical Engineering Handbook* (ed Dyro, J. F.) 155–158 (Academic Press, Burlington, 2004). ISBN: 978-0-12-226570-9.

40. Alonso, A. H. & Hortal, A. *Ética general de las profesiones* ISBN: 9788433017185 (Desclée de Brouwer, 2002).

41. Beauchamp, T. L. & Childress, J. F. *Principles of Biomedical Ethics* ISBN: 9780195335705 (Oxford University Press, 2009).

42. Global Forum for Health Research. *The 10/90 report on health research 2000* (ed Davey, S.) ISBN: 2-940286-01-9 (Geneva, 2000).

Chapter 3

Paper Chemical Dipsticks for Disease Diagnosis Produced with Domestic Inkjet Printers

3.1 Introduction

As previously mentioned, this chapter is focused on the development of chemical dipstick assays, hereinafter referred to as 'dipsticks', that can be simply manufactured in developing countries. We believe that enabling developing countries to design and manufacture their own diagnostic devices would ensure well adapted medical devices to local environments and needs that can be locally maintained, repaired, and further improved. Thus, the high number of malfunctioning and broken devices encountered in developing countries due to the lack of training on correct use and maintenance or absence of in-country spare parts and supplies could be significantly reduced.[1] Specifically, we propose the use of domestic desktop inkjet printers to easily produce dipstick diagnostic assays.

Dipsticks are probably the simplest diagnostic devices and have been in the market for more than 50 years.[2–4] They are paper strips impregnated with chemical reagents that can determine the presence of an analyte in a biological fluid qualitatively or semi-quantitatively through a colorimetric reaction. Most chemical reactions with color change can be achieved on paper in a one-step procedure. Probably the best known dipstick tests are pH strips, such as litmus strips, which

allow detecting alkaline and acid conditions.[5] Test strips to detect metabolic products in urine and blood analytes (such as protein, glucose, salt, etc.) are also very popular.[5,6]

Paper is an ideal substrate for low-cost diagnostics as it is inexpensive, widely available, disposable, biodegradable, flammable, and easy to functionalize due to its physico-chemical properties.[4,5,7] In addition to dipsticks, other point-of-care (POC) diagnostic tests also use paper as substrate: lateral flow immunoassays and microfluidic paper-based analytical devices (mPADS).[8,9] Both of them are relatively low-cost and easy to use; however, their manufacturing process is generally too complex and/or costly to be fully produced in developing countries.[5,10,11]

For depositing liquids on paper, inkjet printers are an attractive solution due to their capability to deposit drops with high accuracy in a low-cost, simple, fast, and reproducible way. Inks can be made of a variety of reagents beyond classical dyes, such as chemical or biological reagents, allowing inkjet technology to evolve from office printing to other industrial process and research applications including diagnostics.[12–15] Drop-on-demand (DOD) piezoelectric and thermal printers are the most widely used technologies for industrial and domestic applications.[16] In piezoelectric printing, applying a voltage to a piezoelectric element in contact with the printer nozzle results in a volume displacement and the ejection of an ink droplet. In thermal inkjet technology, the volume displacement is achieved by the creation of a gas bubble on a heating element inside the nozzle.[16] Piezoelectric technology is usually preferred in applications that involve chemical and biological reagents to avoid damage when exposed to high temperatures.[16] Within piezoelectric printers there are a wide variety of printers with different degrees of sophistication. On the one hand, sophisticated printers are generally used for research applications and allow full control of printing parameters (e.g. choice of nozzle diameter, printing stages, visual confirmation of ink droplet formation) and software (e.g. control of piezo-pulse voltage and duration).[16] On the other hand, consumer printers provide limited user control via the original printer driver and software, but critically are lower cost and user-friendly.[16]

By using domestic printers to produce diagnostic assays we hope to offer people in low-income countries with tools for local diagnostic assay production and

technology transfer, and provide means and ideas for innovation. Thus, as previously anticipated, this assay responds to the prioritization criteria 5 and 7, which emphasize the feasibility of developing an appropriate test and the resources and infrastructure required for POC device production respectively.

As proof of concept, our platform for manufacturing diagnostic test strips was tested for the detection of iodine status. Health conditions derived from a deficient or excessive dietary iodine intake are called iodine deficiency disorders (IDD) and are considered a severe global health problem around the world.[17,18] IDD consequences are varied; goiter, hypothyroxinemia, stillbirth, neurologic disorders, mental retardation or cretinism are some of them.[19] Worldwide, iodine deficiency is the most important cause of preventable mental retardation.[17,20] The WHO estimates that 'people living in areas affected by severe IDD may have an intelligence quotient (IQ) of up to about 13.5 points below that of those from comparable communities in areas where there is no iodine deficiency'.[17] The economic productivity of countries with high number of people suffering IDD is severely affected due to the effect of IDD on health, well-being, intelligence and learning capacity of its habitants.[17,20]

Preventing of IDD is straightforward.[17] Supplementing iodine intake into the diet of people living in areas of endemic iodine deficiency can successfully prevent IDD.[17,21] Iodination of salt is an inexpensive and commonly used method to increase iodine intake in a community.[17,21] Despite the effectiveness and low cost of this intervention, millions remain at risk for IDD.[21] Periodic monitoring and testing for iodine deficiency is key to the success of any supplementation program, for which medical devices play an essential role.

Iodine deficiency was selected as proof of concept since diagnostic assays for this condition should be highly prioritized according to criteria 1, 2, 6, and 8. Diagnostic assays for this condition are expected to highly contribute to reduce the global disease burden (criteria 1 and 2) since nutritional deficiencies and illness are interconnected and are part of a vicious cycle which also includes poverty.[22,23] In Copenhagen in 2008, eight internationally recognized economists selected micronutrient initiatives as the worlds best investment for development.[24] The low cost of food fortification and supplements together with the high rates of return

make these interventions extremely profitable. The diagnosis of nutritional deficiencies, and specifically iodine deficiency, is the first step to combat them. To the best of our knowledge, no diagnostic dipsticks for iodine status determination are currently available in the market and their development follows prioritization criterion 6. People living in developing countries are the most affected by this condition and focusing on them responds to bioethical principles (criterion 8)– most notably the principle of justice.

Iodine is a micronutrient required for normal thyroid function and production of thyroid hormones.[25] Thyroid hormones play a key role in the regulation of protein synthesis, enzymatic activity, hormonal activity and several other biochemical reactions.[25] There are different indicators to assess iodine deficiency including estimation of thyroid size, measurement of thyroid stimulating hormone (TSH) or thyroglobulin levels, and determination of urinary or salivary iodine.[17] IDD control programs use urinary iodine as principal indicator[17–19,26] due to the long response time after supplementation in the case of thyroid size and the high cost of analysis for TSH and thyroglobulin.[17] Urinary iodine is a highly accepted biomarker as short term indicator of recent iodine dietary intake and when used in a large representative population it can provide useful information of iodine status.[17,27] Additionally, urinary samples are easy to collect, store, and analyze, and it is estimated that more than 90 % of the iodine ingested in the diet is released in the urine.[17,25]

Although there are a wide variety of methods to determine iodine and iodide, to date there are no available techniques that fully fit the needs of developing countries.[28] Currently, iodine measurement in biological samples is carried out almost exclusively by inductively coupled plasma mass spectrometry (ICP-MS) or methods based on the Sandell-Kolfhoff reaction.[18,26,28] ICP-MS allows for high sensitivity and reliability; however, its high cost make it unrealistic for widespread use.[26] Methods based on Sandell-Kolfhoff (S-K) reaction rely on iodides role as a catalyst in the reduction of ceric ammonium sulfate (yellow color) to the cerous form (colorless).[17] The main drawback of S-K methods are the toxic waste products generated during urine digestion that is required prior to the colorimetric reaction.[26]

In 1998, Rendl et al. described a sensitive colorimetric method based on iodide function as catalysts in the oxidation of 3,3',5,5'-tetramethybenzidine (TMB) by peracetic acid/H_2O_2 which avoids toxic waste production.[29] We selected this method to perform a proof of concept of the platform here presented. Additionally, initial experiments were performed with the well-known iodine-starch reaction.

The 'holistic approach' for POC medical device development, explained in Chapter 1, is here applied to the development of dipstick assays that are easily and fully manufacturable in low-resource settings using a domestic inkjet printer. Major attention was given to the context, the users, and the end goal of production and implementation of the device. We describe simple chemical ink preparation formulations, easy and rapid methods for ink characterization allowing printing inexpensive diagnostics with domestic inkjet printers, and we provide guidelines for new ink development. Our platform is very versatile and can be used to detect a wide variety of biomarkers of diseases; its application to the detection of iodine deficiency is provided as a proof of concept.

3.2 Materials and Methods

3.2.1 System description and operation procedure

Diagnostic dipsticks were produced with a desktop piezo driven printer Epson Stylus SX420W. Compatible empty refillable cartridges (series T128) were purchased from Prink Ltd. and freshly prepared inks were introduced with a syringe into the cartridges. Once filled, cartridges were introduced into the printer. Previous to printing the diagnostic test, the printer injectors were primed using the 'clean head' function in the printer. Uncoated pure-cellulose filter paper was used as substrate.

The concentration of each ink could be controlled by printing colors that combine the corresponding basic printing color (black, blue cyan, magenta, and yellow) in the desired proportion. For printing only one reagent, only the corresponding basic color was used. For the experiments here presented, a 6×16 cm^2 area was printed for 5 five times over the same area in order to increase the reagent concentration. Then the printed paper was cut in 1.5×1.5 cm^2.

Table 3.1: Reagents and equipment for the production of paper dipsticks.

Name	Reference	Vendor
Reagents		
Soluble starch	33615	Sigma-Aldrich
Sodium nitrite	237213	Sigma-Aldrich
Triton X-100	T9284	Sigma-Aldrich
Tween-80	P1754	Sigma-Aldrich
Benzotriazole	B11400	Sigma-Aldrich
Ethanol 99.8 %	51976	Sigma-Aldrich
Hydrogen peroxide 30 %(w/v)	216763	Sigma-Aldrich
Sulfuric acid 98 %(v/v)	320501	Sigma-Aldrich
Peracetic acid	433241	Sigma-Aldrich
$3,3',5,5'$-tetramethylbenzidine	860336	Sigma-Aldrich
potassium iodide	60399	Sigma-Aldrich
Paper	Uncoated cellulose paper	
Refillable cartridges	T128	Prink Ltd.
Printhead cleaner solution	Magic liquid	Prink Ltd.
Equipment		
Desktop printer	SX420W	Seiko Epson
Drop Shape Analysis System	DSA100	KRÜSS GmbH
Rheometer	AR550	TA Instruments

When replacing ink cartridges and for short term printer storage, the printer nozzles were cleaned using a printhead cleaner solution (Magic Liquid from Prink Ltd.). Chemical ink cartridges were substituted by cartridges filled with printhead cleaner mix with de-ionized water in 1:1 proportion. Then the 'clean head' function in the printer was selected in order to clean the printer nozzles. For long term storage of the printer and unclogging nozzles, the printhead cleaner was directly added to the sponges under the printhead assembly using a syringe. First, the printhead assembly was moved in order to have access to the sponges and once the sponges were saturated, the printhead assembly was moved back over the sponges. The printer was left in this condition until the nozzles were unclogged or until it was used again.

3.2.2 Reagents for ink fabrication

Original inks for the printer Epson Stylus SX420W were purchased from Seiko Epson Corp. and were used to characterize their physico-chemical properties. Reagents used to prepare chemical inks were purchased from Sigma Aldrich Corp. and included Triton X-100, Tween-80, benzotriazole, ethanol 99.8 %, hydrogen peroxide 30 %(w/v), sulfuric acid 98 %(v/v), sodium nitrite, soluble starch, peracetic acid solution 36–40 %(w/v) in acetic acid, 3,3',5,5'-tetramethylbenzidine, and potassium iodide. The composition of the inks is described in Section 3.3.

3.2.3 Methods for determination the physico-chemical properties of an ink

Surface tension and viscosity are the most crucial ink properties since they determine drop formation and jetting performance.[30] The methods used to determine both parameters are described. Since the nature of the ink can affect the chemical integrity (corrosion) of the inkjet printer, a method to determine copper corrosion inside the printer injectors by acidic chemical inks is presented in this section as well.

Surface tension

Surface tension was calculated using a method based in Tate's law (Equation 3.1). For the same capillary radius, the ratio of mass and surface tension is constant for all liquids.

$$m \cdot g = 2 \cdot \pi \cdot r \cdot \gamma \tag{3.1}$$

$$\frac{m_1}{\gamma_1} = \frac{m_2}{\gamma_2} \tag{3.2}$$

where m is the drop mass, g is the gravity, r is the capillary radius, and γ is the surface tension.

The surface tension of a fluid was determined using water as reference. The mass of 25 drops of water and the fluid were measured, the surface tension of water

is known (72 mN/m at 25 °C)[31] and the surface tension of the fluid was calculated from Equation 3.2. Additionally, confirmatory surface tension measurements were taken with Drop Shape Analysis System DSA100.

Dynamic viscosity

Dynamic viscosity was determined using AR550 rheometer from TA Instruments. A shear stress between 0 and 50 Pa was applied to the samples for 5 min. A 60 mm diameter plate and a 250 μm gap were used. Results were analyzed using TA Data Analysis.

Corrosion quantification

Corrosion was determined by weighting 1 mm thick copper plates before and after incubation in an acidic solution with or without the addition of a corrosion inhibitor for 12 days. The mass loss due to corrosion under accelerated conditions was calculated as the mass difference between the initial and final copper plates mass. Benzotriazole was used as corrosion inhibitor.

3.3   Results

3.3.1   Materials selection and chemical inks preparation and description

Inkjet printers are widely available worldwide, easy to use and inexpensive. For the experiments presented here a \$60 Drop-On-Demand (DOD) piezoelectric based inkjet printer was used. As previously described, pure cellulose filter paper was used as substrate. All the inks here described were successfully printed on filter paper, reagents were homogeneously deposited on paper, properly absorbed and color differences from colorimetric reactions performed on filter paper were well distinguished. For depositing inks on paper, hand dispensing and direct immersion were tested as well. These techniques led to uneven distribution of reagents, and when the colorimetric reaction took place, the heterogeneous color formation made

semi-quantification impossible. The superior performance of printing versus hand dispensing and direct immersion, led us to focus on this technique.

In order to print chemical/biological reagents, they should be compatible with the printer materials and should be similar to commercial inks in terms of its physico-chemical properties.[30] As described in the Materials and Methods section, the most important ink physico-chemical properties are the surface tension and viscosity since they determine drop shape and jetting operation.[30] Water or aqueous buffers are the most common solvents for the different inkjet-printed chemical and biochemical analytical assays that target ions, proteins, antigens or metabolites. Water has a surface tension and viscosity of 72 mN/m and 1 mPa·s at 25 °C respectively. In addition to water or aqueous solutions, general ink compositions for piezo electric printers include a surfactant to adjust the surface tension and sometimes require a viscosity modifier.[14,30] Triton X-100 is generally used as a nonionic surfactant to adjust surface tension, and glycerols and glycols are commonly used as viscosity modifiers.[14]

The physico-chemical properties of the commercial pigmented ink for our selected printer were determined as explained in Section 3.2.3. The surface tension is 25.75 mN/m. Ink viscosity is 2.7 mPa·s and was calculated form Figure 3.1, which shows the rheological properties of the ink. Figure 3.1 A shows proportionality between shear stress and shear rate indicating Newtonian fluid behavior.
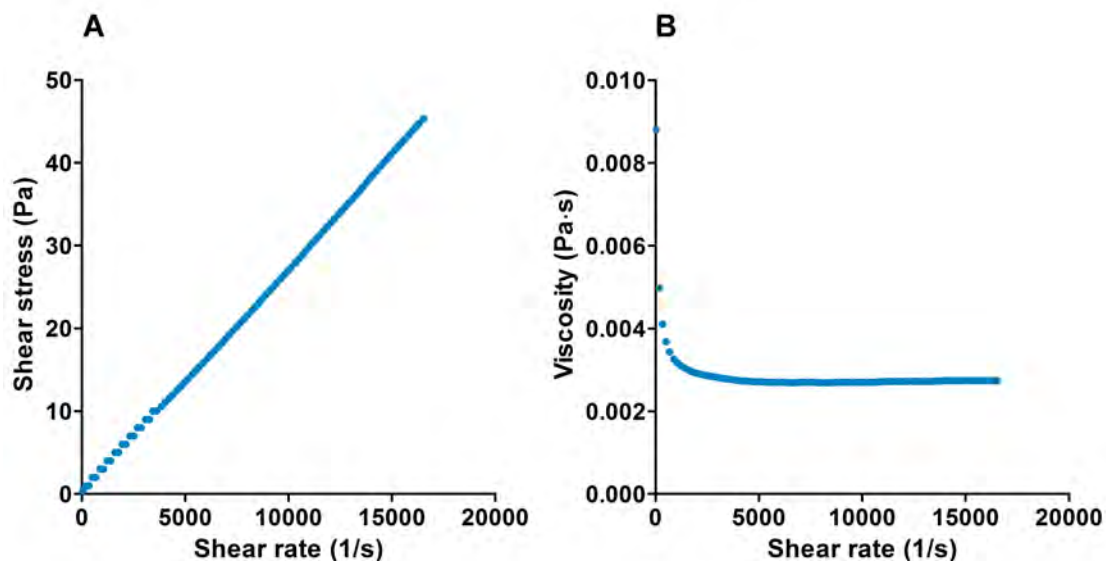
Figure 3.1: Ink rheometric curves of the commercial pigmented ink for our selected printer at 25 °C. A) Shear stress versus shear rate. B) Viscosity versus shear rate.

As proof of concept, it is described the development of chemical inks for two colorimetric reactions for iodide detection: the iodine-starch reaction and the TMB reaction.[29]

3.3.2 Starch-iodine reaction

The specific reaction between amylose in starch and iodine leads to the formation of a deep blue complex that can be used as a semiquantitative test for iodine. In presence of iodide, water insoluble iodine leads to triiodide anion (Reaction 3.3) which is highly soluble and complexes with amylose causing the deep blue color (Reaction 3.4). Iodine can be produced reacting sodium nitrite with potassium iodide and sulfuric acid (Reaction 3.5).[32]

$$I_2 + I^- \rightarrow I_3^- \tag{3.3}$$

$$I_3^- + starch \rightarrow blue\ colored\ complex \tag{3.4}$$

$$2NaNO_2 + 2KI + 2H_2SO_4 \rightarrow I_2 + 2NO + K_2SO_4 + Na_2SO_4 + 2H_2O \tag{3.5}$$
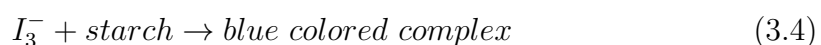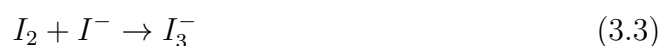
As start point to develop sodium nitrite, sulfuric acid, and starch inks, the concentrations recommended by Burriel et al. were used.[33] To 0.5 ml of sample,

1 or 2 drops of sulfuric acid 1 M were added until the sample turned acidic, then 210 g/L of soluble starch and one solid crystal of sodium nitrite were added. In order to assure that iodide is the limiting reagent and since all inks should be in liquid state, a very concentrated sodium nitrite solution was prepared: 0.7 g/ml. In the case of the soluble starch solution, a filtration step was carried out to separate amylopectin, which does not participate in the colorimetric reaction and is insoluble in water compromising the stability of the ink. Only an amylose solution was used for ink preparation. 1 M sulfuric acid solution was also prepared. Using these reagents, Reaction 3.5 was tested on paper. Color changes were successfully observed on paper; however as previously mentioned, due to imprecise manual reagent deposition on paper, discrimination of various iodide concentrations was not possible. Afterward, we proceeded to fabricate inks from these reagents.

The three solutions -sodium nitrite, sulfuric acid, and amylose– are aqueous. Sodium nitrite and sulfuric acid solutions present very similar surface tension and viscosity compared to water. However, amylose solution presents a very high viscosity due to its high concentration (see Figure 3.2, pink data set). Filtered amylose solution was diluted using water in order to decrease the viscosity to make it more closely match the viscosity of water. Shear stress versus shear rate was measured for each dilution and in Figure 3.2 the corresponding rheological curves can be observed. Commercial ink rheological curves are included for comparison. As can be observed, amylose solution has a pseudoplastic behavior. As expected, the more water added to the amylose solution, the lower the viscosity. For 10 %(v/v) amylose solution, the viscosity is approximately 9 mPa·s. We verified that although the viscosity of 10 %(v/v) amylose solution and pigmented inks differ in 6.3 mPa·s, adjustment of the viscosity was not required for good inkjet printing. Thus, 10 %(v/v) amylose solution, which corresponds to 21 g/l of filtered soluble starch, was selected.

Next, different experiments were conducted with each of the solutions to determine the appropriate composition of additives required for proper inkjet printing. The surface tension of the chemical solutions is around 72 mN/m, approximately three times higher than the surface tension of standard pigmented ink (25.75 mN/m). Triton X-100 and Tween-80 were used as surfactant to reduce the
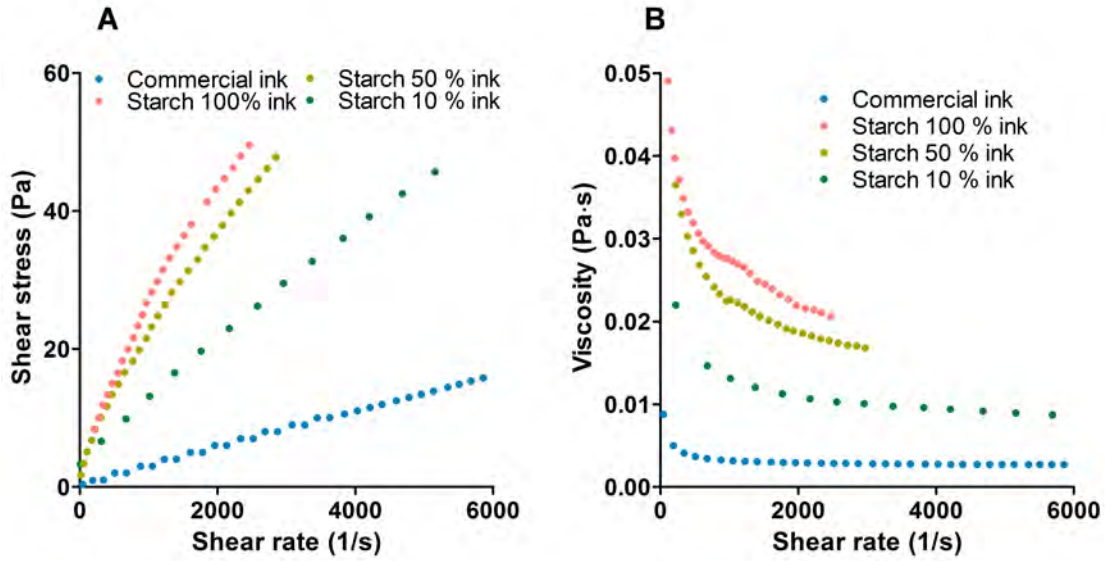
Figure 3.2: Rheometric curves of the different concentrations (expressed in %(v/v)) of amylose solution at 25 °C. A) Shear stress versus shear rate. B) Viscosity versus shear rate. Commercial ink rheological curves are shown for comparison purposes.

surface tension of the chemical solution; the results at different surfactant concentrations are shown in Table 3.2. 1 %(v/v) Triton X-100 resulted to be the most efficient achieving values between 27–30 mN/m for the different inks and allowing for good jetting performance. Higher concentrations of Triton X-100 did not decrease the surface tension substantially. Regarding viscosity, as previously mentioned, viscosity values similar to water did not need to be adjusted for good inkjet printing.

Table 3.2: Starch, sodium nitrate, and sulfuric acid ink surface tension varying the concentration of two surfactants, Tween-80 and Triton X-100.

| Surfactant | Surfactant surface tension (mN/m) | | | | | |
| conc. | *Starch ink* | | *Sodium nitrite ink* | | *Sulfuric acid ink* | |
% (v/v)	Tween	Triton	Tween	Triton	Tween	Triton
0,1	66,53	37,34	53,24	34,72	43,44	33,25
0,5	54,85	30,86	38,93	28,86	38,13	28,45
1	51,08	29,65	37,79	27,35	36,67	27,34
2	48,28	29,49	36,92	27,29	34,52	27,12

When formulating the inkjet printing ink, the compatibility of the ink with the printer components need to be taken into account.[30] Thus, in the case of the

sulfuric acid ink, corrosion studies were conducted as acids mays corrode copper in the printer injectors and as a result damage the printer. 1 M solution of sulfuric acid and 4 different concentrations of the corrosion inhibitor benzotriazole were used. 1 M benzotriazole concentration was the minimum concentration of inhibitor required in order to form a passivating benzotriazole self-assembly monolayer that protects the copper from corrosion (Figure 3.3). For 1 M benzotriazole, the mass loss of the copper plate was less than 0.1 % as can be seen in Table 3.3, which was considered negligible.
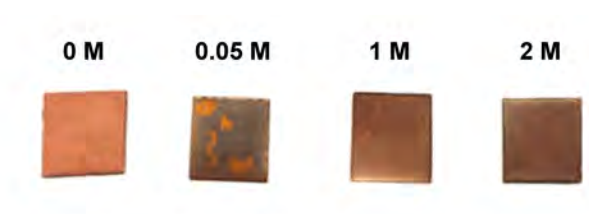
Figure 3.3: Copper plates incubated for 12 days in a 1 M solution of sulfuric acid with different concentrations of benzotriazole. Benzotriazole concentrations indicated above each copper sample.

Table 3.3: Corrosion inhibition study by 1 M sulfuric acid on copper in presence of different concentrations of benzotriazole.

Benzotriazole concentration [M]	Weight loss [%(w/w)]
0	0.33
0.05	0.17
1	0.09
2	0.08

Table 3.4 summarizes the composition of the sodium nitrite, sulfuric acid and starch inks (Lanes 1-3). Once the three chemical inks that participate in the reactions 3.3–3.5 were developed, analytical test strips were produced. Amylose, sodium nitrite, and sulfuric acid inks were printed following that order over the same paper area. Each chemical ink was introduced in a different printer cartridge and by selecting the equivalent colored cartridge it was possible to select which ink was printed at each time. The dipstick was tested through immersion in solutions with different iodide concentration. Results were evaluated after 30 s (Figure 3.4).

Table 3.4: Composition of various chemical inks.

Ink	Main component	Additives	γ (mN/m)	μ (mPa·s)
Starch	21 g/L filtered soluble starch	1 % Triton X-100	29.7	1.53
Sodium nitrite	0.7 g/ml $NaNO_2$ in H_2O	1 % Triton X-100	27.3	3
Sulfuric acid	1 M H_2SO_4 in H_2O	1 % Triton X-100, 1 M benzotriazole	27.3	0.99
3,3',5,5-TMB	2.5 mM 3,3',5,5-TMB in ethanol	–	22.1	1.21

References: γ is the surface tension; and μ is the viscosity.
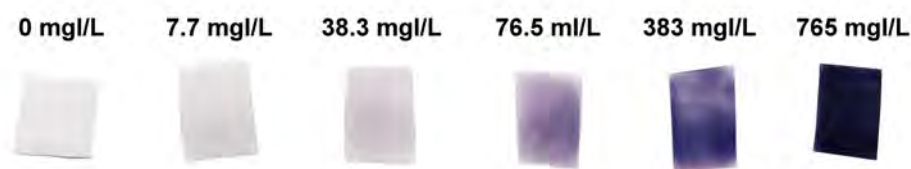
Figure 3.4: Color observed in printed paper with amylose, sodium nitrite and sulfuric acid inks after immersion in potassium iodide solutions of different concentrations. Iodide concentrations indicated above each corresponding colored paper.

Figure 3.4 shows how color differences allow determining semi-quantitatively a wide range of iodide concentrations demonstrating successful ink preparation and printing. However, while this worked as proof of concept, the level of detection was not sufficiently low to detect physiological levels of iodine in the urine. It should be noted that chemical reagents, chemical inks and printed paper strips were stored at room temperature without observing activity loss or ink instability for several months.

3.3.3 Reaction with 3,3',5,5'-tetramethylbenzidine (TMB)

TMB reaction is more sensitive and allows detecting iodine in the concentration present in the urine (20–300 μgI/L).[29] This method is a colorimetric assay in which iodide catalyzes the oxidation of 3,3',5,5'-tetramethylbenzidine (TMB) by peracetic acid/H_2O_2 yielding colored products (Figure 3.5). A blue charge-transfer

complex exists in rapid equilibrium with the TMB-radical cation. Depending on the color of the products it is possible to estimate the range of iodide concentration.

It should be considered that for this method urine needs to be pretreated. However, contrary to Sandell-Kolfhoff methods which require digestions with high toxic waste production, Rend et al. developed simple carbon activated columns which remove the interfering substances without producing toxic wastes.[29] Since these reactions are presented as proof of concept of the system, solutions with different concentrations of iodide were used as samples and no urine experiments were performed.
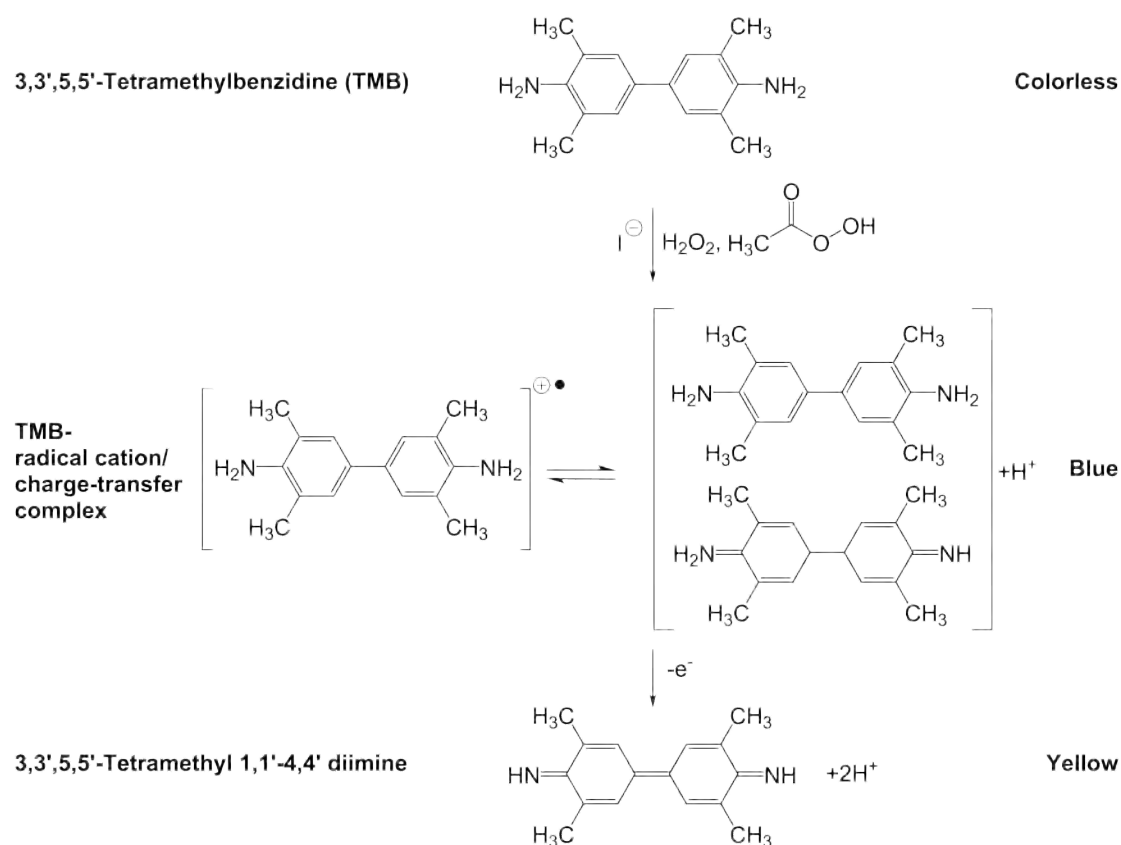
Figure 3.5: 3,3',5,5'-tetramethylbenzidine (TMB) reaction. 3,3',5,5'-tetramethylbenzidine (TMB) is oxidized in the presence of peracetic acid/H_2O_2 and iodide generating colored products.[29]

As a starting point, the concentrations described by Rend. et al were used.[29] The reagents required were: 2.5 mM 3,3',5,5'-TMB in ethanol and 1.2 % peracetic acid in 30 % H_2O_2. Reagents implicated in the reaction were prepared and the change in color was observed on paper.

Since the concentration of TMB is low, the properties of this solution are considered to be very similar to ethanol properties. Thus, ethanol studies were carried out. Ethanol surface tension and viscosity are 22.0 mN/m and 1.04 mPa·s at 25 °C respectively. Both parameters are very close to pigmented ink parameters and good jetting performance was observed with ethanol and TMB ink without the need of additives. The composition of TMB ink is shown in Table 3.4 Lane 4. Peracetic acid in H_2O_2 was not converted to an ink format due to its very oxidative power. If peracetic acid was printed on TMB printed paper, TMB was instantly oxidized impeding its later use.

Paper strips printed with TMB were tested by introducing them into solutions with different iodine concentration in the range present in urine. A drop of peracetic acid in H_2O_2 was added at the end to start the catalytic reaction. The results were read 2 min after the addition of peracetic acid and are shown in Figure 3.6. Different read-out times were tested, and 2 min produced the greatest color differences between the iodide concentrations evaluated. Shorter times produced lighter colors and longer exposures led to color saturation for the higher iodide concentrations. TMB ink and paper strips were stable for several months stored at room temperature without observing activity loss.
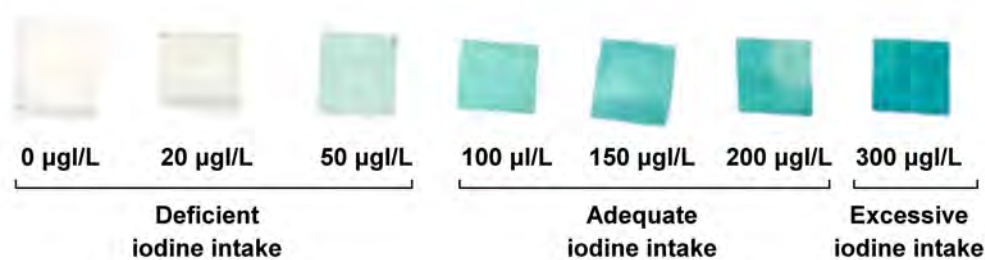
Figure 3.6: Color observed in paper printed with TMB reagent after immersion in iodide solutions of different concentration and addition of a drop of peracetic acid/H_2O_2. Iodide concentrations indicated below each corresponding colored paper.

In Figure 3.6 it can be observed how the color differences, when comparing with a printed colored scale, allow for semi-quantitative determination of the iodine concentration which could identify iodine deficiency and the degree of severity. The WHO considers the iodine nutritional state as: severe deficiency when urinary

iodine is below 20 μg/L, moderate deficiency for 20–49 μg/L, mild deficiency in case of 50–99 μg/L, optimal when urinary iodine is 100–199 μg/L, mild iodine excess for 200–299 μg/L, and severe excess when urinary iodine is higher than 300 μg/L.[17] Although differences between some of the iodine concentrations tested are subtle, differences between deficient (20 μgI/L, 50 μgI/L), adequate (100 μgI/L, 150 μgI/L, 200 μgI/L) and excessive (300 μgI/L) iodine intake groups can be well discriminated unambiguously.

3.3.4 Cost analysis

A cost analysis for dipstick production using TMB reaction was performed. Taking into account the price of the chemical reagents and paper, considering the average cartridge yield provided by the manufacturer (approximately 165 pages/3.5 ml cartridge), and a 2.25 cm^2 dipstick surface area, it is estimated that more than 5000 dipsticks assay can be manufactured with less than \$10 consumables. Additionally, the cost of an inkjet printer and compatible empty inkjet cartridges should be considered. As previously mentioned, for the experiments here presented a \$60 printer was used and 4 empty cartridges which cost \$20. Thus, a 100,000 population could be screened for merely \$200.

3.4 Discussion

3.4.1 Advantages of iodine determination using low-cost dipsticks

We have here presented dipsticks that can be produced locally using inkjet printers. As proof of concept, this method was applied to the determination of urinary iodine, and TMB reaction turned to be particularly useful. 3,3',5,5'-TMB, ethanol, peracetic acid, and H_2O_2 were the only chemical reagents required for the semi-quantification of iodine in the same concentration range as present in the urine.

Our semi-quantitative urinary dipstick assays are well suited for epidemiological purposes.[34] IDD is a nutritional deficiency that is primarily the result of deficiency of iodine in soil which in turn leads to the lack of iodine in groundwater and foods

grown locally in those areas.[34] Communities living in the same areas have usually similar levels of bodily iodine. Urinary dipsticks would allow identifying endemic regions, communities at risk of IDD, and establishing public health programs, such as inexpensive salt iodization interventions, to address this problem.[35] Even after IDD elimination in a community, control programs should be constantly maintained[17] and locally produced urinary dipsticks would be highly useful. Singe individual estimates are also possible; taking several measurements during different days and/or times of the day would help to increase the accuracy.

Chemical handling for ink preparation and paper dipsticks production should be performed at health clinics; then, the dipsticks could be used at the patient site. Providing small rural clinics with low-cost and rapid diagnostics to assess iodine status would motivate them to promote the consumption of iodized salt or other sources of iodine if the iodine status of the community is low.

3.4.2 Comparison with other currently available methods

Local production and technology transfer is key to increase access to medical devices, especially in low- and middle-income countries (LMICs). It is estimated that a mere 13 % of medical device manufacturers are located in LMICs.[36] However, few technologies are developed to facilitate local production in developing countries. Some interesting examples of health technologies in this line are the MediKit[37], which includes modular components to allow medical professionals to design their own appropriate solutions, and Pharmacy-on-Demand[38], which consist in a portable system can be configured to produce at small scale different drugs locally. Our system allows local production of diagnostic devices because its main component is an inkjet printer, which are low-cost and available in every country around the world. Thus, our approach for innovation was to adapt methods and designs to new functions rather than the typical innovation approach based on designing new technologies.[22]

Wide varieties of bio(chemical) sensing devices use inkjet printers during their manufacturing process.[16] Electrochemical and optical-based devices have been reported. Inkjet-printed features include electrodes, hydrophobic barriers, chemical solutions, antibodies, and enzymes which were printed in substrates such as paper

(filter, chromatographic, nitrocellulose) and electrodes.[16,39–44] In most cases research printers were used, especially when printing costly and/or sensitive reagents such as antibodies.[16,42,44] In few of them, if any, the whole assay was inkjet-printed, but rather specific parts of the assay were printed.[16] Additionally, to the best of our knowledge, none of them is simple enough to be fully produced in poor-resource settings. One of the main advantages of our assay is its simplicity which allows to be fully be manufactured using merely a desktop printer and few inexpensive resources.

Regarding the techniques for iodine detection in biological samples, to the best of our knowledge, no available techniques are appropriate to meet the needs of low-income countries.[28] As previously described, ICP-MS and methods based on Sandell-Kolthoff reaction (S-K) are the most common methods used for iodine measurement in biological samples.[28] The sensitivities of both methods are adequate for the detection of severe iodine deficiency in iodine samples; however, each of them present an important shortcoming. In the one hand, S-K reaction requires complete mineralization of the sample, which is usually performed through digestion techniques using perchloric acid for which special precautions are required due to explosion hazards.[28] In the other hand, ICP-MS is a sophisticated and costly technique unaffordable for widespread use.[28] Other techniques worth mentioning include inductively coupled plasma optical emission spectrometry (ICP-OES), neutron activation analysis (INAA), and atomic absorption spectrometry (AAS). All these techniques are sensitive for severe iodine determinations but present similar limitations to S-K based reactions or ICP-MS: they require extensive sample preparation and/or are costly.[28]

3.4.3 Guidelines for the development of new inks

When developing new inks, the first step is to identify a one-step colorimetric chemical reaction that monitors the target analyte. Two situations can be observed depending on reagents that participate in the chemical reaction. The first situation is when the concentration of a chemical reagent in the solution is low and does not considerably alter the viscosity and surface tension of the solvents. In this case, when ethanol is the solvent, the solution can be directly used as ink.

As previously shown, the surface tension and viscosity are very close to pigmented inks parameters and good jetting performance was observed with ethanol based inks without the need of additives. For water-based formulations, the addition of 1 %(v/v) Triton X-100 is enough to sufficiently modify the surface tension while the viscosity does not require modification for good jetting performance. In the case of a reagent that is added to the reaction in the solid state, a solvent should be used to dissolved it in. The second situation is when the properties of the chemical solutions differ from the ones of water or ethanol solvents, or when using a different solvent, more ink studies need to be performed. Viscosity and surface tension should be measured and additives need to be added until both properties resemble those of pigmented inks. In our experience, the addition of Triton X-100 in the range of 0.5–2 %(v/v) is a good method to achieve adequate surface tension. For the determination of surface tension, only a scale and pipette or thin capillary are required. In the case of viscosity, viscosities between 1 and 9 mPa·s did not required modification of their viscosity for good jetting performance. Moreover, as previously mentioned, new inks developed need to be compatible with the printer components.[30] In the case of using reagents that might damage the printer, such as corrosive reagents, experiments to guarantee the printer stability need to be performed. Similar experiments to the described herein for corrosion need to be implemented. Depending on the acid of intended use, its concentration, and the intended time for the ink to be inside the printer cartridge, performing corrosion experiments as described in the materials and methods section is highly recommended as the ink here presented is just an example.

In addition to iodine deficiency, this versatile method to design and produce inkjet-printed dipsticks can be applied to detect biomarkers of other diseases. Urinary dipsticks are widely available and use well known reactions to detect analytes that may signal abnormal conditions.[45] For example, high sugar levels in the urine may indicate diabetes; nitrites and/or leukocytes could be present due to urinary tract infection; high protein levels might be indicative of kidney disease; large amounts of ketones are present in the urine due to diabetes, starvation or a diet low in vegetables or carbohydrates; red blood cells may be a sign of urinary tract, kidney disease, or tumors.[45,46] Chemicals needed to produce common urinary dip-

sticks could be converted into inks and then inkjet-printed on paper. In the same way as with urinary dipsticks, analytes present in other biological fluids -blood, saliva, sweat– could be used to detect other diseases, dietary conditions, or drug abuse situations.[4,47]

Furthermore, this platform may be suitable to print immunoassays. Immunoassays are based on the interaction between antigens and antibodies to detect target proteins from pathogens or the host immune reaction and have been successfully used to detect a wide variety of pathogen types (viruses, bacteria, and parasites), and non-communicable diseases.[48] Immunoassays have been produced using inkjet printers;[11] however, to best of our knowledge, no immunoassays have been developed using inexpensive desktop printers.[16] We performed preliminary experiments printing 'capture' antibodies on nitrocellulose paper. Printed antibodies were fully functional. They recognized a 'detection' antibody conjugated to Alexa Fluor® (Thermo Fisher Scientific). These preliminary experiments show great promise to produce fully printed deployable immunoassays using consumer printers. More information about these preliminary experiments can be found in Appendix B.

We are currently working on expanding the amount of inks and increasing the application to other diseases that are mostly prevalent in emerging nations. Additionally, an online database with ink formulations and properties could be developed and shared between users around the world. Next steps include applying this system in developing countries with printers and resources locally available and providing mentorship when needed.

To conclude, although there are a wide variety of diagnostic assays for developing countries, they very rarely can be produced locally. Future research in the area of diagnostics for developing countries should prioritize the end goal of fabricating the diagnostic devices by locals, with local resources, and giving more autonomy to the local population.

3.5   Concluding Remarks

We herein described simple chemical ink preparation formulations, and easy and rapid methods for ink characterization allowing printing inexpensive diagnostics with domestic inkjet printers. A successful proof of concept for iodine determination in the concentrations present in the urine is provided, demonstrating the versatility of this fabrication method. With only a low-cost inkjet printer, few chemical reagents, and easy to follow chemical ink preparation recipes, it is possible to develop diagnostic strips for biomarkers of a wide variety of diseases. The fact that no high-tech infrastructure and no highly trained personnel is needed, makes this technology ideal to be exploited in developing countries. When medical devices are fabricated by locals with local resources, they are no longer black boxes that cannot be repaired when they breakdown or malfunction, but rather they are technologies that can be locally sustained and fixed, and open the door to innovation.

Bibliography

1. World Health Organization. *Medical devices: Managing the mismatch* ISBN: 978 92 4 156404 5 (Geneva, 2010).

2. Comer, J. P. Semiquantitative Specific Test Paper for Glucose in Urine. *Analytical Chemistry* **28,** 1748–1750. ISSN: 0003-2700 (1956).

3. Free, A. H., Adams, E. C., Kercher, M. L., Free, H. M. & Cook, M. H. Simple specific test for urine glucose. *Clinical chemistry* **3,** 163–8. ISSN: 0009-9147 (1957).

4. Then, W. L. & Garnier, G. Paper diagnostics in biomedicine. *Reviews in Analytical Chemistry* **32,** 269–294. ISSN: 2191-0189 (2013).

5. Hu, J. *et al.* Advances in paper-based point-of-care diagnostics. *Biosensors and Bioelectronics* **54,** 585–597. ISSN: 18734235 (2014).

6. St John, A. & Price, C. P. Existing and Emerging Technologies for Point-of-Care Testing. *The Clinical biochemist. Reviews* **35,** 155–67. ISSN: 0159-8090 (2014).

7. Pelton, R. Bioactive paper provides a low-cost platform for diagnostics. *Trends in Analytical Chemistry* **28,** 925–942. ISSN: 01659936 (2009).

8. Martinez, A. W., Phillips, S. T., Butte, M. J. & Whitesides, G. M. Patterned Paper as a Platform for Inexpensive, Low-Volume, Portable Bioassays. *Angewandte Chemie International Edition* **46,** 1318–1320. ISSN: 14337851 (2007).

9. Mao, X. & Huang, T. J. Microfluidic diagnostics for the developing world. *Lab on a Chip* **12,** 1412. ISSN: 1473-0197 (2012).

10. Klasner, S. A. *et al.* Paper-based microfluidic devices for analysis of clinically relevant analytes present in urine and saliva. *Analytical and Bioanalytical Chemistry* **397,** 1821–1829. ISSN: 16182642 (2010).

11. Abe, K., Kotera, K., Suzuki, K. & Citterio, D. Inkjet-printed paperfluidic immuno-chemical sensing device. *Analytical and Bioanalytical Chemistry* **398,** 885–893. ISSN: 1618-2642 (2010).

12. Abe, K., Suzuki, K. & Citterio, D. Inkjet-printed microfluidic multianalyte chemical sensing paper. *Analytical Chemistry* **80,** 6928–6934. ISSN: 00032700 (2008).

13. Sirringhaus, H. *et al.* High-Resolution Inkjet Printing of All-Polymer Transistor Circuits. *Science* **290,** 2123–2126. ISSN: 0036-8075 (2000).

14. Yamada, K., Henares, T. G., Suzuki, K. & Citterio, D. Paper-Based Inkjet-Printed Microfluidic Analytical Devices. *Angewandte Chemie International Edition* **54,** 5294–5310. ISSN: 14337851 (2015).

15. Martinez, A. W., Phillips, S. T., Whitesides, G. M. & Carrilho, E. Diagnostics for the developing world: microfluidic paper-based analytical devices. *Analytical chemistry* **82,** 3–10. ISSN: 1520-6882 (2010).

16. Komuro, N., Takaki, S., Suzuki, K. & Citterio, D. Inkjet printed (bio)chemical sensing devices. *Analytical and Bioanalytical Chemistry* **405,** 5785–5805. ISSN: 1618-2642 (2013).

17. World Health Organization. *Assessment of iodine deficiency disorders and monitoring their elimination* tech. rep. (Geneva, 2001).

18. World Health Organization. *Iodine status worldwide WHO Global Database on Iodine Deficiency* tech. rep. (Geneva, 2004).

19. Soldin, O. P. Controversies in urinary iodine determinations. *Clinical Biochemistry* **35,** 575–579. ISSN: 00099120 (2002).

20. De Benoist, B., McLean, E., Anderson, M. & Rogers, L. Iodine deficiency in 2007: Global progress since 2003. *Food and Nutrition Bulletin* **29,** 195–202. ISSN: 03795721 (2008).

21. Food and Agriculture Organization & CAB International. *Combating micronutrient deficiencies: food-based approaches* (eds Thompson, B. & Amoroso, L.) ISBN: 9781845937140. doi:10.1079/9781845937140.0000 (Wallingford, 2010).

22. Chin, C. D., Linder, V. & Sia, S. K. Lab-on-a-chip devices for global health: past studies and future opportunities. *Lab on a chip* **7,** 41–57. ISSN: 1473-0197 (2007).

23. World Bank. *Global Burden of Disease and Risk Factors* (eds Lopez, A. D., Mathers, C. D., Ezzati, M., Jamison, D. T. & Murray, C. J.) ISBN: 0821362623 (Washington, 2006).

24. Flour Fortification Initiative *et al. Investing in the future: A united call to action on vitamin and mineral deficiencies* tech. rep. (Ontario, 2009).

25. Institute of Medicine. *Dietary Reference Intakes for Vitamin A, Vitamin K, Arsenic, Boron, Chromium, Copper, Iodine, Iron, Manganese, Molybdenum, Nickel, Silicon, Vanadium, and Zinc* ISBN: 978-0-309-07279-3. doi:10.17226/10026 (National Academies Press, Washington, D.C., 2001).

26. Khazan, M., Azizi, F. & Hedayati, M. A Review on Iodine Determination Methods in Salt and Biological Samples. *Scimetr* **1,** 1–9. ISSN: 2213-7610 (2013).

27. *Laboraroty support for the diagnosis of thyroid disease* (eds Demers, L. M. & Spencer, C. A.) (National Academy of Clinical Biochemistry, 2002).

28. Shelor, C. P. & Dasgupta, P. K. Review of analytical methods for the quantification of iodine in complex matrices. *Analytica chimica acta* **702,** 16–36. ISSN: 1873-4324 (2011).

29. Rendl, J, Bier, D, Groh, T. & Reiners, C. Rapid urinary iodide test. *Journal of Clinical Endocrinology and Metabolism* **106 Suppl,** S12–6. ISSN: 0947-7349 (1998).

30. *Inkjet-Based Micromanufacturing* (eds Korvink, J. G., Smith, P. J. & Shin, D.-Y.) ISBN: 9783527647101. doi:10.1002/9783527647101 (Weinheim, 2012).

31. Vargaftik, N. B., Volkov, B. N. & Voljak, L. D. International Tables of the Surface Tension of Water. *Journal of Physical and Chemical Reference Data* **12,** 817–820. ISSN: 0047-2689, 1529-7845 (1983).

32. Prakash, S. *Advanced Inorganic Chemistry* ISBN: 9788121902632 (S. Chand Limited, 2000).

33. Burriel Marti, F., Lucena Conde, F., Arribas Jimeno, S. & Hernández Méndez, J. *Quimica Analitica Cualitativa* ISBN: 9788497321402 (S.A.Ediciones Paraninfo, Madrid, 2002).

34. WHO, UNICEF & ICCIDD. *Assessment of Iodine deficiency Disorders and Monitoring their Elimination : A guide for Programme Managers* ISBN: 978 92 4 159582 7 (Geneva, 2007).

35. Golden, M. H. Proposed recommended nutrient densities for moderately malnourished children. *Food and nutrition bulletin* **30,** S267–342. ISSN: 0379-5721 (2009).

36. World Health Organization. *Local Production and Technology Transfer to Increase Access to Medical Devices: Addressing the barriers and challenges in low- and middle-income countries* ISBN: 978 92 4 150454 6 (Geneva, 2012).

37. Little Devices Laboratory. *MEDIKit: DIY Technologies for Health* <https://littledevices.org/research/> (2016).

38. Adamo, A *et al.* On-demand continuous-flow production of pharmaceuticals in a compact, reconfigurable system. *Science* **352,** 61–67. ISSN: 0036-8075 (2016).

39. Määttänen, A. *et al.* Paper-based planar reaction arrays for printed diagnostics. *Sensors and Actuators, B: Chemical* **160,** 1404–1412. ISSN: 09254005 (2011).

40. Määttänen, A. *et al.* A low-cost paper-based inkjet-printed platform for electrochemical analyses. *Sensors and Actuators B: Chemical* **177,** 153–162. ISSN: 09254005 (2013).

41. Phongphut, A *et al.* A disposable amperometric biosensor based on inkjet-printed Au/PEDOT-PSS nanocomposite for triglyceride determination. *Sensors and Actuators B: Chemical* **178,** 501–507. ISSN: 09254005 (2013).

42. Fu, E. *et al.* Two-dimensional paper network format that enables simple multistep assays for use in low-resource settings in the context of malaria antigen detection. *Analytical Chemistry* **84,** 4574–4579. ISSN: 00032700 (2012).

43. Lu, R., Shi, W., Jiang, L., Qin, J. & Lin, B. Rapid prototyping of paper-based microfluidics with wax for low-cost, portable bioassay. *Electrophoresis* **30,** 1497–1500. ISSN: 01730835 (2009).

44. Su, S., Ali, M. M., Filipe, C. D. M., Li, Y. & Pelton, R. Microgel-Based Inks for Paper-Supported Biosensing Applications. *Biomacromolecules* **9,** 935–941. ISSN: 1525-7797 (2008).

45. Fischbach, F. *A Manual of Laboratory and Diagnostic Tests* (Lippincott Williams & Wilkins, 2003).

46. Roche Diagnostics. *Compendium of urinalysis Urine test strips and microscopy* tech. rep. (Rotkreuz, 2011), 1–180.

47. Pate, L. A., Hamilton, J. D., Park, R. S. & Strobel, R. M. Evaluation of a saliva alcohol test stick as a therapeutic adjunct in an alcoholism treatment program. *Journal of Studies on Alcohol* **54,** 520–521. ISSN: 0096-882X (1993).

48. *Point-of-Care Diagnostics on a Chip* (eds Issadore, D. & Westervelt, R. M.) ISBN: 978-3-642-29267-5. doi:10.1007/978-3-642-29268-2 (Berlin, Heidelberg, 2013).

Chapter 4

Low-cost, real-time, continuous-flow PCR and RT-PCR systems for pathogen detection

4.1 Introduction

As described in previous chapters, currently the diagnosis of infectious diseases is usually done by culture (bacterial), immunoassays, or nucleic acid assays. However, each format has its drawbacks. Cultures are very slow (18–48 h) and are typically performed in centralized laboratories by trained personnel, making adaptation to POC devices cumbersome. Immunoassays are an improvement over cultures in that they can be very rapid but unfortunately, they can exhibit poor sensitivity in many cases. Nucleic acid assays are rapid and sensitive but are historically costly and nearly always require trained personnel. The sensitivity and rapidity of nucleic acid-based tests have prompted us, and others, to re-engineer these types of tests to substantially reduce the associated costs and training required. A nucleic acid based POC device would be highly desirable and particularly promising for developing countries. They would allow rapid diagnosis of pathogens and diseases which otherwise would be impossible in terms of rapidity, sensitivity, and prompt treatment initiation. As previously described in Chapter 2, the development of this

nucleic acid device addresses the prioritization criteria 1, 5, 6, and 8 for device development. First of all, this device would aid to reduce the burden of infectious diseases (criterion 1). Criterion 5 (feasibility of developing an appropriate test) was selected for inclusion because the individual technologies required to build the system are very close to hitting low-cost, and large-scale production benchmarks. Currently, there are few nucleic acid-based POCTs available in the market; therefore their development should be prioritized according to criterion 6 (availability of tests in market and their sensitivity and specificity). Additionally, since infectious diseases are more prevalent in developing countries, which have the fewest economical resources, the bioethical justice principle (criterion 8) is emphasized.

Three cases where prompt diagnosis and treatment of infectious disease would substantially reduce patient morbidity are *Chlamydia trachomatis*, *Escherichia coli* O157:H7 and Ebola virus (EBOV). *C. trachomatis* is the most common bacterial sexually transmitted disease and the single most important infectious agent associated with blindness (trachoma).[1] Approximately 92 million people are infected with *C. trachomatis* each year with more than two thirds of them living in developing countries.[2] Long-term infected patients may develop pelvic inflammatory disease, infertility, or miscarriage.[3,4] Worldwide, approximately 84 million people suffer *C. trachomatis* eye infections and 8 million are irreversibly visually impaired by trachoma.[5] Diagnosis of the bacteria and initiating treatment in the first clinical encounter is key for increasing treatment success rates. *C. trachomatis* infection is very often asymptomatic (approximately 80 % of women and 40 % of men)[2] and most prevalent in young people, who generally are less prone to seek for medical attention, return to second medical appointments, or follow lengthy treatments, especially when asymptomatic.[6] As previously stated, the expected impact of a new test to diagnose often asymptomatic chlamydial infections is very high (prioritization criterion 2).

Infection with *E. coli* O157:H7 can cause hemorrhagic diarrhea and kidney failure and is associated with consuming contaminated food or drinking-water (fecal-oral route).[7,8] Diarrheal disease is the second leading cause of death due to infection in children under five years of age worldwide.[9,10] Diarrheal diseases are responsible for more than 15 % of all deaths of children between 1 month and 5

years of age in low-income countries and more than 30 % of all deaths due to infectious diseases for the same population group.[11] The risk of dying due to diarrheal diseases is 100 times higher for a child living in low-income countries compared to one of high-income countries.[11] Diarrheal diseases can be caused by a variety of bacterial, viral, and parasitic organisms. Making a prompt and accurate diagnosis of the responsible pathogen would allow for rapid initiation of the right treatment and would avoid the overuse of antibiotics and the rise of antibiotic resistance.[6,12] Diagnostic devices for diarrheal causative pathogens should be prioritized according to criterion 4 (availability, expense and toxicity of treatment). The importance of receiving the right treatment is even more critical in the case of these enterohemorrhagic strains of *E. coli* as receiving the wrong treatment often makes the disease worse.[7,13]

Ebola virus disease (EVD) is an acute, severe, and often fatal illness in humans which is caused by infection with a virus of the family *Filoviridae*, genus *Ebolavirus*. There are five identified Ebola virus species: Zaire, Bundibugyo, Sudan, Reston and Taï Forest.[14,15] The virus is transmitted to people from wild animals and spreads in the human population through human-to-human transmission.[14] Currently, most of the infections occur in equatorial Africa. The average EVD case fatality rate is around 50 %, although case fatality rates have varied from 25 % to 90 % in past outbreaks. In the case of 2014 West African outbreak, the case fatality rate was approximately 50 % and was caused by Ebola Zaire virus.[16] EVD is difficult to diagnose through its early symptoms, such as fever, since they are very similar to other common infectious diseases such as malaria, typhoid fever, and meningitis. Prompt and accurate EVD diagnosis is key for successful outbreaks control since it requires isolating patients from the community to prevent continued virus spread. Additionally, early supportive care with rehydration and symptomatic treatment improves survival.[14] Unfortunately, there is no proven treatment or vaccine available for EVD; however, a range of potential treatments and vaccines are being evaluated.[14] The development of a diagnostic device that allows differentiating Ebola disease when the early symptoms appear from other fever related diseases, attends to prioritization criteria 2 and 4.

As previously stated, nowadays there are few POC nucleic acid tests (NAT) to diagnose infectious diseases like those described; however, new technological advances are enabling PCR to be used for POC diagnostic devices. Thus, since the development of the first PCR, there has been ongoing research in the area to miniaturize conventional thermocyclers, allowing for faster amplification, lower fabrication costs, reduction of sample and reagents required, higher portability, and easier integration.[17] These advances are enabling PCR to be used as a POC diagnostic device.

Most nucleic acid assays are based on selective amplification of target nucleic acid sequence through specific *in vitro* enzymatic reactions.[18] Polymerase chain reaction (PCR), invented in 1986, is the preferred method due to its simplicity, well understood methodology, extensively validated standard operating procedure, and availability of reagents and equipment.[19] PCR is based on thermal cycling and generally involves three basic steps: denaturation, annealing, and extension. During the denaturation step, a double-stranded DNA molecule is separated into two single-strands by a heat separation conducted at approximately 95 °C. The annealing step takes place at approximately 55–65 °C during which two oligonucleotide primers (approximately 20 nucleotides) which flank the target sequence, bind in a complementary fashion to the two single strands (annealing). Afterwards, the temperature is increased to approximately 72 °C, at which a DNA polymerase extends the primers (successive additions of deoxy-nucleotide triphosphates dNTPs). At the end of each thermal cycle, the amount of target sequence doubles. Multiple thermal cycles increase the target sequences exponentially.[18]

Most commonly, PCR is performed in a stationary chamber and the temperature of the surrounding reaction chamber is cycled between two or three different temperatures.[20] The first PCR chip, developed in 1993, was based on stationary chamber.[21] However, in 1998, a flow-through PCR chip was developed which utilizes fixed temperatures zones and flows the PCR solution between the heated areas in a cyclic manner.[22] With this design, the device does not have to be heated and cooled and this facilitates faster cycling, and as a consequence, faster PCR. This design also allows higher flexibility to change the reaction rate, reduces the possibility of cross-contamination allowing for very specific amplification, and faci-

litates the integration to other systems.[17,20] Within flow-through PCR, three main design types are usually distinguished: serpentine rectangular channels, circular arrangement of temperature zones, and single straight capillary.[20] A schematic figure of these designs is presented in Figure 4.1.
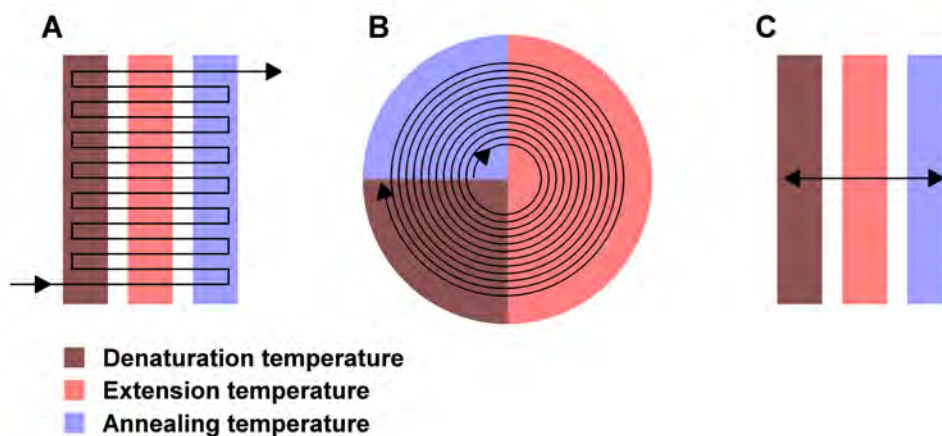
Figure 4.1: Design types of continuous-flow PCR. A) Serpentine channel continuous-flow PCR. B) Spiral channel-based continuous-flow PCR. The sample is introduced at the inlet and pumped unidirectionally towards the outlet. C) Straight channel oscillatory-flow PCR. The sample is introduced in the inlet and pumped back and forth in a straight channel. Temperature zones are provided by three heaters.[23]

In order to achieve rapid heat transfer with any of the PCR designs, the chip substrate material plays a key role. Additionally, the selection of substrate material to create the chip device is also crucial to determine the chip cost, ease of fabrication, disposability, biocompatibility, optical transparence, etc.[20] Much research on chip materials has been conducted over the years. Although no single material is ideal, currently polymeric materials are considered the preferred and most promising option.[17,20]

The success of the amplification can be either detected at the end of the PCR (end-point PCR) or while the amplification takes place (real-time PCR). Real-time PCR allows for fine quantification of the initial DNA template or pathogen load, is faster, more sensitive, and avoids post-sample processing;[20,24,25] however, as expected, it is a more expensive technique than end-point detection. The sensing protocol basically involves the use of reporters or labels that emit a signal when the binding event takes place. The reporters can be of various natures, such as optical, electrochemical, and microgravimetric (mass-sensitive).[18] Among them,

optical methods, and particularly fluorescence-based techniques are the most popular due to the high sensitivity, high selectivity, and commercial availability (and therefore reduced costs) of fluorophores.[18]

While both individual technologies of real-time PCR and continuous-flow PCR have been in use for some time, to the best of our knowledge, there are no continuous-flow quantitative PCR systems available in the market. A possible reason for the absence in the market of these types of devices is that newly proposed devices in the literature are not typically designed with the ultimate production and distribution goal of the device in mind. A standard approach to developing new diagnostic devices is to optimize all features for detection of the disease state without much thought being given to materials used or available industrial-scale manufacturing methods. A severe shortcoming of this approach is that while the device 'works', introduction to the market is often significantly delayed or is prevented altogether because the device cannot be translated to the industrial scale. Thus, many promising diagnostics are stuck in the 'R&D' phase indefinitely.

As previously described in Chapter 2, a 'holistic approach' to POC device design is one in which considerable attention is given to the end goal of introduction to the market by selection of materials and designs that can be used in industrial-scale manufacturing processes. The biology and laboratory work is optimized within the context and constraints of those initial design and material choices. Thus, translation to the market at the end of development is greatly facilitated.

In this context, we present here such a holistic approach to the development of a portable and low-cost POC real-time fluorescence-based continuous-flow PCR system. The system is based on a disposable serpentine channel chip designed for economic manufacture by roll-to-roll methods which would allow for scale-up to industrial-level production. We describe the system design and the chip prototype and production. We specifically discarded designs that had low potential for translation to the industrial scale. The system could be applied to the diagnosis of any DNA pathogen and it was here tested with three infectious pathogens, *C. trachomatis* L2, *E. coli* O157:H7 and Ebola Zaire virus.

4.2 Materials and Methods

4.2.1 Chip design, manufacture, and bonding

Table 4.1: Reagents, equipment, and software for chip design, manufacturing, and bonding.

Name	Reference	Vendor
Reagents		
Chip blank	Zeonex COP690R, 2 mm	Zeon Chemicals L.P.
Chip blank	Zeonex 690R, 0.25 mm	Plitek LLC
Chip cover slip	ZF14–188, 0.185 mm	Zeon Chemicals L.P.
Decahydronaphthalene	D251	Sigma-Aldrich
Ethanol	187380	Sigma-Aldrich
Equipment		
Hydraulic hot press	In-house	Fraunhofer CMI
Milling machine	UPM 0005	Fraunhofer IPT
Oven	IsoTemp Oven 851F	Thermo Fisher Scientifc
Profilometer	Conturograph CV200	Mahr GmbH
Laser cutting machine	Zing 16	Epilog Laser
Ultrasonic cleaner	1510–DTH	Branson Ultrasonics
Plasma Treatment System	PS 0500	Plasma Tech. Systems
Drop Shape Analyzer	DSA 100	KRÜSS GmbH
Software		
Pro/ENGINEER Wildfire	3.0	Parametric Tech. Corp.

Several chips with different characteristics were designed and fabricated during this thesis. All chips were designed in-house using the CAD program Pro/ ENGI-NEER Wildfire 3.0. Chips were fabricated in-house using either an ultra-precision milling machine or by hot embossing as described.

Chip manufacture

Chip milling Blank chips were machined according to the desired design using an ultra-precision milling machine. Once the chips were completed, the chip lubricant was cleaned off using soap and the burrs were removed. Chips were then rinsed with water and stored.

Chip embossing   Embossing is the process by which a metal mold containing the negative image of the device's desired features is pressed into the final device material. Negative molds were produced in-house using an ultra-precision milling machine according to the requested design. A Fraunhofer CMI custom-made hydraulic hot press was used to press the chip blank with the mold. The mold and chip blank were placed between aluminum platens and stainless steel sheets and shims. They were stacked inside the hot press as shown in Figure 4.2 and pressed under vacuum at high temperature and pressure conditions. The specific temperature and pressure conditions were improved over the course of this work and are described in the Improvement section (Section 4.4.1). In Figure 4.3 pictures of the hydraulic hot press and a chip mold are shown.
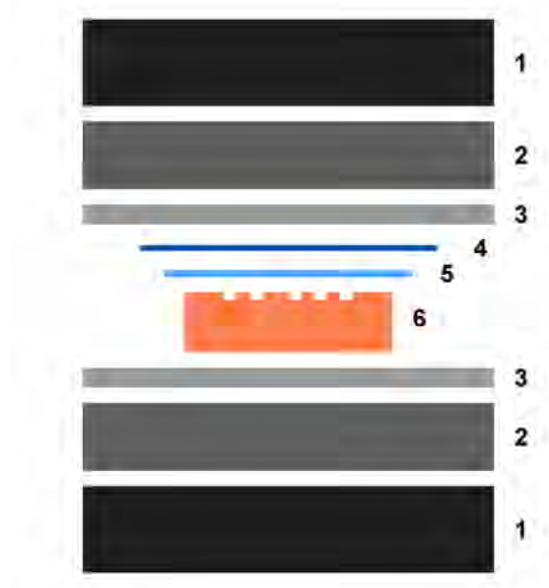
Figure 4.2: Disposition of platens and shims for hot embossing technique. 1, 2) Aluminum platens. 3) Stainless steel sheet. 4) Stainless steel shim. 5) Chip substrate material. 6) Embossing mold.

Once the hot embossing process was completed, inlet and outlet holes were carefully drilled using a screwdriver since they were not fully drilled from the embossing process. Afterwards, chips were cleaned off using soap and then rinsed with water. Chips were dried inside the oven and stored.
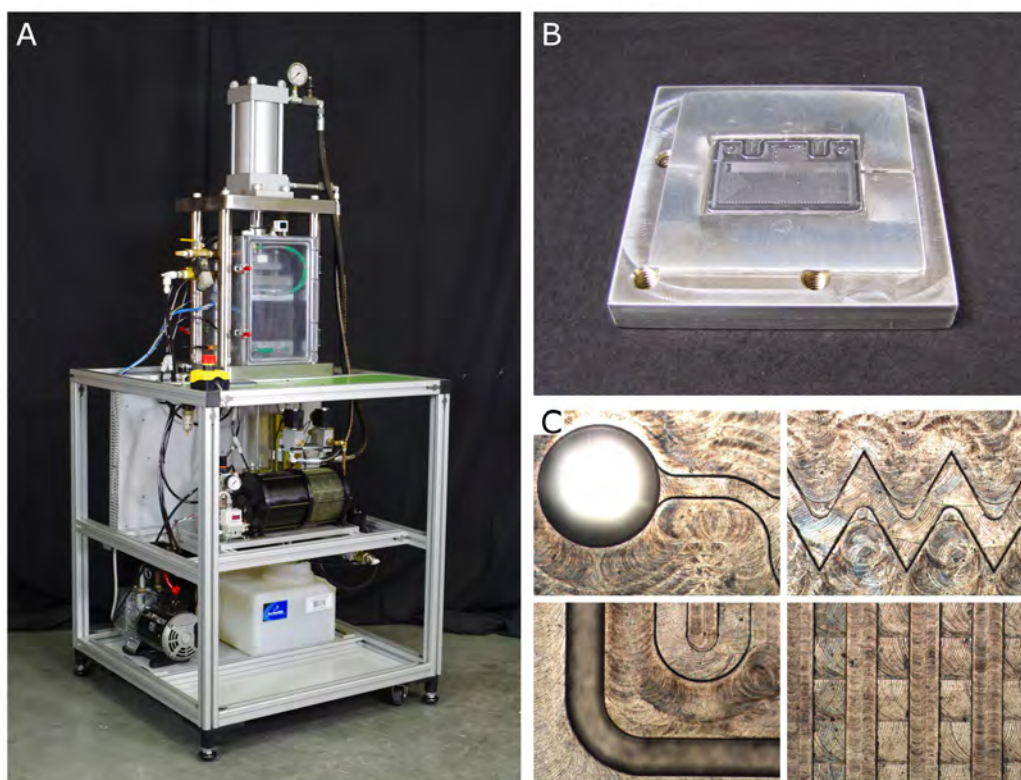
Figure 4.3: Pictures of CMI hot-press and hot embossing PCR mold. A) Picture of CMI custom-made hydraulic hot press. B) Picture of the PCR chip mold used for hot embossing. C) Close view of some features of the PCR chip mold.

Chip bonding

In order to seal the channels, chips were bonded with a cover slip from the same material. Two types of bonding procedures were performed: solvent-assisted bonding and plasma bonding.

Solvent-assisted bonding The surface of the chips and the cover slips were activated for the bonding process. The surface activation steps were performed inside the fume hood using two closed stainless steel containers to avoid evaporation of the chemicals and prevent variations in the chemical composition. The first container was filled with a mixture of decahydronaphthalene:ethanol (35:65 %(v/v)) and the second container with ethanol. Using tweezers, the microstructured chip was placed in the decahydronaphthalene:ethanol mixture container and gently agitated for a specific time period between 30–60 s. Then, the chip was introduced in the ethanol container and agitated constantly for 2 min. Afterwards the chip was dried using compressed air. The same procedure was repeated with the cover slip

with the side to be bonded to the chip facing up. The time inside the decahydro-naphthalene:ethanol mixture container was optimized over the course of this work and is discussed in detail in Section 4.4.1. Briefly, longer times result in stronger bonding while shorter times result in weaker bonding. After the surface of both chip and cover slip was activated, they were pressed together using the Fraunhofer CMI hydraulic hot press. The chip and cover slip were placed inside the hot press between aluminum platens, and stainless steel shims and sheets stacked as shown in Figure 4.4. Chips were hot pressed at 130 °C and 3.93 MPa for 2 min.

Figure 4.4: Arrangement of platens and shims for thermal bonding. 1, 2) Aluminum platens. 3) Stainless steel sheets. 4) Stainless steel shim. 5) Chip. 6) Chip cover slip.

Plasma bonding   A low-pressure Plasma Surface Treatment System Model PS 0500 was used. Chips and cover slips were placed inside the vacuum chamber with the sides to be bonded together facing up. The plasma treatment system was programmed with the desired parameters. Plasma parameters were varied and improved during this thesis and are discussed in detail in the Improvements section. After surface activation, the cover slip was placed on top of the chip, with their activated sides against each other, and were pressed using the Fraunhofer CMI custom-made hydraulic hot press at 130 °C and 3.93 MPa for 2 min.

Annealing step An annealing step after either solvent or plasma-assisted thermal bonding was always performed. Chips were placed inside an oven and the annealing step consisted of a temperature increase of 0.5 °C/min until 125 °C was reached, then the temperature was held at 125 °C for 15 h, and afterwards a temperature decrease of 0.5 °C/min took place until room temperature was reached.

4.2.2   Design and description of the chip surrounding instrumentation

Table 4.2: Reagents, equipment, and software for chip surrounding instrumentation.

Name	Reference	Vendor
Reagents		
FAM	C1359	Thermo Fisher Scientific
Equipment		
Microfluidic connector	3000024	Dolomite Microfluidics
Syringe pump	RS232	KDScientific Inc.
Cartridge Heaters	FIREROD	Watlow
Temperature controller	CN77523	OMEGA Engineering
Thermocouples		
Dichroic mirror	25x35mm	Edmund Optics
Emission filter	65-699	Edmund Optics
Excitation LED light (470 nm)	M470L2	ThorLabs
Excitation LED light (490 nm)	M490L3	ThorLabs
Camera	UI-1480-C	IDS GmbH
Camera	UI-3240CP-M	1st Vision
10x microscope objective	46–144	Edmund Optics
FITC fluorescence filter set	MDF-FITC	ThorLabs
Femtowatt photodetector		Newport Corp.
30/70–beamsplitter, 25 mm^2	MDF-FITC	ThorLabs
Filter cube for detection	56-264	Edmund Optics
Filter cube for excitation	56-264	Edmund Optics
Optical meter	1835-C	Newport Corp.
Software		
ImageJ		NIH

The system was designed around a microfluidic chip with fluidic, thermal, and optical interfaces. A schematic drawing of the system is presented in Figure 4.5. The nucleic acid sample and other PCR reagents were introduced to the chip using a syringe pump. A microfluidic connector was used between inlet and outlet tubes and the microfluidic chip to facilitate easy loading of the chip. Heaters below the chip control the chip temperature in the different zones. Each heater consisted of an aluminum heat block, a Watlow FireRod cartridge heater, a thermocouple, and a programmable temperature controller. Heaters were thermally isolated from each other and the rest of the setup by a ceramic baseplate which has low thermal conductivity.
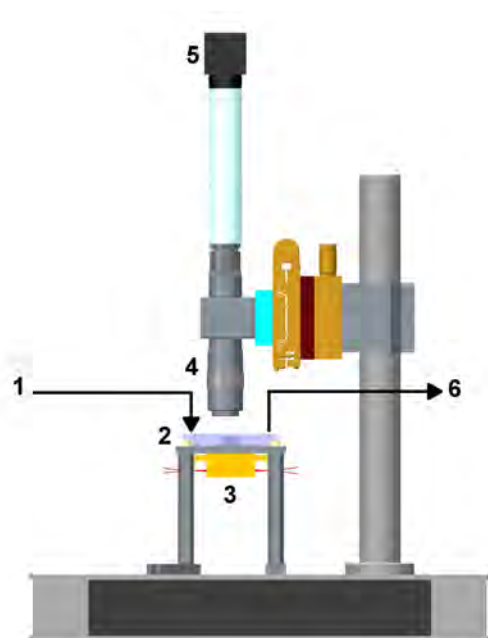
Figure 4.5: Schematic drawing of the instrumentation surrounding the PCR chip. 1) Chip input port connected to a syringe pump. 2) Chip. 3) Heaters. 4) Microscope objective. 5) Camera. 6) Chip output port.

Fluorescein amidite (FAM) probes were used as fluorescent reporters of the amplicons generated during the PCR. Fluorescence was excited by a 490 nm LED source through the standard microscope fluorescein isothiocyanate (FITC) fluorescence filter set with excitation centered at 475 nm and emission centered at 530 nm. The excitation light was focused onto the sample using a 10x microscope objective. Fluorescence generated by the sample was collected through the same microscope objective into the tube lens assembly. The image of the sample fluo-

rescence was formed 200 mm from the back surface of the lens. Collected light was directed to the optical detector/measuring system which was modified during this thesis and more details are provided in the Improvements section (Section 4.4.2). A charge-coupled device (CCD) camera was placed into the sample image plane. During the experiment, the real-time CCD image of the sample was generated with a broadband illumination source placed underneath the sample. The image was used to pre-align the target channel. Further information about the optical system improvements can be found in Section 4.4.2.

4.2.3   PCR reagents and protocol

PCR Reagents

Table 4.3: Reagents, equipment, and software for the preparation of the PCR reagents

Name	Reference	Vendor
Reagents		
Genomic DNA *E. coli* O157:H7	0801622DNA-10UG	ZeptoMetrix
PCR kit for *E. coli*	Path-e.coli-0157-std	PrimerDesign
E. coli IDT primer/probe set 1		
Forward primer	ATGT CAGA GGGA TAGA TCCA	IDT
Reverse primer	TATA GCTA CTGT CACC AGAC AAT	IDT
Probe	CGCT TTGC TGAT TTTT CACA TGTT ACC	IDT
E. coli IDT primer/probe set 2		
Forward primer	TGTC CGTA ACAT CCTG TGTA TC	IDT
Reverse primer	CAAA GAGA GCTG CAAC CTTA AC	IDT
Probe	TCAA GTAG TCGC ATGA GATC TGAC CAGA	IDT
USB VeriQuest® Fast Probe qPCR Master Mix	75680	Affymetrix
C. trachomatis bacteria		Kindly provided by Dr. Michael N. Starnbach
		Continued on next page

Table 4.3 – continued from previous page

Name	Reference	Vendor
Genomic DNA purification kit	51104	Qiagen
C. trachomatis primer/probe set		
Forward primer	GGAG GCTG CAGT CGAG AATC T	IDT
Reverse primer	TTAC AACC CTAG AGCC TTCA TCACA	IDT
Probe	TCGT CAGA CTTC CGTC CATT GCGA	IDT
pcDNA3.1(+) plasmid with target EBOV sequence		Genscript
Competent cells	C2988J	New England Biolabs
Plasmid DNA purification kit	27104	Qiagen
Restriction enz. SmaI	R0141S	New England Biolabs
Restriction enz. NdeI	R0111S	New England Biolabs
Restriction enz. XhoI	R0146S	New England Biolabs
Restriction enz. buffer	CutSmart® Buffer	New England Biolabs
Gel extraction kit	28704	Qiagen
In vitro transcription kit	AM1333	Thermo Fisher Scientific
Purification kit for *in vitro* transcribed RNA	AM1908	Thermo Fisher Scientific
EBOV IDT primer/probe set		
Forward primer	GTCC GTCG TTCC AGTC ATTT	IDT
Reverse primer	CCCT CTTG GATG CTGA GTTA TG	IDT
Probe	TAAG TGAC TCTG CTTG CGGT ACAG C	IDT
DNA Decontamination	AM9890	Thermo Fisher Scientific
RNase Decontamination	10328011	Thermo Fisher Scientific
BSA Blocker™	37525	Thermo Fisher Scientific
PEG 8000	V3011	Promega Corp.
96 well PCR plate	N8010560	Thermo Fisher Scientific
Adhesive Film for PCR plate	4311971	Thermo Fisher Scientific
DNA Ladder	N04745	New England Biolabs
SYBR® Green Nucleic Acid Stain	50513	Lonza
6 % TBE Gels 10 Well	EC6265BOX	Thermo Fisher Scientific
6 % TBE Gels 15 Well	EC62655BOX	Thermo Fisher Scientific
TBE Sample Buffer	LC6678	Thermo Fisher Scientific

Table 4.3 – continued from previous page

Name	Reference	Vendor
Equipment		
qPCR thermal cycler	AB 7500	Thermo Fisher Scientific
Spectrophotometer	NanoDrop Lite	Thermo Fisher Scientific
Rotary shaker	Maxi Rotator	Lab Line Instruments
Electrophoresis chamber	XCell SureLock$^{\text{TM}}$	Thermo Fisher Scientific
Power source	93000-744	VWR International
Blue Light Transilluminator	Safe Imager$^{\text{TM}}$2.0	Thermo Fisher Scientific
Software		
GraphPad Prism	Version 6.07	GraphPad Software

The performance of the PCR and RT-PCR systems were evaluated with *C. trachomatis*, *E. coli*, and Ebola virus (EBOV). Next is described the materials and methods followed for the preparation of the DNA and RNA pathogenic templates and for on-chip and off-chip PCR and RT-PCR.

***C. trachomatis* genomic DNA and primer/probe sets.** *C. trachomatis* genomic DNA was isolated and purified from *C. trachomatis* bacteria using Qiagen kit 51104 following a protocol for isolation of genomic DNA. The purified DNA concentration was measured with NanoDrop Lite Spectrophotometer and diluted to the desired concentration. The number of DNA copies of the target sequence per volume of stock solution (C_s) was calculated using Equation 4.1 and based on the measured concentration (m), and the length of *C. trachomatis* strain L2 (L_s) (1038842 bp, NCBI GenBank database).[26] A molar mass per base pair (M_{bp}) of 660 (g/mol)/bp was used. The primers/probes were designed to amplify a 85 bp long segment of the 16S RNA gene and were custom-made by Integrated DNA Technologies (IDT); their sequences are shown in Table 4.2.

$$C_s = \frac{N_{Av} \cdot m}{L_s \cdot M_{bp}} \tag{4.1}$$

where C_s is the copies of target sequence per volume of stock solution, N_{Av} is Avogadro's number, m is the spectrophotometrically measured concentration, L_s is the target sequence lenght, and M_{bp} is the molar mass per base pair.

***E. coli* genomic DNA and primer/probe sets.** Genomic DNA *E. coli* O157:H7 strain EDL933 was used as target. The DNA concentration in the stock solution was measured using NanoDrop Lite Spectrophotometer and diluted to the desired concentration as indicated. The number of DNA copies of the target sequence per volume of stock solution was calculated using Equation 4.1 and based on the measured concentration, and the length of *E. coli* O157:H7 EDL933 (5528445 bp, NCBI GenBank database).[26] A molar mass per base pair of 660 (g/mol)/bp was used. Three primer/probe sets for *E. coli* 0157:H7 were tested. The first set of primer/probe was designed and purchased from Primer Design. The primers/probe sequences were not provided. The amplicon generated during PCR was 76 bp long and the predicted T_m was 71.5 °C. The two other primer/probe sets were purchased from Integrated DNA Technologies (IDT). Both sets were targeted against the virulence gene STX1A. The primer/probe sequences for both IDT sets are specified in Table 4.2; the amplicon size for set 1 and 2 are 69 bp and 99 bp respectively. Bovine serum albumin (BSA) (Thermo Fisher Scientific Inc., Waltham, MA) at a final concentration of 0.05 %(w/v) was added to VeriQuest® Fast Probe qPCR Master Mix at a final concentration of 1x for both *C. trachomatis* and *E. coli* O157:H7 amplification.

EBOV RNA and primer/probe sets. A pcDNA3.1(+) plasmid vector containing a target region of EBOV L gene was designed in-house from Makona variant EBOV sequences (2014 EBOV outbreak) and was purchased from Genscript®. The L gene was selected as the target since it codes for the well-conserved RNA-dependent RNA polymerase.[23,24] Competent bacteria 5-alpha *E. coli* cells were transformed with the plasmid of interest for plasmid banking and replication purposes. Bacteria containing the target plasmid were selected by exposure to ampicillin antibiotic. The plasmid containing the L gene fragment was isolated and purified using Qiagen kit 27104. The plasmid was then linearized using the restriction enzyme SmaI and subsequently double digested using the restriction enzymes NdeI and XhoI. The cloned L gene fragment was digested and gel purified to provide clean template for RNA *in vitro* transcription using the MEGAscript *in vitro* transcription kit AM1333 and MEGAclear kit AM1908 respectively. The primers/probe were designed to amplify a 120 bp long segment of the L RNA

gene and were custom-made by Integrated DNA Technologies; their sequences are presented in Table 4.2.

Two one-step RT-qPCR master mixes were tested. First, the commercial Affymetrix VeriQuest® Probe One-Step qRT-PCR 75700 was used. It is composed of an RT-enzyme and a standard DNA-polymerase and is referenced as 'commercial' master mix. Secondly, a custom made one-step master mix which combines the RT-enzyme from Affymetrix VeriQuest® Probe One-Step qRT-PCR 75700 and the fast DNA-polymerase included in Affymetrix VeriQuest® Fast qPCR Probe 75680 was kindly provided by Affymetrix Inc. and is referenced as 'custom' master mix. Independently of the master mix used, bovine serum albumin (BSA) at a final concentration of 0.05 %(w/v) was added.

Off Chip-PCR protocol

The working area and pipettes were cleaned with DNA and/or RNAse decontamination solutions to avoid DNA and/or RNAse contamination. DNA/RNAse free reaction tubes were used to prepare the PCR solutions. Each PCR reagent was incorporated to the PCR mix according to the desired PCR mix composition. The final volume of each PCR sample was 20 μl. An optical 96 well PCR plate was used and it was sealed with an optical adhesive film. The PCR plate was shortly centrifuged. An Applied Biosystems 7500 PCR system was used for off-chip real-time qPCR. The thermal profile protocol was programmed as required and fluorescence measurements were acquired during the thermal cycling phase automatically.

In the case of *C. trachomatis* and *E. coli* off chip PCR, the thermal protocol consisted in an initial hold of 2 min at 50 °C and a 95 °C hold for 5 min followed by 40 cycles of 95 °C for 3 s and 60 °C for 30 s. For EBOV off chip RT-qPCR different off-chip thermal profile protocols were followed and they are summarized in Table 4.4. For both master mixes, the 'slow' protocol corresponds to the protocol recommended by the manufacturer.

The ratio of fluorescence emission intensity of the reporter dye to the fluorescence emission intensity of the passive reference dye (ΔRn) was provided by the PCR machine. FAM probes were used as reporter dyes. ΔRn was plotted against

Table 4.4: Thermal profile protocol for off chip RT-qPCR.

Name	RT	Polymerase Activation	Thermal Cycling	
Commercial 1 step RT-PCR mix				
Slow	15 min, 50 °C	10 min, 95 °C	15 s, 95 °C	30 s, 60 °C
Mid	5 min, 50 °C	10 min, 95 °C	15 s, 95 °C	30 s, 60 °C
Rapid	5 min, 50 °C	5 min, 95 °C	3 s, 95 °C	30 s, 60 °C
Custom 1 step RT-PCR mix				
Slow	15 min, 50 °C	5 min, 95 °C	3 s, 95 °C	30 s, 60 °C
Rapid	5 min, 50 °C	5 min, 95 °C	3 s, 95 °C	30 s, 60 °C

the PCR cycle. The C_T values of each PCR curve were provided by the PCR program. The C_T value is the fractional cycle number where the fluorescence passes the fixed threshold of the negative control. The threshold was internally determined by the system. C_T values were plotted versus the concentration of template nucleic acid sample on a logarithmic scale. The slope (s) of the linear regression was used to determine the PCR efficiency (η_{PCR}) according to Eq. 4.2.

$$\eta_{PCR} = 100 \ \% \cdot \left(10^{-\frac{1}{s}} - 1\right) \qquad (4.2)$$

On-chip PCR protocol

Previous to performing on-chip PCR, chips were sterilized. Only chips used for the first time did not require a sterilization step. For sterilization, a 10 %(v/v) bleach solution was flushed through the chip channel for 10 min. Sterile DNA free water was then flushed to remove bleach residue from the chip. The chip was then vacuum dried. In some cases, the inner walls of the PCR chip were statically passivated with 1 %(w/v) BSA prior to performing PCR. BSA was flushed through the system and chip channel for approximately 30 min. The effect of static passivation in on-chip PCR performance was studied and further details are described in the Improvement section.

Once the chip was sterile and ready to be used, the PCR mix solution was prepared and the heaters under the chip were turned on. Heaters were switched on approximately 30 min before starting the PCR experiment to assure stable

heating at the desired temperature. The working area and pipettes were cleaned with DNA and/or RNA decontamination solutions to avoid DNA and/or RNA contamination. DNA/RNA free reaction tubes were used to prepare the PCR solutions. Each PCR reagent was incorporated to the PCR mix according to the desired PCR mix composition. The final volume of each PCR sample varied between 70–250 μl; although most PCRs had a 70 μl total volume. Master mix reagents were pre-mixed prior to start the PCR run. The PCR mix was aspirated through a sterile empty microfluidic tube which was connected to a 1 ml syringe filled with approximately 200 μl of DNA/RNA free water. The water inside the syringe allowed for a more constant flow rate of the PCR mix as fluids are less compressible than air. Air inside the microfluidic tube separated the PCR mix from the water that was used for pushing the PCR sample. The tube containing the PCR mix was connected to one of the input ports of the chip through a Dolomite microfluidic connector. The syringe was placed on the syringe pump and the liquid was pumped into the chip. There is also an option of introducing DNA sample and master mix reagents through different input ports and achieving mixing inside the chip. This option was not used for the experiments described in this thesis but was incorporated in the design for future iterations of the assay.

The flow velocity inside the chip was routinely calculated through the course of the PCR by measuring the time that an air bubble or a fluid front traveled through a known distance. The flow rate set in the syringe pump was adjusted as needed such that the flow velocity was as close as possible to the target. The flow velocity was used to determine the residence time inside the chip (the time it takes for a single fluid voxel to travel through the chip). The amplicons generated during the PCR were detected by real-time fluorescence measurement and/or gel electrophoresis depending on the stage of improvements of the optical system. Thus, the method of collection of fluorescence measurements varied depending on the optical system version. Collected fluorescence measurements in most cases were normalized with the average fluorescence values from PCR cycles 4 to 16. However, in some cases, fluorescence measurements were directly plotted against the PCR cycle. A sigmoidal dose-response (variable slope) curve fit was applied to the data using GraphPad Prism version 6.07 for Windows. Error bars are

presented when there are enough data collected from each data point. Error bars represent the standard deviation. The cycle threshold (C_T) value was interpolated from the curve fit at the intersection with a threshold line, which was set at the average baseline signal of channels 4 to 16 plus two times its standard deviation. In order to determine the PCR efficiency, the cycle thresholds were plotted against the logarithm of the initial template concentration and the slope of the linear regression was used in Eq. 4.2.

Amplicon detection by gel electrophoresis. Amplicons generated by either off-chip or on-chip PCR/RT-PCR were examined by gel electrophoresis. A XCell SureLock™electrophoresis chamber was used with 6 % polyacrylamide Tris/ Borate/EDTA buffer (TBE) gels. TBE 1x was used as running buffer. Samples were prepared by adding TBE sample buffer to the PCR samples in a 1:5 %(v/v) proportion. A low molecular weight DNA ladder, with a 25–766 bp range, was used. Samples mixed with TBE sample buffer were loaded to the gel and run at a constant voltage of 125 V for 40 min. The gel was gently agitated in 50 ml of 1x SYBR® Green staining buffer for 25 min for visualization. A blue light transilluminator was used to visualize the nucleic acid bands. Gel pictures were taken with a digital camera.

4.3 System Description and State-of-the-Art of the Technology

This section aims to provide a vision of the state-of-the-art of the technology concerning microfluidic lab-on-a-chip devices, and it is specially focused on continuous-flow and real-time PCR in order to aid the understanding of the design of our system. Continuous-flow microfluidic PCR systems can be divided in two major components: a microfluidic chip and the instrumentation that surrounds it. Additionally, the reagents required for the amplification also play a key role. Thus, this section is subdivided into three main areas: chip, surrounding instrumentation, and reagents.

4.3.1 Chip

Chip designs state-of-the-art

As previously described, within continuous-flow PCR three main design types are usually distinguished: serpentine rectangular channel, circular arrangement of temperature zones, and single straight capillary.[20] A schematic figure of these designs was presented in Figure 4.1. The serpentine rectangular channel is the most common design used in flow-through PCR due to its simplicity.[22,27–30] Some of the designs included outlets at different channels to allow performing thermal cycling a variable amount of cycles.[27] For the circular design, it is acknowledged that PCR channels can consist of either capillary tubes[31,32] or an on-chip annular channel.[20,33,34] The single straight capillary design is very flexible and allows performing variable amounts of cycles.[20,35–37]

Depending on the DNA-polymerase used, PCR is performed in two or three steps and consequently chips incorporate two[29,30,38] or three[37,39] heating areas. On the one hand, three-step PCR performs a denaturation step at 95 °C, then annealing of the primers takes place at approximately 60 °C, and elongation of the DNA strands occur at 72 °C. Two-step cycling polymerases combine the primer annealing and the elongation step at approximately 60 °C. In the case of continuous-flow RT-PCR chips, an extra heating station can be incorporated to the previous PCR designs to allow reverse transcription to take place.[27] Depending on the chip and system design, RT-PCR is performed in one[40,41] or two[27,39] (RT and PCR) separate steps. Additionally, some authors have reported RT-PCR designs which combine stationary RT step with a continuous-flow PCR step.[42]

During this thesis, a serpentine rectangular channel design was selected with two-step thermal cycling for the PCR and RT-PCR chips.

Chip materials state-of-the-art

For microfluidic lab-on-a-chip (LOAC) devices the selection of materials plays a key role. It determines the chip physical properties, the microfabrication technique, and the chip cost. The evolution of materials for LOAC devices reflects the main requirements of the major user of microfluidic technologies: research laboratories

105

and commercialization. In general, research laboratories are concerned about ease of prototyping and reliability of use; while for commercialization purposes, low production costs and reliability in use are the main driving forces.[43]

The most common materials used for biological microfluidic chip fabrication are glass/silicon, elastomers, thermoplastics, thermosets, hydrogels, and paper. In Figure 4.6 it is shown the materials for microfluidic devices versus fabrication cost and usage in commercial and research applications.[43,44]
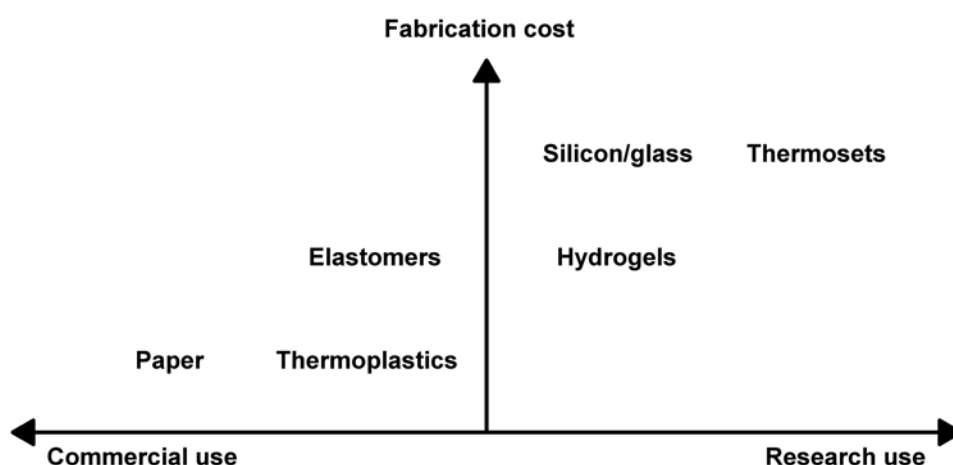
Figure 4.6: Materials for LOAC microfluidic devices versus fabrication cost and usage in commercial and research applications. Figure adapted from Ren et al.[43]

The advantages and disadvantages of the different materials for LOAC are application oriented. For the selection of an appropriate substrate material for on-chip qPCR assays, several requirements should be considered. Firstly, the material should exhibit high heat stability since temperatures up to 95 °C are required during the PCR assay. Secondly, to sensitively measure nucleic acid amplification via fluorescence signals, substrate materials with low-autofluorescence and high optical transparency should be selected. For biological assays that require expensive enzymatic reagents, chemical inertness, and low protein substrate adhesion of the material are important factors. Additionally, for commercialization of a disposable chip, inexpensive substrate materials that can be rapidly manufactured at a low-cost with high reproducibility are preferred. A table with the application oriented advantages and disadvantages of the different materials can be found in Appendix C.[43]

Considering all the requirements for on-chip qPCR, thermoplastics materials stand as the best option as they fulfill most of the requisites. Poly(methyl)-methacrylate (PMMA), polycarbonate (PC), and cyclic olefin polymer and copolymer (COP/COC) are the main thermoplastic materials for used for microfluidic applications. COP/COC present the lowest water absorption (<0.01 % in 24 h) when comparing with other materials. When looking at the glass transition temperature, the glass transition temperature of COC/COP is the highest, it can be up to 180 °C, higher than for other thermoplastic materials. Additionally, the temperatures at which COC/COP deforms under a specified load is high (140/170 °C) and is significantly superior to PMMA or PC. In terms of thermal conductivity, all the different thermoplastic materials have similar low conductivity values, which is highly desirable for PCR chip applications since different temperatures are required at different parts of the chip. Regarding the optical properties, the light transmittance of COP/COC and PMMA is as high as glass (92 %) and the usable transmission range for the three thermoplastic materials is very wide and similar for all of them. Additionally, fluorescence measurements of some commercial thermoplastic polymers were performed and are presented in Section 4.4.1. Due to the advantageous characteristics of COP/COC, this material was selected as substrate for chip production in this thesis. A table with the relevant physical properties of COC/COP, PMMA and PC is provided in Appendix D, in which the properties of Polydimethylsiloxane (PDMS) and glass are also presented for comparison.

Chip production state-of-the-art

Due to the large variety of substrate materials for microfluidic chip applications, numerous manufacturing methods for producing such devices are available.[45] The manufacturing method for lab-on-a-chip (LOAC) devices plays a key role for producing quality, replicable, and especially low-cost chips. During this thesis, special importance was given to the production aspect to assure easy translation to the industrial scale and thus facilitate introduction to the market.

As previously described, thermoplastic polymers allow fast and cheap production. Prototyping can primarily be achieved by direct milling of the positive microstructures. A major drawback of such manufacturing is the significant time

consumption of the setup and machining process. Larger volumes justify the use of replicative manufacturing methods, such as injection molding or embossing, which use complex negative master molds and are characterized by shorter cycle times and higher throughput.[45]

Embossing of thermoplastics is the process by which a metal mold containing the negative image of the devices desired features is pressed into the final device material. Embossing is a preferred technique for nano/micro fabrication as it provides excellent replication accuracy and it is more economic than other micromachining techniques such as injection molding, glass etching, or milling machining.[46] Typical embossing procedures involve either hot embossing[47,48] where the material is heated to a plastic state before applying the mold or by ultraviolet (UV) embossing[49] where the mold is pressed into a semi-solid resin before a final UV cure solidifies the features. For large-scale production, UV embossing is preferred over hot embossing since it can be performed at room temperature at higher speed than hot embossing due to its lower temperature and pressure requirements. A schematic drawing of UV embossing techniques is presented in Figure 4.7.
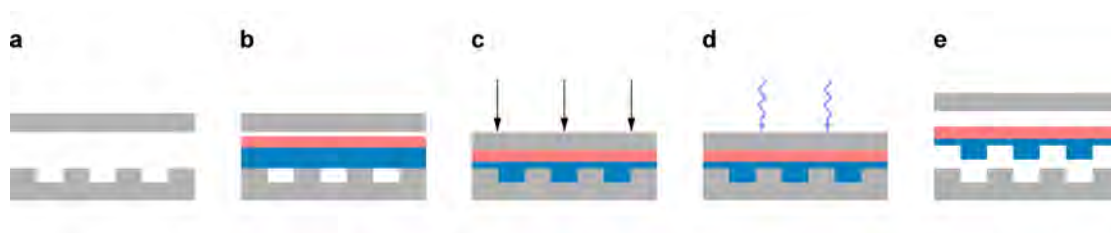
Figure 4.7: Steps for UV embossing technique. a) Mold and cover for UV embossing (shown in grey). b) A semi-solid resin (shown in blue) attached to a polymeric substrate (in pink) is placed between the mold and the cover. c) Pressure is applied to the resin which adopts the mold shape. d) Ultraviolet light is applied to the resin, curing and solidifying it. d) At the end of the process the resin with the mold features is solidified.

However, embossing (either hot or UV) with a flat mold has limited capability for large-scale production as it is difficult to imprint consistently and accurately over a large area with a uniform pressure over the entire surface. Roll-to-roll embossing is a better technique for economic mass production of micro-machined structures as it is a continuous and high-throughput process that can rapidly manufacture large areas at ambient temperatures.[46,50,51] A schematic drawing of a typical roll-to-roll UV embossing system is presented in Figure 4.8.
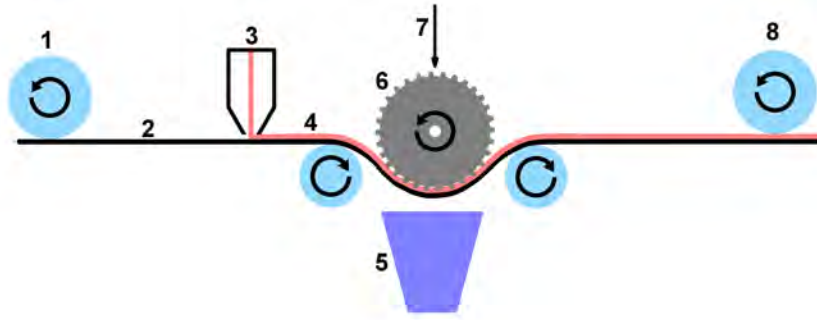
Figure 4.8: Schematic drawing of roll-to-roll ultraviolet (UV) embossing fabrication setup. The numbers indicate the different components of the system. 1) Unwinding module. 2) Polymeric substrate material. 3) Slot die coating unit. 4) Semi-solid resin showed in pink. 5) UV lamp. 6) Embossing mold. 7) Pressure applied to the embossing mold. 8) Rewinding module.

Due to the advantageous characteristics of the embossing technique, and especially ultraviolet roll-to-roll embossing for economical large scale production, this manufacturing technique was selected for chip production in this thesis.

Bonding state-of-the-art

The fabrication of microfluidic chips usually involves a bonding step to seal the microfluidic channels at the microstructured substrate to the non-structured one. The bonding step is a challenging step in which clogging the channels, changing their physical parameters, or altering their dimensions should be avoided.

Gluing is one of the bonding techniques for thermoplastic polymers, commonly used to join two different polymeric parts.[52] However, a common risk of this technique is blockage of the microfluidic channels if the glue layer flows into them. UV adhesives have been used to successfully bond COP parts of a lab-on-a-chip systems.[53,54]

A more frequent technique to bond thermoplastic polymers, such as COP/COC, is thermal bonding. This technique involves heating the substrates to the glass transition temperature (T_g) of the polymers and pressing them together.[54,55] Using this physical bonding technique, the polymer chains in-between the polymeric parts entangle and adhere to each other. An annealing step after the bonding step (in which the pressure is removed but high temperatures are maintained) is

usually performed to release tension due to entangled polymers which results in stronger bonds.

A common variant of this thermal bonding technique is solvent bonding. Solvent bonding method uses a solvent which dissolves the surface of the polymers and enables a better entanglement of the polymer chains, since these become more mobile across the bonding interface.[54] This technique can achieve a higher bond strength at lower temperatures than regular thermal bonding. The time inside the solvent, and the bonding temperature and time are crucial for this process and need to be optimized. As a solvent, decalin:ethanol solution is commonly used. Wallow et al. sealed microfluidic channels which withstood pressures up to 13–16 MPa by immersing COP pieces in a decalin:ethanol solution at room temperature prior to thermal bonding.[54,56] Other solvent mixtures have been used, such as hexadecane and isopropanol.[54,57]

Plasma activation thermal bonding is another technique to increase the bonding strength of standard thermal bonding. Plasma activates and creates radicals on the surface of the polymeric substrates. When plasma-activated substrates are pressed together at high temperatures, the radicals form strong covalent chemical bonds in addition to the physical entanglement of the polymer chain. Plasma activation is probably the most common surface activation method. O_2 plasma has been proven to be more effective than either N_2 or a mix of both gases.[58]

Although there are other techniques for bonding thermoplastic lab-on-a-chip devices, plasma-assisted thermal bonding and solvent bonding are the most common ones and are the ones used and optimized during this thesis.[54]

4.3.2 Surrounding instrumentation

Surrounding instrumentation state-of-the-art

Systems for continuous-flow PCR are usually designed around the microfluidic chip. Heaters, thermal sensors and controllers, and pumps are common elements for most of the systems. The most differentiating features between the systems described in the literature relates to the detection system. Detection can be performed either off-line or on-line. Off-line detection is usually performed by gel

electrophoresis and thus, detection is not integrated to the PCR system.[27,40,41] In this case, post sample processing time should be taken into consideration. On-line detection systems incorporate the detection element into the system. Within the on-line systems, the detection can be performed either at the end of the PCR (end-point detection) or while the PCR takes place (real-time PCR). Probably the most common end-point detection techniques is laser-induced fluorescence (LIF).[32,39] Regarding real-time detection techniques used for PCR microfluidic applications, optical detection and especially fluorescence-based is the most common technique due to its advantageous characteristics in terms of sensitivity, selectivity, and availability.[18] However, other techniques such as electrochemical, or microgravimetric have been used.[18]

As previously anticipated, due to the advantages of real-time fluorescence based detection, the focus of this thesis is in this type of detection. In Figure 4.9, a schematic drawing of a standard continuous-flow and real-time system is shown. The nucleic acid sample (DNA/RNA) with other PCR reagents are introduced to the chip through an inlet port generally by using a microfluidic pump. Below the chip, there are heaters that control the chip temperature in two or three zones. By thermally cycling the sample, the nucleic acids are amplified and detected in real-time via fluorescence measurements. This type of system was used for this work.
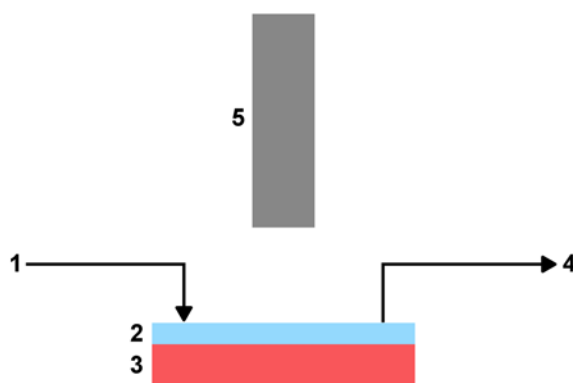

Figure 4.9: Schematic drawing of a standard continuous-flow PCR platform with optical detection. 1) Inlet port to the microfluidic chip. 2) Microfluidic chip. 3) Heaters. 4) Outlet port of the microfluidic chip. 5) Optical detection system.

4.3.3 Reagents

In addition to the sample, the PCR and RT-PCR reaction mixtures involves multiple components with very diverse properties –oligonucleotide primers, dNTPs, enzymes, metal ions, buffers. The optimization of these reagents is crucial for the success of the amplification. Additionally, it should be taken into account that the possibility for one or more of the PCR reaction components to bind to the internal surface is significant, especially for microfluidic devices. Next, the approaches to prevent unspecific binding of the PCR reagents to the chip surface are discussed.

Surface passivation state-of-the-art

The possibility of adverse interactions between the internal surface of a microchip and/or the sample is critical for microdevices in which the surface area/volume ratio is 20-fold or greater than for conventional PCR tubes.[59] Therefore, several passivation procedures for the inner surface of microdevices have been proposed. They are usually classified into static and dynamic passivation. Static passivation consists in pre-coating the inner walls of the microchip prior to the biological process and usually during microchip fabrication. In dynamic passivation, a passivating agent is added to the reaction mix itself to prevent nonspecific surface binding.[59] Common passivation agents for both static and dynamic passivation include proteins and polymers. The inexpensive globular protein bovine serum albumin (BSA) and polymers such as polyethylene glycol (PEG) have been successfully used for microfluidic applications. These substances bind preferentially to the inner surface of the microchip and prevent binding by components of the sample or reagent mixture.[59,60]

Another approach for static passivation and/or addition of an extra functionality is the use of plasma treatment to functionalize the surface. Plasma treatment is a powerful method to efficiently and flexibly functionalize the surface of materials by making nanometer thick films of tailored functional group densities.[61] Although surface functionalization using vacuum plasma is well documented in the literature; there are few studies regarding plasma functionalization in a roll-to-roll process. A corona system, which uses atmospheric plasma, is a more appropriate method for roll-to-roll surface functionalization. In-line slot die coating or direct immersion

in a solution with the target molecule are commonly used to deposit molecules on the corona-activated surface. An approach to generate a surface which prevents the attachment of oligonucleotides or enzymes consists of surface activation using corona treatment to generate radicals on the surface which then are allowed to react with other molecules with hydrophobic/hydrophilic character. By controlling the hydrophobic/hydrophilic character of the surface, it is possible to prevent/control molecules attachment.

During this thesis, the process conditions using dynamic and static passivation techniques including plasma methods were studied.

Summarizing, this section provided an overview of the state-of-the-art of the current technology used for microfluidic lab-on-a-chip applications. The next section is focused on the improvement of the chip, system, and reagents for nucleic acid amplification.

4.4   System Improvement

In this section the development and improvements in the PCR and RT-PCR systems are described. The system was design around a disposable and low-cost chip, which is surrounded by heaters, thermal sensors, and an optical system. As a starting point, a chip and system designed by Fraunhofer Center for Manufacturing Innovation (CMI) were used. Fraunhofer CMI has extensive experience on-chip manufacturing for diagnostic purposes.[62] In September 2012, as part of the international research project Multilayer MicroLab (ML^2) funded by the European Commission within the Seventh Framework Programme, the development of a chip and a system for nucleic acid amplification was initiated. During this thesis, the chip was improved for a more economic chip production and less reagent consumption, the system was enhanced to allow real-time detection with high sensitivity, and different biological reagents were as well tested for faster and more specific nucleic acid amplification for the different target pathogens. This section is subdivided into the three main areas: chip improvements, the surrounding system, and reagent improvements.

4.4.1 Chip improvements

Chips have a long serpentine channel that connects the input to the output ports. They work by introducing the pathogen sample along with nucleic acid reagents into the microfluidic channel that travel first along a 95 °C heated area, where the polymerase is activated and DNA double strands are melted. Afterwards the reagents are thermally cycled between the 95 °C and 62 °C heated areas where annealing, DNA synthesis, and denaturation take place every cycle.

In this section, the optimization of PCR and RT-PCR chips that were designed for amplification of DNA and RNA respectively are described. Chips were optimized in terms of chip dimensions (internal and external), materials, production method, and bonding protocol to seal the channels. The chip optimization was conducted with the chip to amplify DNA and the improvements were later applied to the design and fabrication of the chip for RNA amplification.

Chip generations

Chip features and dimensions were modified through the course of this thesis. Figure 4.10 shows a schematic drawing indicating the different chip elements that were subject to modification through the different chip generations.

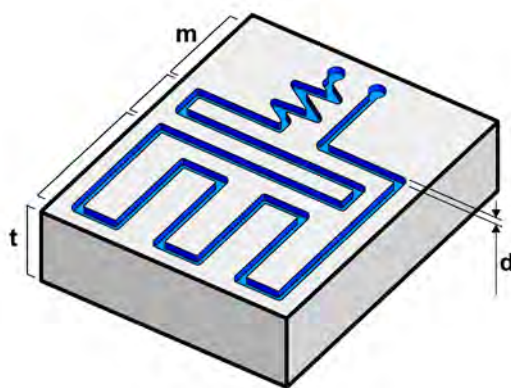Figure 4.10: Chip schematic drawing showing the different chip elements that were subject to modification through the different chip generations. t: chip thickness; m: mixer; d: channel depth.

PCR-chip generation 1 was developed and manufactured by milling machining techniques at Fraunhofer CMI before the start of this thesis. PCR-chip generation 1's outer dimensions are 47.4 mm x 46.0 mm x 2.2 mm. A 1486 mm long and

350 μm deep thin channel connects the two input ports to the output. The total volume of the chip is 135 μl. The channel has two different sections: a 325 mm long activation section and an 1161 mm long thermal cycling section which has 40 repetitive serpentine channels. The chip has one input port and one output port in the top section; both ports are connected to the microfluidic tubes through a manifold homemade at Fraunhofer CMI. With chip generation 1 successful PCR amplification was obtained. Figure 4.11 shows a schematic drawing of the first generation PCR chip with the heaters superimposed and DNA-polymerase activation and thermal cycling zones marked. Additionally, PCR-chip generation 1 is also shown in Figure 4.12A for comparison with the other PCR chip generations.
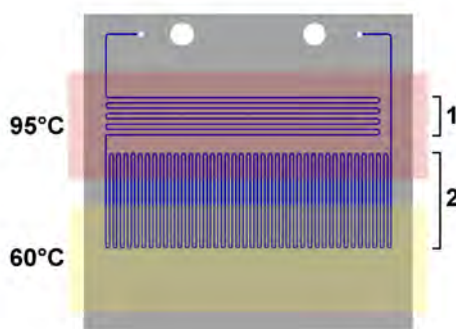
Figure 4.11: A: Schematic drawing of a PCR chip with heaters superimposed. 1) DNA-polymerase activation zone. 2) Thermal cycling zone.

In the case of PCR-chip generation 2, the depth of the chip features was reduced to a mere 50 μm while keeping all other chip dimensions and elements the same. This channel depth reduction was mainly dictated by the requirements in the production methods that will be described later. The reduction in channel depth resulted in a total chip volume of 20 μl instead of 135 μl (see Table 4.6) which allowed lower reagent consumption and thus reduced costs. The reduction of channel depth also had dramatic consequences regarding optical detection, the increase of fluidic resistance, and the modification of the surface/volume ratio which could affect the PCR master mix reagent composition. First, since fluorescence optical measurements were taken from a small section of each PCR cycle, when the channel depth was merely 50 μm, only approximately 50 nl were monitored within the optical field of view, compared to approximately 350 nl for a 350 μm channel depth (a 7-fold volume reduction). Secondly, the decrease of channel depth to
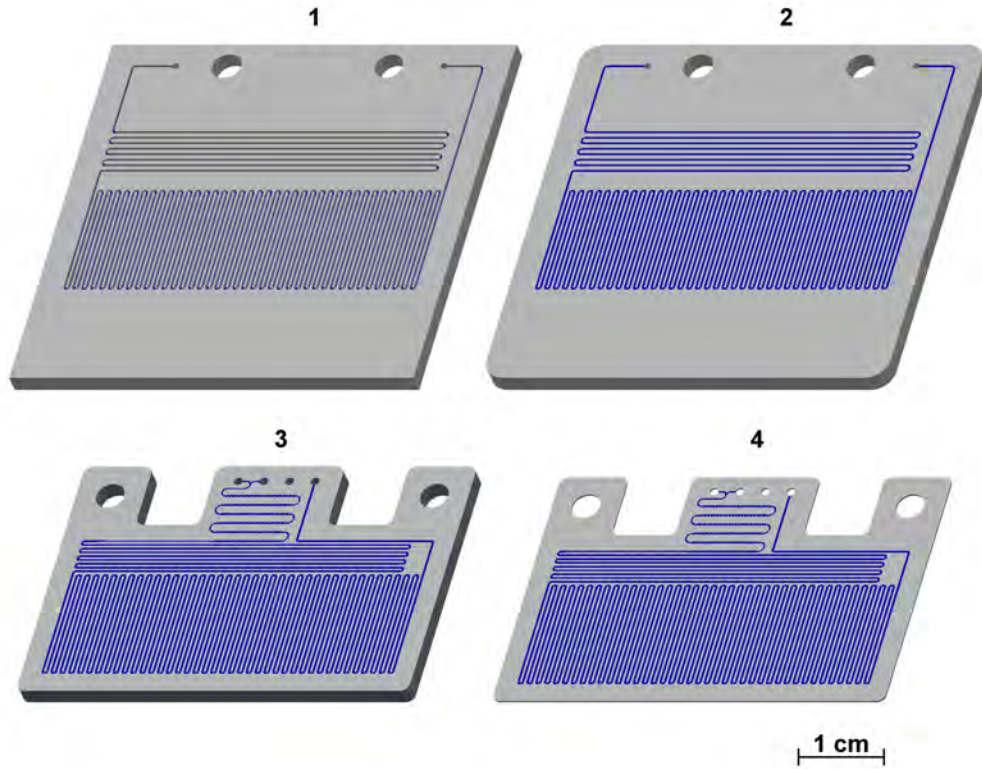
Figure 4.12: PCR-chip generations. 1) 1st PCR-chip generation. The outer dimensions of this chip generation are 47.4 x 46.0 x 2.2 mm, and the chip feature depth is 350 μm. 2) 2nd PCR-chip generation. The outer dimensions of this chip generation are 47.4 x 46.0 x 2.2 mm, and the chip feature depth is 50 μm. 3) 3rd PCR-chip generation. The outer dimensions of this chip generation are 46.0 x 30.9 x 2.2 mm, and the chip feature depth is 50 μm. This chip generation also includes a mixing section. 4) 4th PCR-chip generation. The outer dimensions of this chip generation are 46.0 x 30.9 x 0.4 mm, and the chip feature depth is 50 μm.

50 μm resulted in more than 300 times increase in fluidic resistance, making more challenging achieving a constant flow rate inside the chip and increasing the risk of leakages at the junctions. The fluidic resistances for chip generation 1 and 2 were 1.4 and 488.3 KPa·s/μl and were calculated using Equation 4.3; the viscosity of the fluid was considered equal to 0.89 mPa·s as an average for buffer solutions.

$$R = \frac{12L\mu}{d^3w} \tag{4.3}$$

where R is the flow resistance for a rectangular channel; L is the length of the channel; μ is the viscosity; d is the depth; and w is the width.

Thirdly, due to the modification of the surface/volume ratio, additional experiments were performed to assure adequate master mix reagent composition.

Despite these challenges, since the shallow channel design was necessary for economic industrial scale production, we directed our energies into optimizing our optical system and assay rather than just make deeper channels.

On-chip PCRs with PCR-chips generation 1 and 2 were performed to evaluate if despite the challenges, similar amplification could be obtained with chip generation 2. In Figure 4.13 A and B the gel electrophoresis of on-chip amplification of *E. coli* target amplicon (76 bp) using chip generation 1 and 2 respectively are shown. The composition of the master mix and the initial DNA template was the same in both cases. As can be observed, the amplification with both PCR-chip generations provided comparable successful results.

Figure 4.13: Gel electrophoresis of on-chip *E. coli* O157:H7 amplicons (76 bp) with 10^4 DNA copies/μl initial template concentration. Primer Design primers were used. A) Chip generation 1. Lane L: ladder. Lane 1: On-chip positive control. Off-chip PCR results are shown in Lane 2 (10^4 DNA copies/μl) and Lane 3 (0 DNA copies/μl) for comparison. B) Chip generation 2. Lane L: ladder. Lane 1: On-chip positive control. Lane 2: Off-chip positive control. Lane 3: On-chip negative control (0 DNA copies/μl). Lane 4: Off-chip negative control (0 DNA copies/μl).

A new chip generation 3 was later designed, which incorporated a new inlet port and a new feature: a mixer. The mixing section has large zig-zag turns for achieving optimal mixing; its dimensions are included in Table 4.6. The mixer allows the introduction of DNA sample and master mix through different inlet ports and achieving mixing inside the chip. This option was not used for the experiments described in this thesis but was incorporated in the design for future iterations of the assay. This chip generation was also designed to facilitate the microfluidic connection between the PCR chip and the microfluidic tubes. As previously stated, both chip generation 1 and 2 used an in-house manifold as the connector. However, microfluidic manufacturers are now developing standards for microfluidic connections to facilitate the use of products from different providers.

Dolomite Microfluidics is one of the main microfluidic manufacturers worldwide and PCR chip generation 3 was adapted to fit one of their universal microfluidic connectors. Figure 4.14 A and B show Fraunhofer CMI homemade microfluidic connector manifold and Dolomite microfluidic connector respectively.
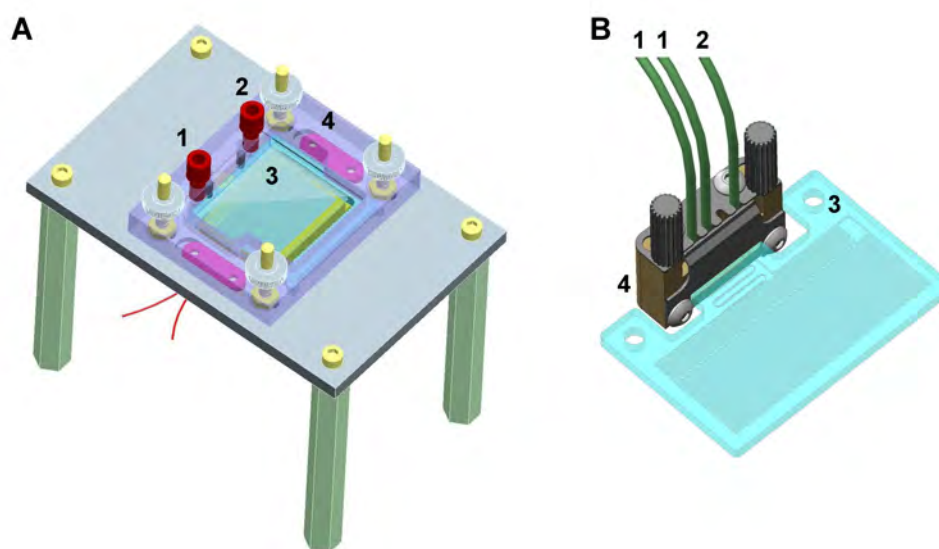
Figure 4.14: Microfluidic connectors between the PCR chip and microfluidic tubes. A) Fraunhofer CMI homemade microfluidic connector manifold. 1) Inlet port. 2) Exit port. 3) PCR chip. 4) Manifold. B) Dolomite microfluidic connector. 1) Entrance port. 2) Outlet port. 3) PCR chip. 4) Manifold.

PCR-chip generation 4 has the same channel dimensions compared with the 3rd chip generation but it has a lower outer thickness. This reduction of the outer thickness was possible due to the use of a different manufacturing method. While chip generations 1, 2, and 3 were produced through milling machining, PCR-chip generation 4 was produced through hot embossing, a preferred technique for industrial scale manufacturing and one step closer to the target of ultraviolet roll-to-roll manufacture. Hot embossing technique allowed microstructuring a thinner substrate (0.2 mm), which was more difficult to achieve when using a milling machine. Thus, this 4th chip generation has a mere 0.4 mm of thickness (see Table 4.5). The use of a thinner substrate reduced the costs of materials and more importantly, improved the sensitivity of the fluorescence measurements. The thinner the substrate, the less background substrate autofluorescence and less

fluorescence dispersion through the substrate. A schematic drawing and picture of the last PCR-chip generation, generation 4, is shown in Figure 4.15.
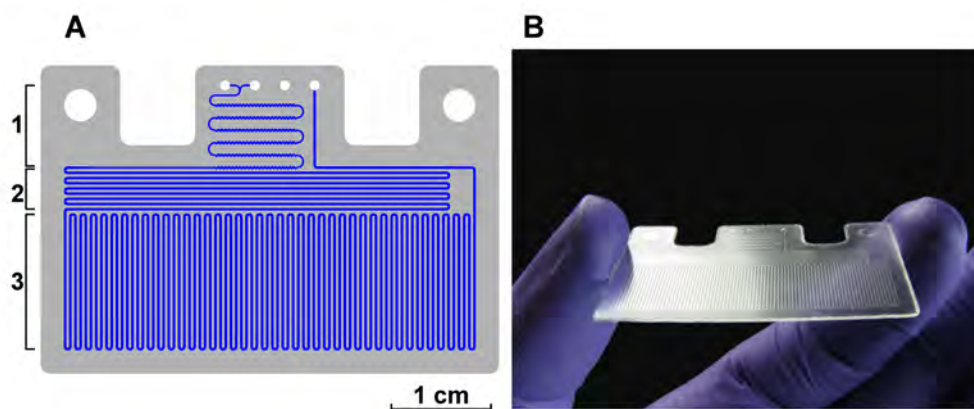
Figure 4.15: 4th generation PCR chip. A) Schematic drawing of 4th generation PCR-chip. 1) Mixing zone. 2) DNA-polymerase activation zone. 3) Thermal cycling zone. B) Picture of the chip.

After the successful fabrication by hot embossing and the amplification results obtained with the 4th generation PCR-chip, new chip designs were proposed to allow the amplification of RNA. In this case, in addition to the functionalities present in the PCR chip, a new 50–55 °C heated area was incorporated to allow reverse transcription (RT) to take place. Two RT-PCR chip designs were proposed.

The 1st RT-PCR chip design (Figure 4.16 1) uses only two heaters and requires to be operated in two steps; the first step is stationary and the second continuous-flow based. During the first step, the RT-PCR master mix is kept stationary at 50–55 °C at the RT section placed at the bottom of the chip using one of the heaters. This section has the same volume as the polymerase activation and thermal cycling section together. Once the RT step is completed, both heaters are set to the temperatures required for thermal cycling. The PCR master mix is pushed in a continuous-flow mode through the polymerase activation section and the thermal cycling section. Both, the polymerase activation and the thermal cycling zones are identical to those present in the 3rd and 4th PCR chip generation. This design presents several disadvantages. First, it prevents a continuous-flow system. Second, it would increase the time to results since after the RT step is completed; the temperature of both heaters need to be increased and approximately 15 min are required to achieve stable temperatures before the RT-PCR can be continued.

Third, only 16.1 μl (the volume of the RT section) of PCR master mix could be amplified each time. As a consequence of all these operational disadvantages, this chip design was discarded before being manufactured.

The 2nd RT-PCR chip design (Figure 4.16 2) includes a third heater. The RT section is placed close to the inlet and outlet ports to avoid deactivation of the RT polymerase when travelling close to the 95 °C area. The length and inner channel dimensions of the RT section are equal to those of the polymerase activation zone. Both, the polymerase activation and the thermal cycling zones are identical to those present in the 3rd and 4th PCR chip generation. This 2nd generation RNA chip was manufactured by hot embossing technique. Schematic drawings of both RT-PCR chip designs are presented in Figure 4.16. In Figure 4.17, a frontal schematic drawing of the 2nd RT-PCR chip and a picture of the chip are shown.
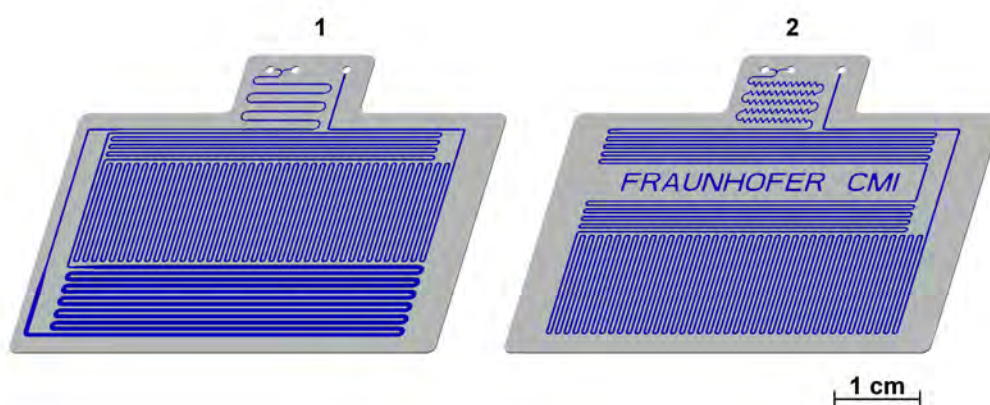
Figure 4.16: Schematic drawing of RNA chip design generations. A) 1st RNA chip generation. B) 2nd RNA chip generation.

A summary of the chip outer dimensions for the different DNA and RNA chip generations is presented in Table 4.5. For the same chips, the dimensions of the inner chip features is shown in Table 4.6.
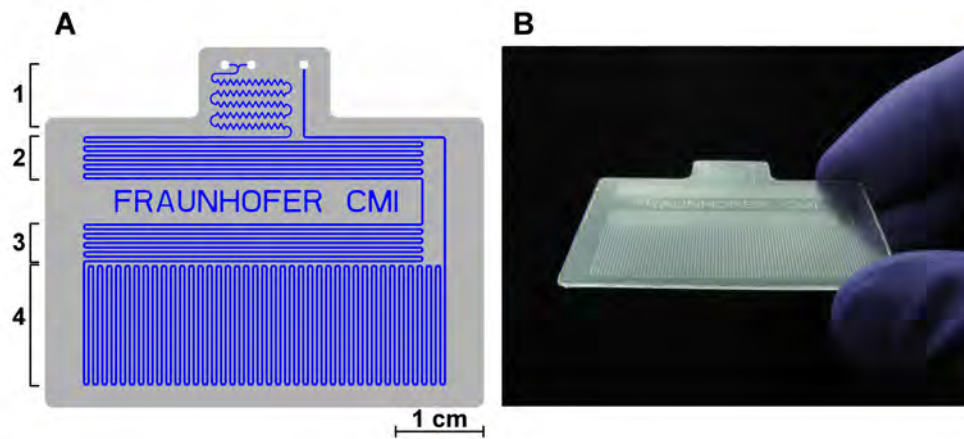
Figure 4.17: 2nd generation RT-PCR chip. A) Schematic drawing of the RT-PCR chip. 1) Mixing zone. 2) Reverse transcription zone. 3) Polymerase activation zone. 4) Thermal cycling zone. B) Picture of the chip.

Table 4.5: Chip outer dimensions for the different DNA and RNA chip generations.

Chip generation	Length (mm)	Width (mm)	Height (mm)
1st & 2nd PCR chip	47.4	46	2.2
3rd PCR chip	46	30.9	2.2
4th PCR chip	46	30.9	0.4
1st & 2nd RT-PCR chip	50	41	0.4

Table 4.6: Inner dimensions of the chip features for the different DNA and RNA chip generations.

Chip section	Length (mm)	Width (mm)	Depth (mm)	Volume (μl)
1st PCR chip generation				
Polymerase activation	325	0.26	0.35	29.6
Cycles	1161	0.26	0.35	105.6
Total	1486			135.2
2nd PCR chip generation				
Polymerase activation	325	0.26	0.05	4.2
Cycles	1161	0.26	0.05	15.1
Total	1486			19.3
3rd and 4th PCR chip generation				
Mixing	80	0.18	0.05	0.7
Polymerase activation	325	0.26	0.05	4.2
Cycles	1161	0.26	0.05	15.1
Total	1566			20
1st RT-PCR chip generation				
Mixing	87	0.18	0.05	0.8
RT section	547	0.59	0.05	16.1
Polymerase activation	329	0.26	0.05	4.3
Cycles	1134	0.26	0.05	14.7
Total	2099			36
2nd RT-PCR chip generation				
Mixing	95	0.18	0.05	0.9
RT section	372	0.26	0.05	4.8
Polymerase activation	354	0.26	0.05	4.6
Cycles	1131	0.26	0.05	14.7
Total	1952			25

Chip materials

In Section 4.3.1, the advantages/disadvantages and the relevant physical properties of the materials commonly used for microfluidic chip applications were described. To complement these physical properties, autofluorescence of several commercial thermoplastic materials was measured. Autofluorescence values were measured using the same settings and optical system as was used during experimental on-chip measurements. The values are presented in Table 4.7. Zeonex 690 R and both PMMA types show low autofluorescence values; however, other materials such as polyethylene terephthalate (PET) or O-carboxyanhydride (OCA) present higher autofluorescence and thus are less desirable for our microfluidic chip application.

Table 4.7: Autofluorescence of several commercial thermoplastics materials. Values taken using the same disposition and optical system as when recording experimental fluorescence on-chip measurements.

Sample	Mean fluorescence (W)
Air	$1.77 \cdot 10^{-11}$
Zeonex 690 R	$2.00 \cdot 10^{-11}$
PMMA 200 μm, Evonik Plexiglas 0F058	$1.78 \cdot 10^{-11}$
PMMA 250 μm, Microsharp	$2.37 \cdot 10^{-11}$
PET 100 μm, HiFi Films PMX17C	$5.76 \cdot 10^{-11}$
PET 50 μm, HiFi Films PMX17C	$4.12 \cdot 10^{-11}$
OCA 50 μm, Tesa 69402	$2.99 \cdot 10^{-11}$
OCA 50 μm, 3M 8172	$3.90 \cdot 10^{-10}$
Polyolefin sealing film 100 μm, HJ-Bioanalytik 900320	$2.14 \cdot 10^{-11}$
PET 140 μm, Novacentrix Novele IJ-220	$8.11 \cdot 10^{-11}$
PET 120 μm, DuPont Tejin Films Melinex STCH11/500	$3.36 \cdot 10^{-11}$

Considering the advantages/disadvantages, the relevant physical properties of the materials commonly used for microfluidic chip applications, together with the requirements for on-chip qPCR, COC/COP was selected as substrate material (see also Section 4.3.1). Specifically, Zeonex, a brand name for COC, was chosen.

Chip production

Chips produced during this thesis were specifically designed to be compatible with roll-to-roll UV embossing production due to its advantageous characteristics for large-scale production as previously described in Section 4.3.1. Due to the requirements of this technique, the depth of the chip features was 50 μm, which is an appropriate depth for the structure to be produced on a roll-to-roll ultraviolet embossing process according to companies in this sector[63,64] and a private communication from Dr. Xin Li from Microsharp Innovation.

Initial chip prototypes were directly machined using a milling machine. Once the prototype was successful, an embossing mold was produced and chips were hot embossed. Most of the experiments presented in the following sections were performed using hot embossed chips. Milled machined and hot embossed chips present very different characteristics. While milled chips have sharp edges and controlling the exact depth is difficult, embossed chips present smother surfaces and chip features are almost identical when using the same mold for several chips. The high chip replicability achieved through embossing is highly important for comparison purposes between PCR runs conducted using different chips. Since the fluorescence optical measurements are taken from a small section of each PCR cycle, differences in channel depth affect the volume, and thus the absolute fluorescence monitored within the optical field. When chips are identical among themselves, differences in fluorescence are only dependent on the success of the PCR run. Figure 4.18 shows the channel depth profile of the measurement of 3 different milled chips and 3 different embossed chips. In all cases the target channel depth was 50 μm. It can be observed how the depth of embossed chips is 50 μm $\pm$ 3 μm; however, in the case of milled chips, they differ in more than 50 μm from the target. Because of the smooth edges, the replicable depth profile, and the low-cost of embossing versus milling, embossing was the selected technique for the manufacture of our microfluidic chips.

The protocol for hot embossing Zeonex was previously studied at Fraunhofer CMI.[65] The procedure consisted in the application of a pressure of 12.6 MPa at 157 °C for 2 min in vacuum conditions. It should be noted that the embossing temperature was 20 degrees above Zeonex 690R glass transition temperature,
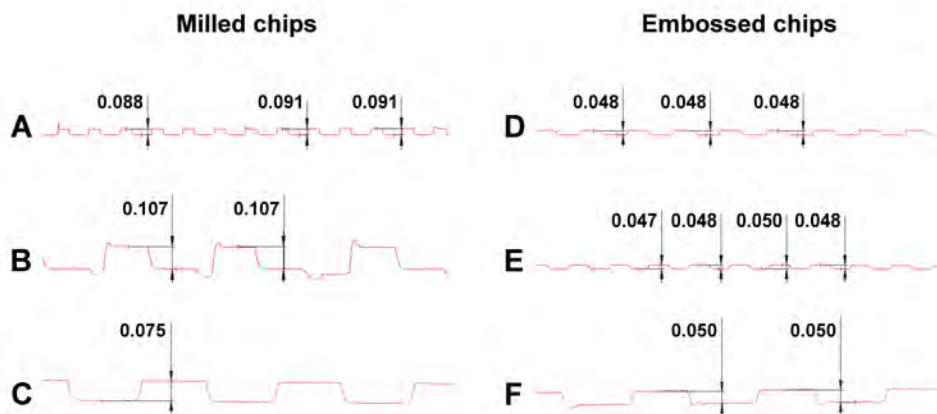
Figure 4.18: Channel depth profile of different milled (A, B, and C) and embossed chips (D, E, and F). Values in mm. In all cases the target channel depth was 50 μm.

136 °C.[66] Nevertheless, this protocol failed to provide successful embossed chips repetitively; in many cases the substrate did not fully fill the mold. As a result the temperature and/or pressure were increased until good Zeonex chip embossing was achieved constantly. 163 °C and 15.73 MPa for 2 min in vacuum conditions provided repetitively sucessful chips (conditions summarized in Table 4.8).

Table 4.8: Hot embossing parameters for Zeonex 690R.

Temperature (°C)	163
Embossing time (min)	2
Pressure (MPa)	15.73
Vacuum	On

The improvement of this protocol allowed for the reliable manufacture of high-quality hot embossed chips. It should be noted that the depth of the chip features (50 μm) and the chip fabrication process –including imprinting, bonding, and cutting steps– were designed to be compatible with ultraviolet roll-to-roll embossing production independently if they were fabricated by milling or hot embossing techniques. Although no chips were produced through roll-to-roll embossing, we anticipate using this technique for our chip manufacture in the near future.

125

Chip bonding

During this thesis, to seal the microfluidic channels, both solvent bonding and plasma-assisted thermal bonding were employed. At Fraunhofer CMI, solvent-assisted bonding was previously used to bond microstructured Zeonex substrates with 350 μm deep channel features. The microstructured part and the unstructured cover were immersed in a decalin:ethanol mixture (35:65 % v/v) for 1 min, followed by 2 min immersion in denatured ethanol to remove excess decalin and then dried with pressurized air. Afterwards, thermal bonding was applied in two steps, the first step was carried at 110 °C and 12.27 MPa for 10 min followed by a second step at 134 °C and 2.67 MPa for 2 min. While these conditions worked successfully with chips with 350 μm deep channel features, when the channel depth was decreased to 50 μm, channels began to clog. The harsh bonding conditions caused an extreme compression of the microfluidic channels and loss of microfluidic functionality. In Figure 4.19 some channel clogs are shown; in Figure 4.19 A and B it can be observed how the channels are dissolved.
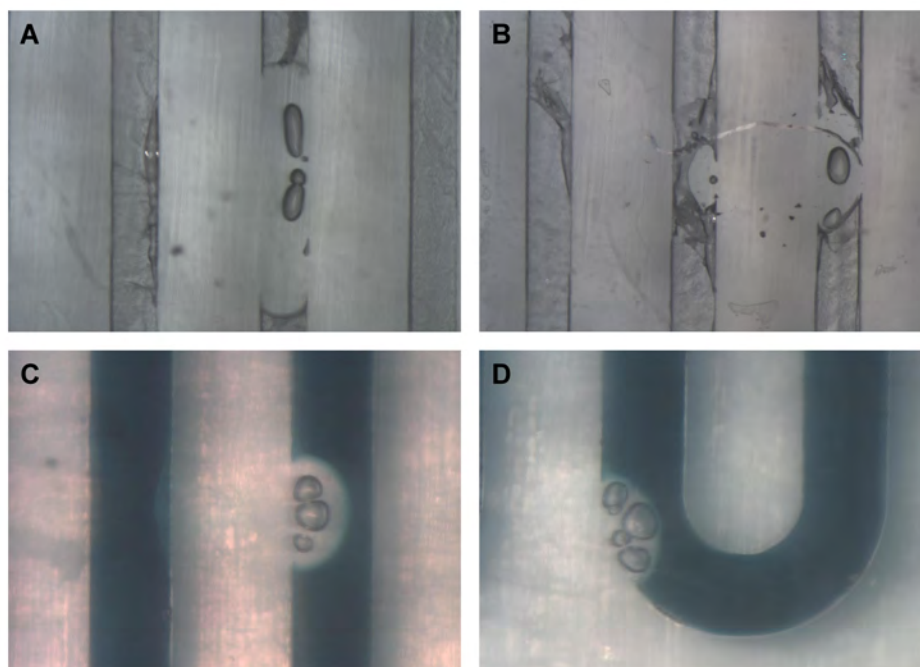

Figure 4.19: Clogged channels from a microfluidic chip with 50 μm chip features.

The protocol for solvent bonding was studied in order to achieve a sufficient and reliable sealing of the microfluidic channels while maintaining, as much as

possible, the channel integrity. In order to solve this problem, different strategies were followed. First, an additional ultrasonic cleaning step was introduced prior to solvent activation to remove any extra material from the channels that could contribute to the clogs. The ultrasonic cleaning step included an initial ultrasonic wash in water with detergent followed by several ultrasonic washes in distilled water. The incorporation of this step reduced clogging, but it did not solve it completely. A second approach was comprised of optimizing bonding temperature/pressure parameters. This optimization was conducted by Philipp Ganser during his master thesis at Fraunhofer CMI.[65] Philipp Ganser considered a wide array of temperature, pressure, and time parameters. In contrast with the two bonding steps previously used, a one-step thermal bonding at 130 °C and 3.93 MPa for 2 min was considered optimal. Thirdly, a reduction in the immersion time of microstructured substrate inside the solvent was attempted. Several combinations of immersion times for the microstructured and the unstructured substrates were tested. 30 s immersion time for both substrates was sufficient to achieve a reliable sealing; lower immersion times resulted in unsuccessful bonding.

Solvent activation of polymeric surfaces is characterized by a significant swelling of the top surface; however, the chemical inertness of the material is persistent. In contrast, plasma-assisted thermal bonding leaves the gross surface topography unaffected but modifies the chemical reactivity of the surface. Plasma-assisted thermal bonding was also studied during this thesis. Different plasma conditions were tested. In all the cases the optimized one-step thermal bonding process was used after surface activation. Plasma machine variables included: power, gas flow rate, process time, and maximum pressure allowed inside the vacuum chamber in order to start the plasma process. Several parameter values were selected for each variable. The testing conditions were: power 10, 50, 100 W; gas flow rate 0.1, 1, 10, 25 cm^3/min at standard temperature and pressure (sccm) of O_2 gas; process time 1, 2, 5, 10 min; base pressure 3.33, 4, 6.67, 13.33 Pa. Combinations of the previous parameter conditions were tested for delamination using samples replicates of each condition. The optimal results were obtained for 1 sccm, 100 W, 2 min process time and 4 Pa of initial base pressure. Higher gas flow rates, increased power, longer process times or lower initial base pressure did not improve the bonding strength.

Additionally, corona treatment was test as a substitute of O_2 plasma activation; however, the bonding strength was lower and chip delamination occurred more frequently.

An annealing step after either solvent bonding or plasma-assisted thermal bonding was always performed (details described in Section 4.2.1). Annealing at high temperatures close to the glass transition temperature of the material enhances the degradation of any residual stresses within the material.

A summary of the optimized bonding protocols for Zeonex substrate is shown in Table 4.9 and Table 4.10 for solvent and plasma activation respectively.

Table 4.9: Solvent activation parametes for Zeonex 690R bonding.

Chip	
Immersion time in decalin/ethanol mix	30 s
Immersion time in ethanol 100 %	2 min
Cover slip	
Immersion time in decalin/ethanol mix	30 s
Immersion time in ethanol 100 %	2 min

Table 4.10: Plasma activation parameters for Zeonex 690R bonding.

Parameters	Values
Power (W)	100
O_2 flow rate (sccm)	10
Process time (min)	2
Base pressure (Pa)	4

4.4.2 Surrounding instrumentation improvements

Temperature on the chip

As previously described, heaters below the chip control the chip temperature in different zones. A programmable temperature controller regulates the temperature on each heater. The temperature in the PCR and RT-PCR chip plays a key role for

successful amplification, especially in the case of the lower temperature heater (50–60 °C) compared to the high temperature one (95 °C). Stable annealing and reverse transcription (in the case of RT-PCR) temperatures are essential for effective PCR performance. However, the denaturing temperature allows higher temperature variations (approximately 90–97 °C) without altering the amplification process.

Verifying the temperature in the area of interest is a difficult task in microfluidic systems without altering the process in a substantial manner. To determine the actual temperature inside the chip for a given heater temperature, a thermal measurement chip was built for a previous chip generation which had the same shape as chip generations 1 and 2. The chip is shown in Figure 4.20, it has equidistant measurement channels located in a similar depth as the PCR microfluidic channel. A thermocouple is embedded in high temperature silicone in every channel. The channels are sealed using a regular cover slip. Six thermocouples measure the temperature in the middle area of the chip while the other six provide temperature values of the outer area of the chip. Thermocouples were read out using a digital thermometer. For different given temperatures, the temperatures of the thermocouples inside the measurement chip were recorded. Approximately, for the 60 °C heater temperature, the temperature inside the chip was 2 °C below; while for a heater temperature of 95 °C, the temperatures inside the chip were in the range 90–92 °C. Given these results, for on-chip experiments, the heaters were set 2 °C above the target temperature. In the case of target temperature of 95 °C inside the chip, heaters were set to 97–98 °C to prevent boiling effects.
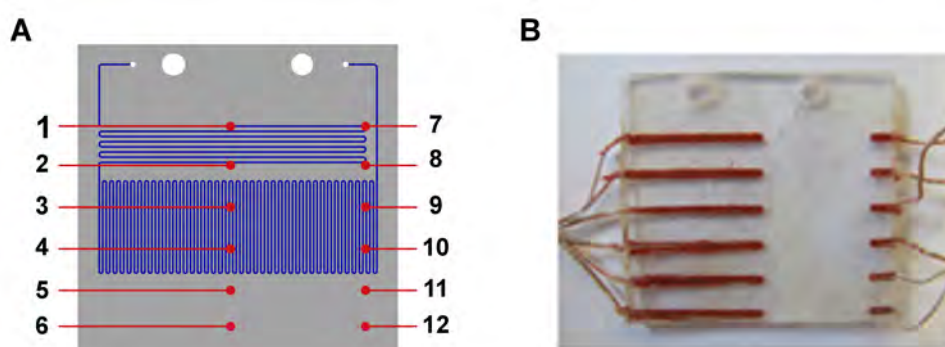

Figure 4.20: Thermal measurement chip with 12 thermocouples. A) Schematic drawing. Numbers 1–6 show the inner thermocuples and 7–12 the outer thermocuples. B) Picture.

Optical system

As previously stated, optical methods are the most common methods to detect amplification products in real-time. Among them, the fluorescence-based technique is the most popular one due to its high sensitivity, high selectivity, and commercial availability of fluorophores.[18] Commercial real-time PCR machines monitor fluorescence in approximately a total volume of 20 μl; however, for on-chip-PCRs, only a small section of each PCR cycle was monitored. As previously described, for the chip generations with 50 μm channel depth (PCR chip generations 2, 3, 4 and both RT-PCR chip generations) the approximate monitored volume within the optical field of view was a scant 50 nl. In the case of the 1st PCR chip, the monitored volume was 350 nl due to its higher channel depth (350 μm).

Fraunhofer CMI developed an optical detection system previous to the start of this PhD thesis. The system was composed of a light-emitting diode (LED) source which excited fluorescence through a standard microscope FITC fluorescence excitation and emission filter set. The excitation light was directed to the sample and the fluorescence generated by the sample was collected and directed to a charge-coupled device (CCD) camera placed into the sample image plane. Photo images were taken with the camera, which were latter analyzed using Image J program. Unfortunately, this system was not sensitive enough for monitoring on-chip amplification, and post sample processing through gel electrophoresis was required to determine the success of the amplification. A schematic drawing of the optical system and a CAD drawing are shown in Figure 4.21 A and B respectively.

In order to increase the sensitivity of the system, a photodetector was incorporated. Collected light was split into two detection paths using a broadband beam splitter with 30/70 intensity split ratio. In the first detection path, a CCD camera was placed into the sample image plane. In the second detection path, a photodetector surface to maximize intensity response was located. The changes in the photodetector current were measured using an optical power meter. The camera was used to pre-align the target channel onto the opening in the second detection path. A schematic drawing of the optical system and a CAD drawing are shown in Figure 4.22 A and B respectively.
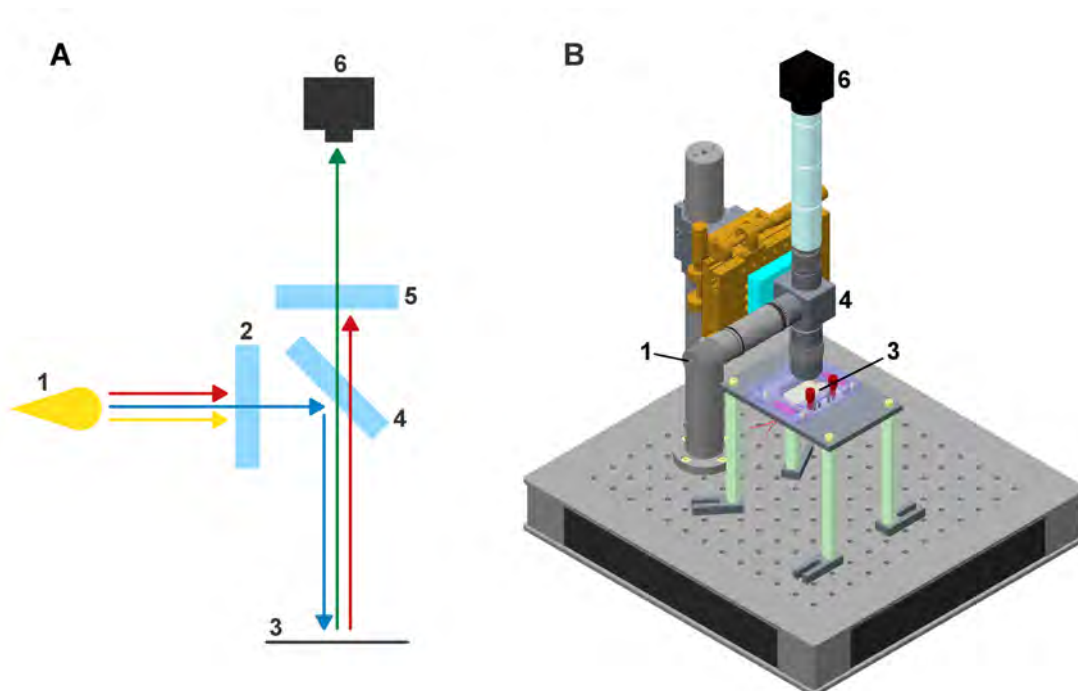
Figure 4.21: First version of the optical system. A) Schematic drawing. B) CAD drawing. For both A and B figures numbers are as follows. 1) LED light. 2) Excitation filter. 3) Sample. 4) Dichroic filter. 5) Emission filter. 6) Camera.

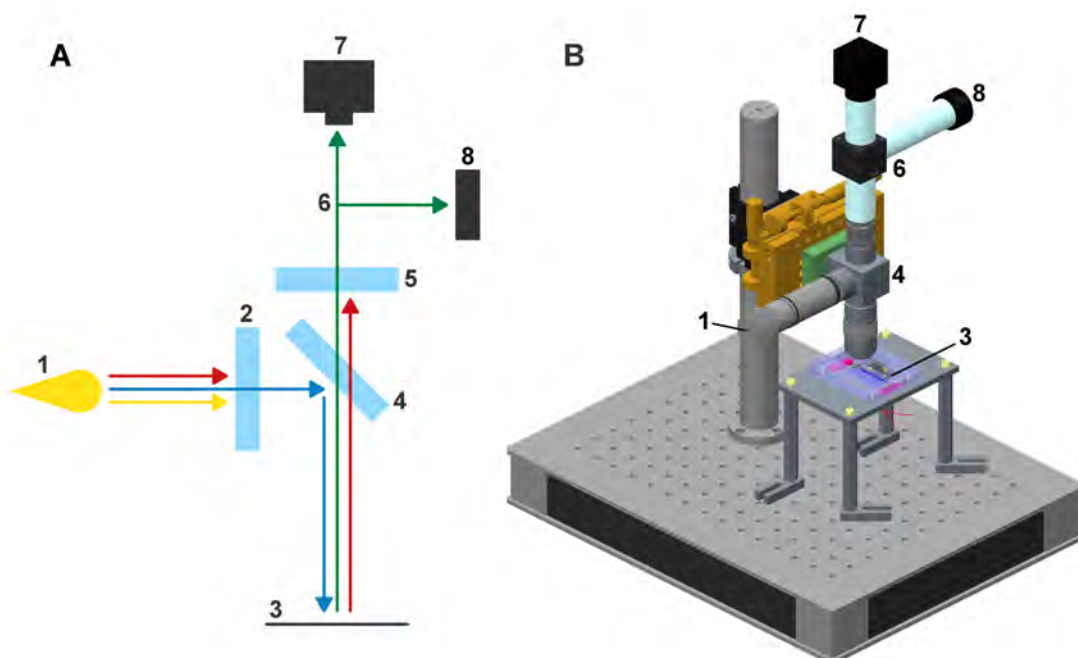Figure 4.22: Second version of the optical system after the addition of a photodetector. A) Schematic drawing. B) CAD drawing. For both A and B figures numbers are as follows. 1) LED light. 2) Excitation filter. 3) Sample. 4) Dichroic filter. 5) Emission filter. 6) Beam splitter. 7) Camera. 8) Photodetector.

The use of the photodetector surface increased the sensitivity of the system and allowed real-time on-chip measurements. Using this optical set up, several additional improvements were made to enhance the sensitivity, improve data collection, and data accuracy. Initially, values were directly read out from the power meter; however, the rapidly fluctuating values led to inaccurate data collection. By connecting the output of the power meter to a computer this problem was solved and fluorescence intensity was read-out through the computer. Moreover, data collection was improved with the incorporation of a computer program. This program allowed for a more consistent data acquisition by collecting a desired number of data points in an established time interval. During the optical system improvement process, an attenuating effect in the fluorescence values due to the platform on top of the chip was discovered. The platform was reshaped to avoid interferences in the fluorescence data collection. Additionally, the sensitivity of the system was improved by placing in the photodetector path a rectangular-shaped opening into the sample image plane limiting throughput of the fluorescence to a single channel.

In Figure 4.23, the on-chip PCR graphs associated with different optical system iteration are shown. It can be observed that the different iterations have very similar profiles and the C_T value is very similar for the second and third iterations. The last iteration allows for consistent data collection and provides high quality and sensitive fluorescence curves. It should be noted that since all the system improvement experiments –regarding the chip, system and reagents– were performed at the same time as the improvements in the optical system, the on-chip PCR data shown during the improvement of the different sections varies depending on the available optical system.

The next steps to further improve the optical system should be focused in reducing the overall costs. For example, the microscope stage could be removed if the chip could be positioned in the same identical plane. In the case of the CCD camera, it could also be eliminated if an integrated system that automatically moves through the chip channels was available.
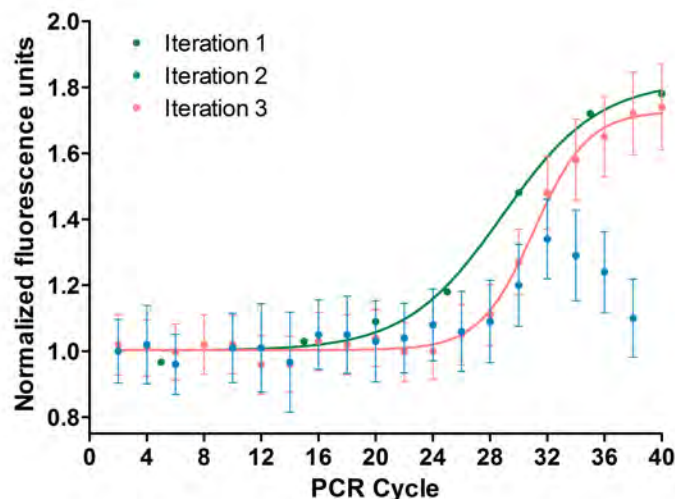
Figure 4.23: Iterations to improve the optical system. Experiments conducted with *E. coli* O157:H7 and initial template concentration 10^4 DNA copies/μl. IDT primers used. Iteration 1: optical data were directly read out from the power meter. No error bars were obtained. Iteration 2: optical data read out from the power meter connected to a computer. Attenuating effect in the fluorescence values due to interference with the chip platform can be observed. Iteration 3: optical data collected through a computer program consistently.

4.4.3 Reagents improvements

Given the importance of the optimization of the components involved in the PCR reaction as described in Section 4.3.3, during the following subsections the selection of oligonucleotide primers, enzymes and passivation agents for the microfluidic chip is described.

Passivation

At Fraunhofer CMI before the start of this thesis, both static and dynamic passivation were routinely performed prior to the PCR process. Static passivation was implemented with bovine serum albumin (BSA) protein for 2 h. Additionally, BSA and polyethylene glycol (PEG) were used as dynamic passivation agents and were added to the PCR mixture to avoid nonspecific binding to the channel walls. The main drawback of static passivation with BSA is the incompatibility with roll-to-roll processes. As previously described, another passivation method compatible with roll-to-roll production line uses plasma treatment for surface biofunctionalization.

Experiments intended to improve the process conditions using both dynamic and passivation strategies were performed and are described in this section. Experiments using plasma treatment are first described. A corona system (which uses atmospheric plasma) was used to activate the surface of the polymers. To deposit molecules on the activated surface, either in-line slot die coating or direct immersion in a solution with the target molecule were used. Tests were performed at Eurecat Technology Centre of Catalonia (Barcelona, Spain) using an in-line roll-to-roll system. Power tests and experiments with molecules of different nature were conducted. A full surface characterization was accomplished by measuring contact angle values and performing time-of-flight secondary ion mass spectrometry (TOF-SIMS) analysis.

Polyethylene terephthalate (PET) and cyclic olefin copolymer (COC) were used as substrate materials. The feeding speed was kept constant throughout all the experiments and was equal to 0.2 m/min. When not specified otherwise, corona power density was 1200 W·min/m². This corona power density was selected based on former experiments where almost no improvements were obtained when increasing the power density more than 1200 W·min/m². Figure 4.24 shows the contact angles before and after corona treatment for PET and COC substrates. PET and COC contact angles decreased until approximately 20°, being very hydrophilic after corona treatment.

Secondly, the contact angles of PET samples treated with corona were monitored over time in order to follow its evolution stored in air. Contact angle can be directly correlated with the number of radicals and reactivity. Results are shown in Figure 4.25. Immediately after corona treatment the highest number of radicals was found. Contact angle increased with time (until approximately 45°) as radicals stabilize with each other and with air oxygen and nitrogen.

Afterwards, corona activated substrate polymers were subsequently treated with slot die coating or direct immersion for 5 s in aqueous solutions with different hydrophilic/hydrophobic character in order to evaluate its surface adhesion. The solutions used were: water, polyethylene glycol (PEG 6000) 200 μM (hydrophilic), aminoethoxyethanol 10 mM (hydrophilic), and decylamine 1 mM (hydrophobic). Afterwards, samples were dried with nitrogen gas and the contact angle was imme-
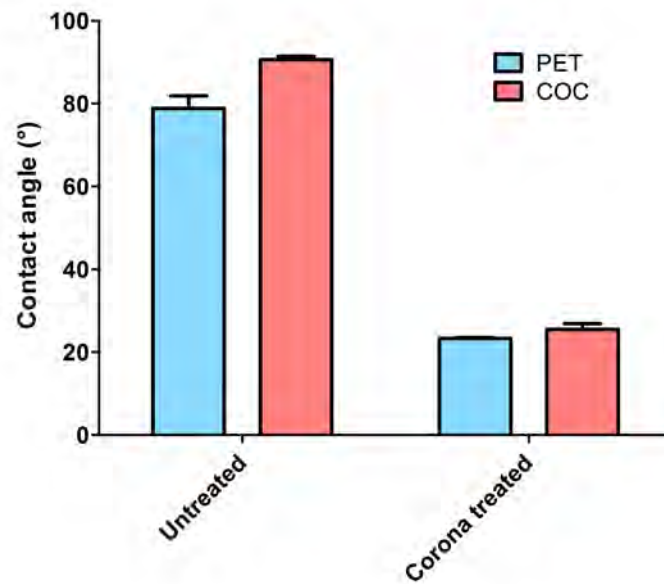
Figure 4.24: Contact angles before and after corona treatment for PET and COC substrates.
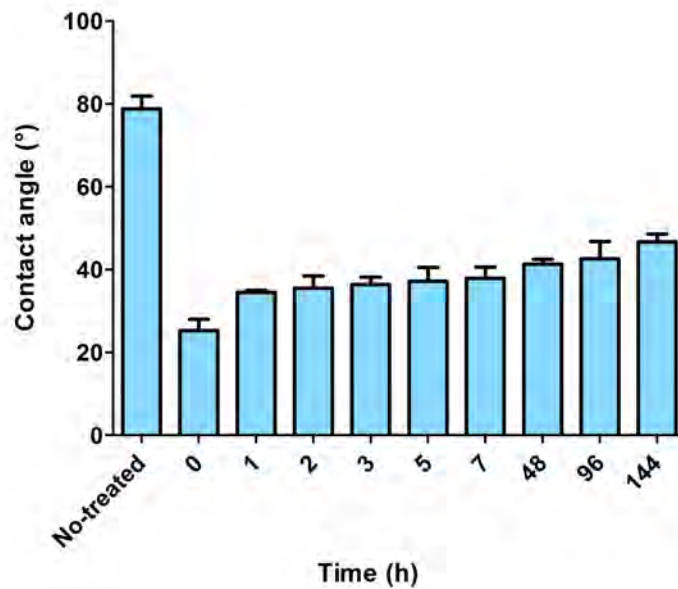
Figure 4.25: Contact angles of PET samples treated with corona and stored in air over time.

diately measured. Direct immersion experiments were only conducted with PET substrate. Figure 4.26 shows the results obtained.
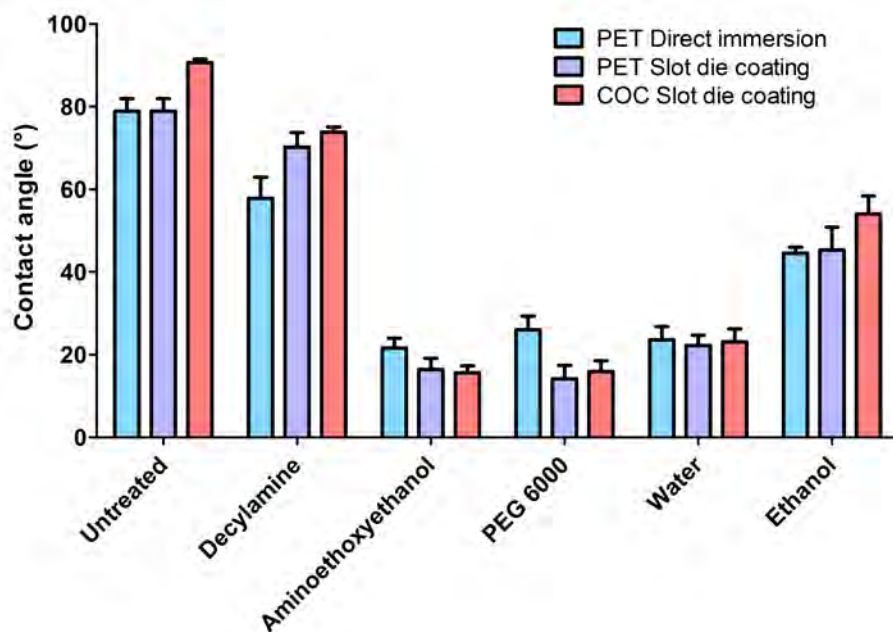
Figure 4.26: Contact angles of PET and COC substrates treated with corona and slot die coating or direct immersion in water, polyethylene glycol (PEG 6000) 200 μM, aminoethoxyethanol 10 mM, and decylamine 1 mM.

As can be observed in Figure 4.26, both substrates present very similar behaviors. High contact angle differences between the tested solutions were observed for both PET and COC polymers: water (22°), PEG (15–20°), aminoethoxyethanol (16–20°) and decylamine (60–70°). Hydrophilic solutions created low contact angles while hydrophobic solutions generated higher contact angle values, as was expected. When comparing the effect of direct immersion and slot die coating for each of the solutions, both mean values and standard deviations were very similar. Both techniques seem equally adequate for biofunctionalization of corona-treated surfaces. Based on these results, it seems that the molecules are well attached to the surface confirming the feasibility of using a corona system for surface biofunctionalization.

In order to accelerate the drying time after slot-die coating or immersion in the different solutions, a subsequent washing step in ethanol was introduced. After surface biofunctionalization and the ethanol washing step, samples were dried with nitrogen gas and contact angles were measured. Figures 4.27, 4.28, and 4.29 show the contact angle results for direct immersion with PET polymer and slot die

coating with PET and COC respectively. For comparison purposes, the contact angles of samples which did not undergo an ethanol washing step are also included.

Figure 4.27: Contact angles of biofunctionalized PET samples through corona treatment and direct immersion in water, polyethylene glycol (PEG 6000) 200 μM, aminoethoxyethanol 10 mM, and decylamine 1 mM. Shown with shading those samples which underwent a subsequent washing step in ethanol.

Looking at figures 4.27, 4.28, and 4.29, ethanol seems to have a high influence in the contact angle of the biofunctionalized samples. Although it is still possible to see the differences between samples treated with hydrophilic and hydrophobic solutions, contact angle values tended towards the ethanol contact angle (approximately 45°). Based on these results, performing a washing step with ethanol seems to be detrimental.

Time-of-flight secondary ion mass spectrometry (TOF-SIMS) analysis was used to confirm contact angle results. Three samples were analyzed: PET substrate after treatment with corona (sample 1), PET after corona treatment and addition of pentafluorophenol dissolved in water (sample 2), and in ethanol (sample 3). Pentafluorophenol was selected since it is easier to recognize its characteristic mass-to-charge ratio (m/z) peaks generated by TOF-SIMS than the peaks generated by other biomolecules including PEG, decylamine, or aminoethoxy ethanol. Samples were first activated with corona and pentafluorophenol was then deposited by slot die coating. Table 4.11 shows the relative abundance for m/z peak 183,

Figure 4.28: Contact angles of biofunctionalized PET samples through corona treatment and slot die coating in water, polyethylene glycol (PEG 6000) 200 μM, aminoethoxyethanol 10 mM, and decylamine 1 mM. Shown with shading those samples which underwent a subsequent washing step in ethanol.
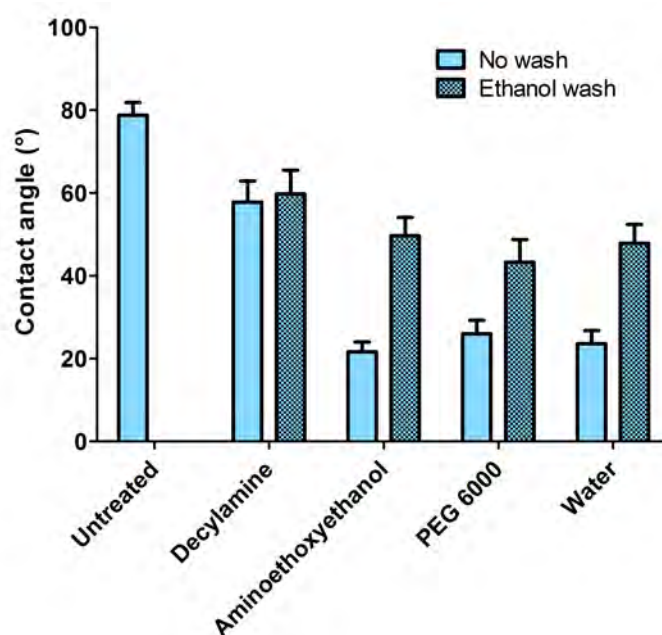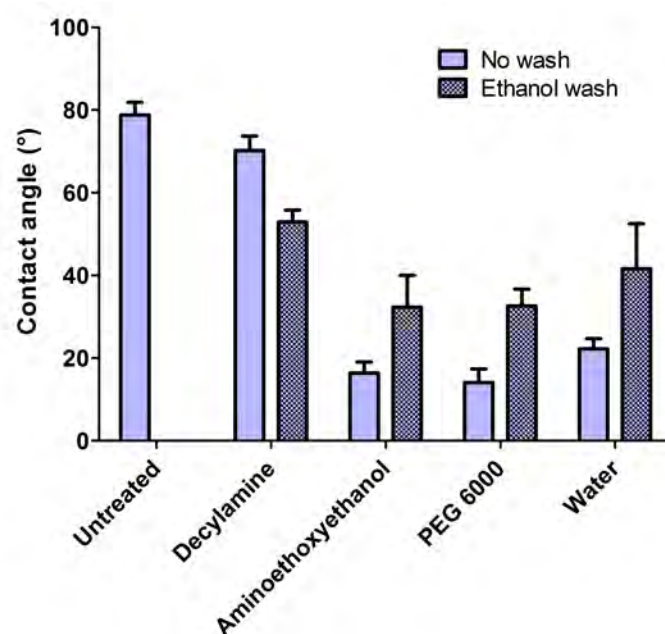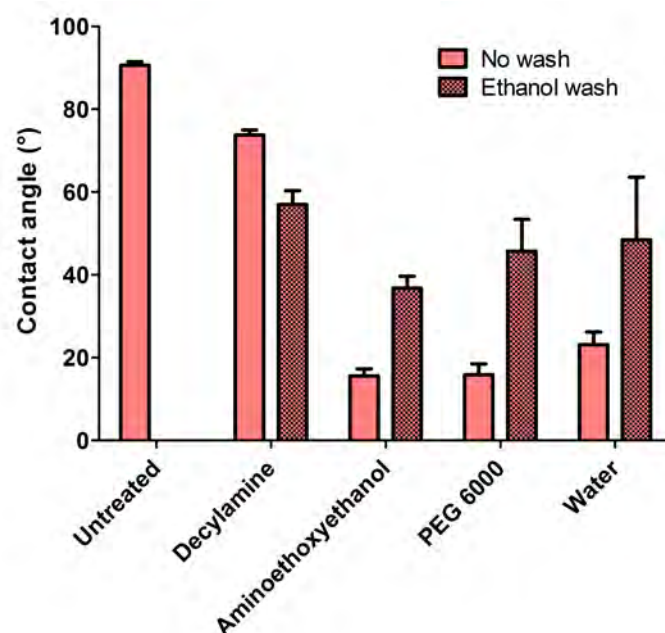

Figure 4.29: Contact angles of biofunctionalized COC samples through corona treatment and slot die coating in water, polyethylene glycol (PEG 6000) 200 μM, aminoethoxyethanol 10 mM, and decylamine 1 mM. Shown with shading those samples which underwent a subsequent washing step in ethanol.

which correspond to pentafluorophenol ion without a hydrogen atom and is one of the typical mass fragments of pentafluorophenol. The molecular structures of pentafluorophenol and its 183 m/z fragment are shown in Figure 4.30.

Table 4.11: Relative abundance of m/z 183 peak measured by TOF-SIMS analysis of three samples: PET substrate after treatment with corona, PET after corona treatment and addition of pentafluorophenol dissolved in water, and in ethanol. The abundance of peak 183 was normalized with C-12 peak.

Sample	Normalized abundance of m/z 183 peak
Corona	8.9
Corona+pentafluorophenol in water	16.7
Corona+pentafluorophenol in ethanol	13.7
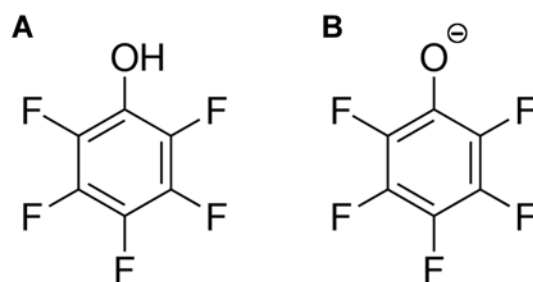
Figure 4.30: Molecular structure of pentafluorophenol. A) Pentafluorophenol molecule, m/z=184. B) Pentafluorophenol anion, m/z=183.

Comparing the three samples, it can be observed how the addition of pentafluorophenol increases the 183 peak, both in water and ethanol. This is attributed to pentafluorophenol attachment to the surface of the samples. The signal when the solvent is water is slightly higher than with ethanol as a solvent. These results agree with previous contact angle results. As it has been stated before, treating the substrate with corona followed by treatment with the desired molecules seems to provide adequate surface attachment. Better biomolecule attachment to the substrate is obtained when water is used as solvent solution and no ethanol wash is performed.

Finally, a drying step was considered at the end of the process (after corona treatment and slot die coating/immersion in solutions with different biomolecules). Different temperatures were tested. The original feeding speed was 0.2 m/min and

the oven was 1 m long. A temperature of 100 °C with aqueous solution was not enough to dry the samples, a longer oven or a slower feeding speed are required. However, when samples were washed with ethanol before entering in the oven, 95 °C dried all the substrates well.

Summarizing, surface functionalization proof of concept was successfully performed using a roll-to-roll plasma system. Molecules were well attached to the surface based on contact angle results and TOF-SIMS analysis.

The next step was to statically passivate the surface of a PCR chip through plasma biofunctionalization with PEG molecules and test its performance. A chip and its cover slip were activated with corona treatment followed by direct immersion in a 1 mg/ml PEG aqueous solution for 3 h. Next, the chip was solvent-assisted thermally bonded following the protocol described in the Materials and Methods section. On-chip qPCR was performed with *E. coli* target, 10^4 DNA copies/μl initial template concentration, 25 min residence time and using the 3rd PCR chip generation. Optical measurements were taken. Additionally, for comparison purposes, an on-chip PCR was run in a chip statically passivated with BSA using a previously validated protocol. In both cases, BSA and PEG were added to the master mix as dynamic passivating agents. The results are shown in Figure 4.31.

As can be observed in Figure 4.31, amplification was obtained using the two differently statically passivated chips. It should be remarked that BSA and PEG were used as dynamic passivating agents. Both optical curves present similar cycle thresholds (C_T) and shapes. Thus, these results confirm that static passivation with BSA for 2 h can be substituted by static passivation using a plasma system and subsequent PEG attachment which allows chip biofunctionalization in a roll-to-roll system.

The next experiments were focused on investigating if any of the static and dynamic passivating agents was unnecessary and could be eliminated from the passivation protocol. As previously described, static passivation is more time consuming and costly than dynamic passivation (especially when static passivation is performed with BSA) and consequently dynamic passivation is usually preferable than any type of static passivation. On-chip PCR experiments were conducted with different combinations of dynamic blocking agents (BSA and PEG) and with

Figure 4.31: Static passivation experiments. *E. coli* O157:H7 25 min residence time on-chip qPCR results with 10^4 DNA copies/μl initial template concentration. Milled chips and IDT primers were used. BSA and PEG were added to the master mixes for dynamic passivation. A) On-chip qPCR optical detection data for different passivated conditions. The passivation conditions of each run are indicated in the legend. Static passivation with BSA was performed for 2 h. Plasma static passivation was performed with corona treatment followed by immersion in a PEG solution. NC is the negative control performed with a BSA static passivated chip. Each data curve was normalized with its average baseline from cycles 4 to 16. B) Gel electrophoresis of on-chip amplicons (69 bp) with varying passivation conditions as shown in figure (A). Lane L indicates the ladder. Lane 1 and 3 corresponds to the passivation conditions shown in the legend of figure (A) following the same order. Off-chip PCR results are shown in Lane 4 (10^4 DNA copies/μl) and Lane 5 (0 DNA copies/μl) for comparison.

and without prior static blocking with BSA. Static passivation was performed with BSA instead of plasma due to simplicity reasons; however, as previously demonstrated, experiments performed with BSA static passivation can be substituted with static passivation with plasma biofunctionalization. Experiments were performed under the same optical system conditions and with the 3rd chip generation, using *E. coli* DNA as target with 10^4 DNA copies/μl initial template concentration, and for 25 min residence time. In Figure 4.32 the qPCR results are shown.

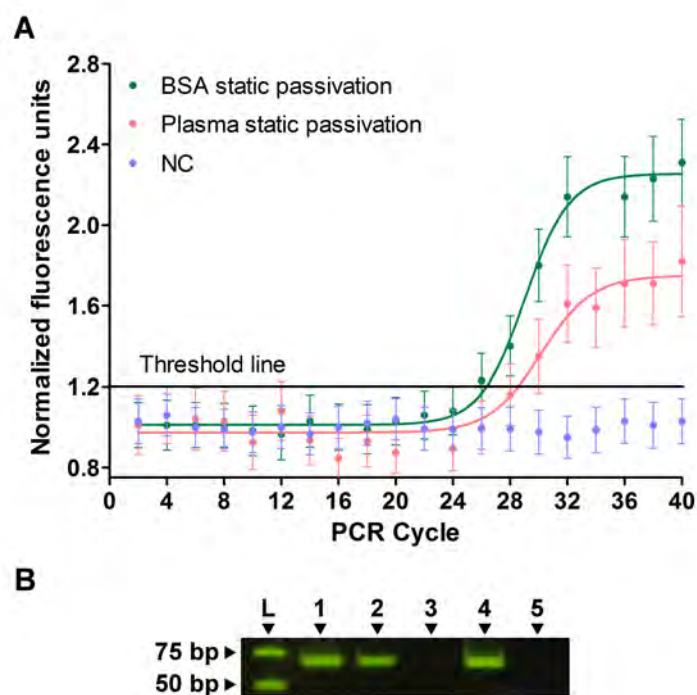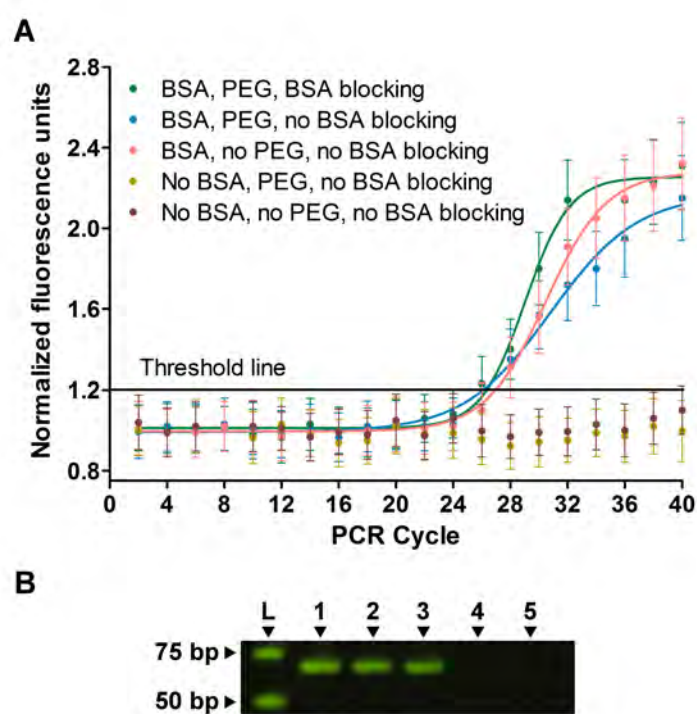Figure 4.32: Static and dynamic passivation experiments. *E. coli* O157:H7 25 min residence time on-chip qPCR results with 10^4 DNA copies/μl initial template concentration. A) On-chip qPCR optical detection data for different passivated conditions. The passivation conditions of each run are indicated in the legend. BSA, and PEG refers to dynamic passivation with those reagents while BSA blocking refers to static passivation with BSA. Each data curve was normalized with its average baseline from cycles 4 to 16. B) Gel electrophoresis of on-chip amplicons (69 bp) with varying passivation conditions as shown in figure (A). Lane L indicates the ladder. Lane 1 to Lane 5 corresponds to the passivation conditions shown in the legend of figure (A) following the same order.

From the amplification curves (Figure 4.32 A) and gel electrophoresis results (Figure 4.32 B), it is observed that three of the curves achieved comparable levels of amplification: (1) static passivation with BSA and dynamic passivation with BSA and PEG (green curve); (2) no static passivation and dynamic passivation with

BSA and PEG (blue curve); (3) no static passivation and dynamic passivation with BSA (pink curve). Based on these result, it can be concluded that static passivation with BSA is unnecessary and that the addition of BSA to the PCR mix as dynamic passivation agent is enough to prevent non-specific binding of the PCR components to the internal microfluidic channel surface. Within the chip, BSA in the PCR master mix binds to the channel surface and prevents PCR components from potentially absorbing to the channel walls.[59] When neither static nor dynamic passivation was performed or when passivation was implemented with only PEG as dynamic agent, no amplification was observed (brown and light green curves respectively).

These findings allowed for chip passivation using only BSA as dynamic agent during the subsequent experiments with our PCR chips. The elimination of the static passivation step (either with a BSA pre-coating step or using plasma bio-functionalization) facilitates chip manufacture and decreases its costs. Dispensing with PEG contributes to the reduction of the PCR reagents costs and thus the assay costs.

Primer/probe optimization for *E. coli* O157:H7

Specific primer and probe sets for each of the pathogen targets were designed to be detected through the FAM channel and exploit the TaqMan principle. High quality primers and probes are essential for the success of the PCR. In the case of *E. coli* O157:H7 target, 3 sets of primers/probes were tested, one primer/probe set from Primer Design Ltd. and two sets of primer/probe purchased from Integrated DNA Technologies, Inc. (IDT). The sequences of the primers and probes are specified in Section 4.2.3. Initial experiments were performed using Primer Design primer/probe set with successful results. However, the 6 times higher price of Primer Design primer/probe set compared to custom made primers/probes by IDT, led us to test other IDT primer/probe sets. To assess its performance, off-chip and on-chip experiments were performed using *E. coli* DNA as target with initial template concentration of 10^4 DNA copies/μl. Off-chip qPCR experiments are shown in figures 4.33 and 4.34 for Primer Design and IDT respectively.

Figure 4.33: Off-chip qPCR results using Primer Design primer/probe set and *E. coli* DNA as target. Initial template concentration of 10^4 DNA copies/μl was used for the positive control.
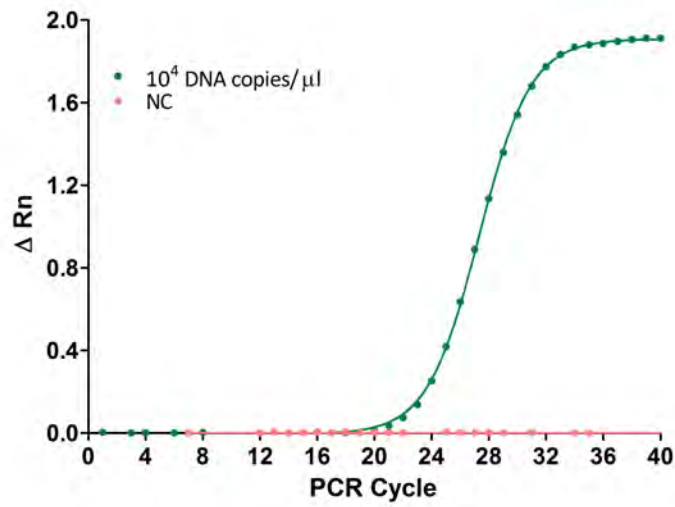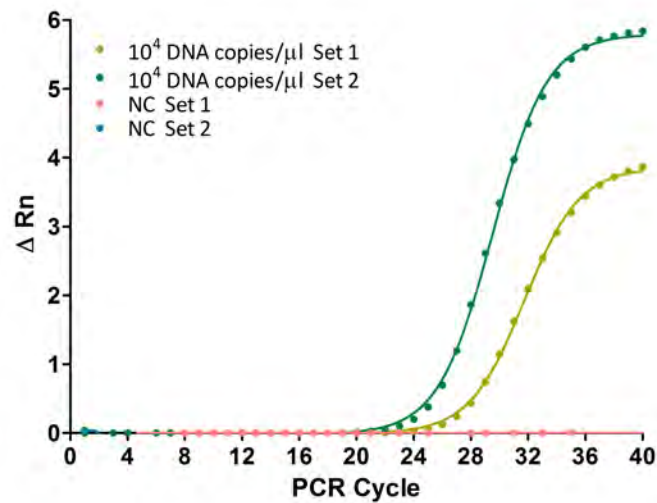

Figure 4.34: Off-chip qPCR results using Primer Design primer/probe set and *E. coli* DNA as target. Initial template concentration of 10^4 DNA copies/μl was used for the positive controls.

On-chip experiments were performed with the 3rd generation PCR chip for 25 min residence time. The optical system was not sensitive enough at the time these experiments were perform and gel electrophoresis was used to analyze the success of the on-chip runs. Figures 4.35 and 4.36 show the results for Primer Design and IDT primer/probe sets respectively.
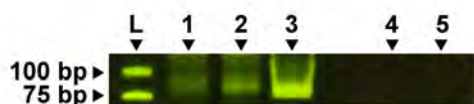
Figure 4.35: Gel electrophoresis of on-chip amplicons (76 bp) using Primer Design primer/probe set and *E. coli* DNA as target. Initial template concentration of 10^4 DNA copies/μl were used for the positive controls. On-chip PCR results are shown in Lane 1 (10^4 DNA copies/μL) and Lane 3 (0 DNA copies/μL). Off-chip PCR results are shown in Lane 2 (10^4 DNA copies/μL) and Lane 4 (0 DNA copies/μL) for comparison.

Figure 4.36: Gel electrophoresis on-chip amplicons using IDT primer/probe set 1 (69 bp) and 2 (99 bp). 10^4 DNA copies/μl of *E. coli* target were used as initial template concentration for the positive controls. Amplicons in Lane 1 and 2 were obtained through on-chip PCR performed with primer/probe set 1 and 2 respectively. The on-chip negative control (0 DNA copies/μL) is shown in Lane 5. For comparison, off-chip PCR results are shown in Lanes 3 and 4 (10^4 DNA copies/μL) for primer/probe set 1 and 2 respectively, and Lane 6 (0 DNA copies/μL).

Based on both off-chip and on-chip PCR results, the tree primer/probe sets seem to perform similarly. Looking at the C_T values of off-chip PCR curves, Primer Design and IDT set 2 show a very similar C_T, which are slightly lower than the C_T of IDT set 1. Comparing the gel electrophoresis bands of on-chip amplicons no significant differences were observed between the three primer/probe sets. Given the slight differences in terms of performance, other selection criteria were considered. Price was an important factor contemplated. Due to the higher price of Primer Design primer/probe set compared to IDT, the latter were preferred. IDT primer/probe set 1 was selected over set 2 due to the smaller amplicon size since small amplicons have higher possibilities to be fully amplified during on-chip

PCR. Thus, IDT primer/probe set 1 was selected for PCR chip characterization experiments (Section 4.5.1) when *E. coli* was used as target.

During this section we described the improvements in different aspects of the PCR and RT-PCR. Significant consideration was given to the disposable chip to assure rapid and economic production at industrial scale. The price of both PCR and RT-PCR chips is expected to be under $0.4. In addition to disposable components, in any POC system, considerable attention needs to be given to the surrounding instrumentation. Components within the instrument must likewise be robust and the biological assays should be optimized around instrumentation cost constraints rather than vice versa. For our prototype instrument, the components were limited to two heaters, the optical system including a detector, a pump, and a computer for data processing. A picture of the prototype system is shown in Figure 4.37. This instrument was assembled with simple off-the-shelf components and the approximate cost was below $9,000. The cost of such instrumentation is driven lower when producing in larger quantities and components are able to be purchased in bulk. While satisfied with the costs of the first prototype, we are in the process of incorporating even smaller and lower-cost components. Currently, this work involves incorporating lower-cost optics, and miniaturizing the pump and heaters. When the system improvements are incorporated, the price of the instrument is expected to be below $2,000.

During next section, the function of the chip and surround instrumentation is demonstrated with three infectious pathogens.
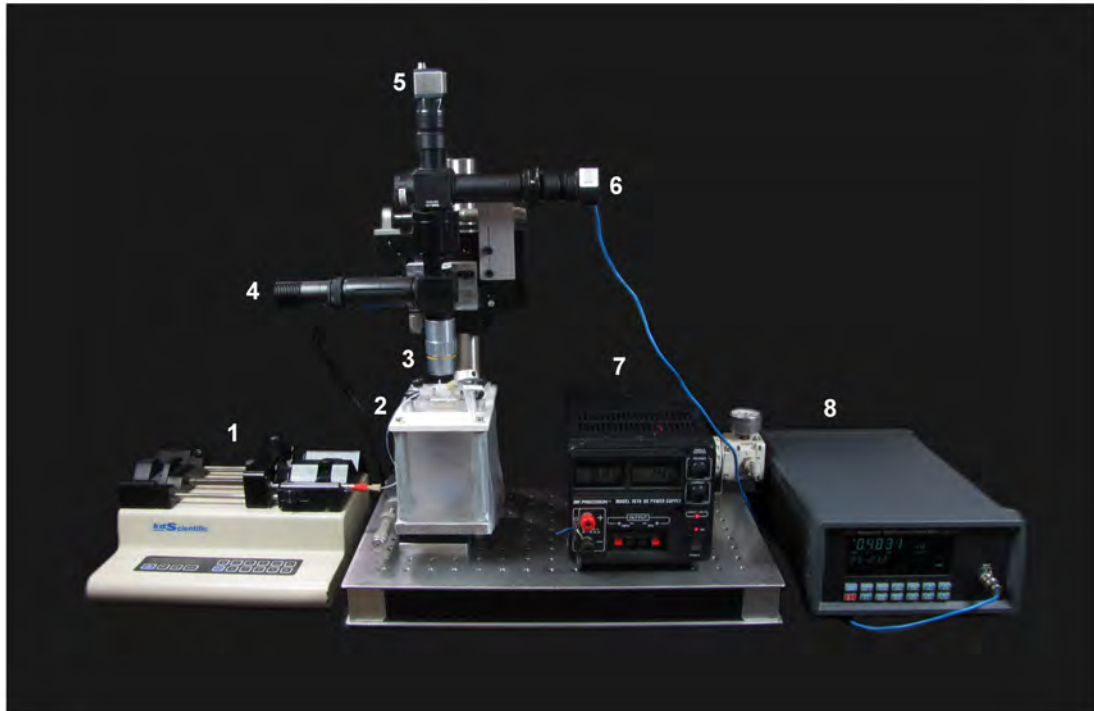
Figure 4.37: Picture of the instrumentation used for qPCR experiments.[67] 1) Syringe pump. 2) Chip baseplate. Two block heaters are placed below the chip. 3) Microscope objective. 4) LED source. 5) Camera. 6) Photodetector. 7) Power source. 8) Optical power meter.

4.5 Characterization

At the end of the previous section, a PCR system that allows for amplifying DNA and RNA-based pathogens and detecting them in real-time was achieved. This section is focused on the characterization of both PCR and RT-PCR chips using three infectious pathogens. *Escherichia coli* and *Chlamydia trachomatis* were selected to characterize the PCR chip, and Ebola virus (EBOV) Zaire to test the RT-PCR chip.

Infection with *C. trachomatis*, when untreated or if treatment is delayed, can lead to ocular infection, pelvic inflammatory disease, or infertility.[1,3] Infections with *E. coli* O157:H7 can lead to hemorrhagic diarrhea and hemolytic uremic syndrome.[7,8] Ebola virus disease (EVD), formerly known as Ebola haemorrhagic fever, is a severe illness in humans, with an average case fatality rate around 50 %.[14] EVD early symptoms are non-specific (fever, sore throat, muscular pain, headaches). As the disease progress, vomiting, diarrhea, decreased function of liver and kidneys, and in some cases bleeding internally and/or externally follows.[14] A rapid diagnosis

147

of these pathogens would be crucial for prompt initiation of the right treatment, increased treatment success, avoidance of the spread of the infections, and reduction in the rise of antibiotic resistances due to broad prophylactic antibiotic use.

For both bacteria and virus, different flow velocities were tested for determining the maximum speed at which DNA amplification could occur and the limit of detection (LOD) of the system was identified. First we describe the characterization experiments regarding the PCR chip and later the tests performed with the RT-PCR chip.

4.5.1 PCR Chip

The influence of the residence time in the on-chip PCR system was tested to explore how quickly we could run each assay and to determine the optimal flow-rate. The same initial template concentration, 10^4 DNA copies/μl, was used for all the residence time experiments. On-chip amplifications were conducted for 40, 30, 20 and 10 min residence times. The optical data and the corresponding gel electrophoresis amplicons are presented in Figure 4.38 and Figure 4.39 for *C. trachomatis* and *E. coli* O157:H7, respectively. The cycle threshold (C_T) for 30 and 40 min residence times was almost identical suggesting that both reactions achieve the maximum total amplification possible. At these low speeds, the enzymes likely have sufficient time to complete polymerization of all targets. When the residence time is 20 min the C_T shifts to the right a couple of units.

For 10 min residence time, although no optical signals were measured above the threshold for either bacteria, the fluorescence is slightly higher at the last PCR cycles indicating some DNA amplification. Shown below each set of curves, is the gel electrophoresis results for each amplification. Note that while we did not optically detect product for the 10 min samples, faint bands were detected for these conditions by gel electrophoresis for *C. trachomatis* and *E. coli* O157:H7 (see Figure 4.38 B Lane 4 and Figure 4.39 B Lane 4 respectively). 20 min residence time is probably the best tradeoff between sensitivity and speed; it allows achieving high sensitivity while keeping the time to result low.

To further explore the limit of detection (LOD) of the system, determinations were done by a DNA dilution series ranging from 10^5 to 1 DNA copies/μl by
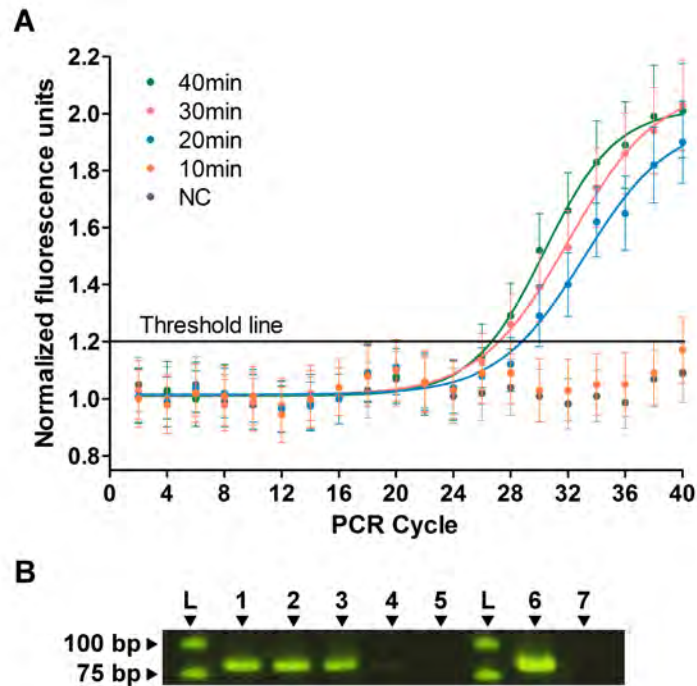
Figure 4.38: *C. trachomatis* on-chip qPCR results with 10^4 DNA copies/μl initial template concentration.[67] A) On-chip qPCR optical detection data for different on-chip residence time. Each data curve was normalized with its average baseline from cycles 4 to 16. Independent trials were run for 40, 30, 20, and 10 minutes total on-chip residence times as indicated. B) Gel electrophoresis of on-chip amplicons (85 bp). Amplicons in Lane 1 had a total on-chip time of 40 min and times decreased by 10 minutes until a final on-chip time of 10 min as shown in Lane 4. The negative control (0 DNA copies/μl for 25 min) is shown in Lane 5. Off-chip PCR for 1 h with 10^4 DNA copies/μl (Lane 6) and 0 DNA copies/μl (Lane 7) are shown for comparison purposes.
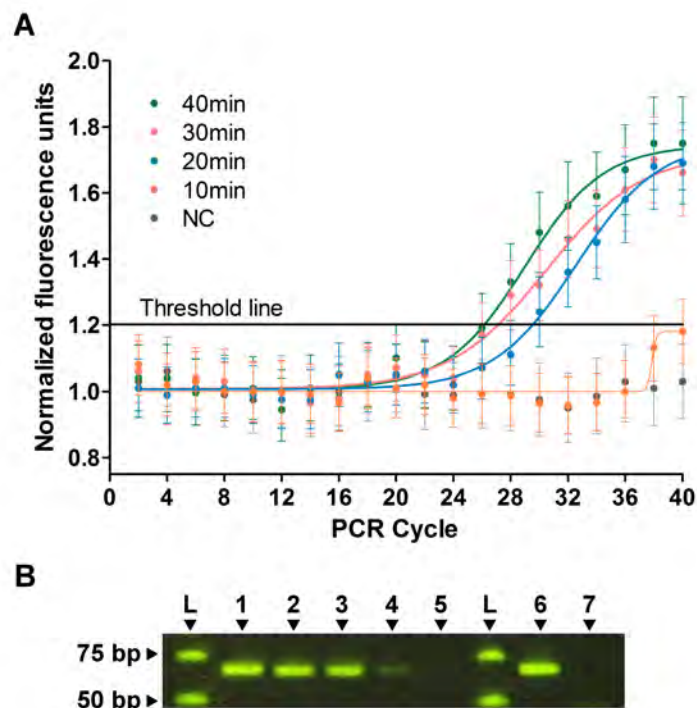
Figure 4.39: *E. coli* O157:H7 on-chip qPCR results with 10^4 DNA copies/μl initial template concentration.[67] A) On-chip qPCR optical detection data for different on-chip residence time. Each data curve was normalized with its average baseline from cycles 4 to 16. Independent trials were run for 40, 30, 20, and 10 minutes total on-chip residence times as indicated. B) Gel electrophoresis of on-chip amplicons (69 bp). Amplicons in Lane 1 had a total on-chip time of 40 min and times decreased by 10 minutes until a final on-chip time of 10 min as shown in Lane 4. The negative control (0 DNA copies/μl for 25 min) is shown in Lane 5. Off-chip PCR for 1 h with 10^4 DNA copies/μl (Lane 6) and 0 DNA copies/μl (Lane 7) are shown for comparison purposes.

factors of 10. On-chip qPCR of serially diluted DNA is presented in Figure 4.40 for *C. trachomatis* and Figure 4.41 for *E. coli* O157:H7 for 25 min residence time. The limit of detection for our on-chip qPCR system for both *C. trachomatis* and *E. coli* O157:H7 is 10 DNA copies/μl. It should be considered that for very low DNA concentrations, stochastic sampling (the probability of retrieving a single copy of DNA in the microliter) can lead to variations in the optical signals. For large devices that process larger sample volumes, this effect of stochastic sampling is obviously minimized. However, for all microfluidic approaches with small volumes, these probabilistic limits need to be kept in mind when discussing LOD measurements.

When doing 1 h-long qPCR experiments off-chip with a commercial thermocycler, the LOD was 1 DNA copy/μl, an order of magnitude below our on-chip data. However, it is remarkable that the on-chip PCR was done in less than half of the time than that of the off-chip thermocycler. In addition, it should be pointed out that the off-chip cycler measures the fluorescence from 20 μl, while in our on-chip system the optical data is taken from a small section of each PCR cycle, which is approximate 50 nl. This makes the comparison between on- and off-chip difficult regarding PCR sensitivity or in terms of the total number of template copies.

The PCR efficiencies, calculated as described in the Materials and Methods section, are 93$\pm$3 % and 95$\pm$5 % for *C. trachomatis* and *E. coli* O157:H7 respectively. These PCR efficiencies are equivalent to those obtained from benchtop thermocyclers. It can be observed how a 10-fold increase in the initial template concentration produced a 3.3 threshold cycle shift. The data obtained matched classic quantitative PCR amplification curves. Off-chip amplification results are presented for comparison in Appendix E (figures E.1 and E.2). Gel electrophoresis data (Figure 4.40 C and Figure 4.41 C for *C. trachomatis* and *E. coli* O157:H7) confirm the successful on-chip amplifications and shows the same detection limit (10 DNA copies/μl) as the on-chip optical detection system.

When comparing the data from *C. trachomatis* and *E. coli* O157:H7 (Figure 4.40 and Figure 4.41), it can be observed that optimized assays yielded similar results in terms of the on-chip fluorescence curves, the limit of detection, the PCR efficiency, and gel electrophoresis results for both bacteria. As each assay tar-
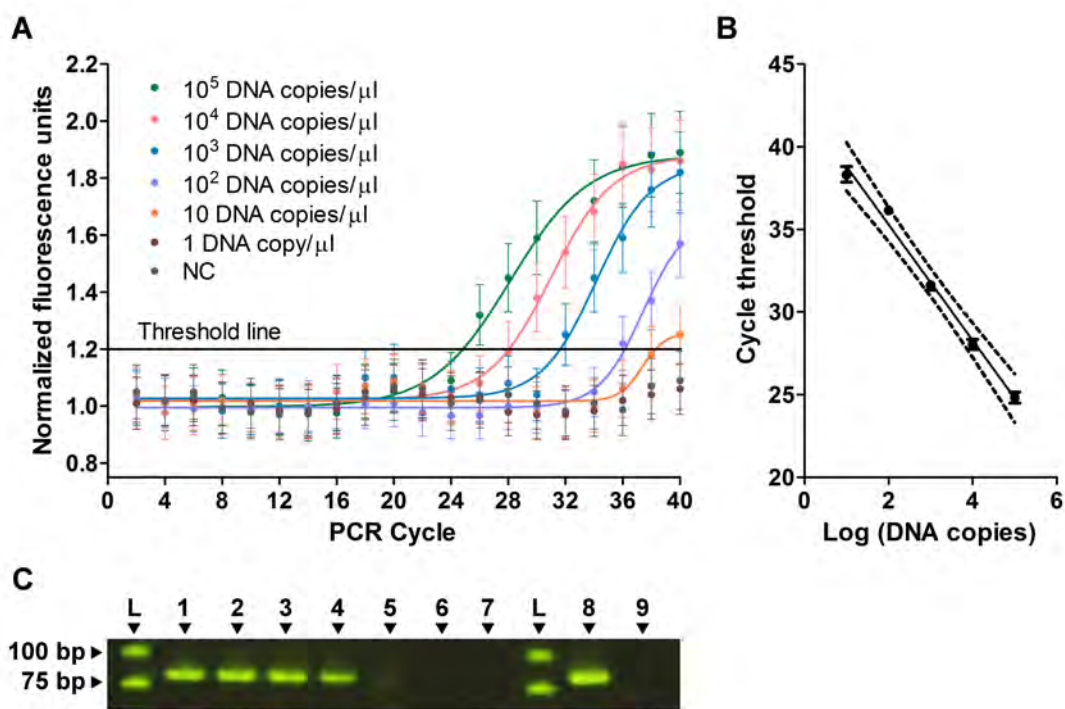
Figure 4.40: *C. trachomatis* 25 min residence time on-chip qPCR results.[67] A) On-chip qPCR optical detection data for serially diluted DNA template. Each data curve was normalized with its average baseline from cycles 4 to 16. Template concentrations begin at 10^5 DNA copies/μl and are reduced by one order of magnitude until the final trial of 1 DNA copy/μl. Also included is the negative control (0 DNA copies/μl). B) On-chip qPCR efficiency graph representing the cycle threshold versus the initial template concentrations in a logarithmic scale. Dotted lines represent 95 % confidence interval. The slope is 3.50$\pm$0.19 which correspond to a PCR efficiency of 93$\pm$3 %. C) Gel electrophoresis of on-chip amplicons (85 bp) with varying levels of template as shown in (A). Lane 1 has an initial template of 10^5 DNA copies/μl and template concentrations are reduced by one order of magnitude until the final trial of 1 DNA copy/μl in Lane 6 and the negative control (0 DNA copies/μl) in Lane 7. Off-chip PCR results are shown in Lane 8 (10^4 DNA copies/μl) and Lane 9 (0 DNA copies/μl) for comparison.
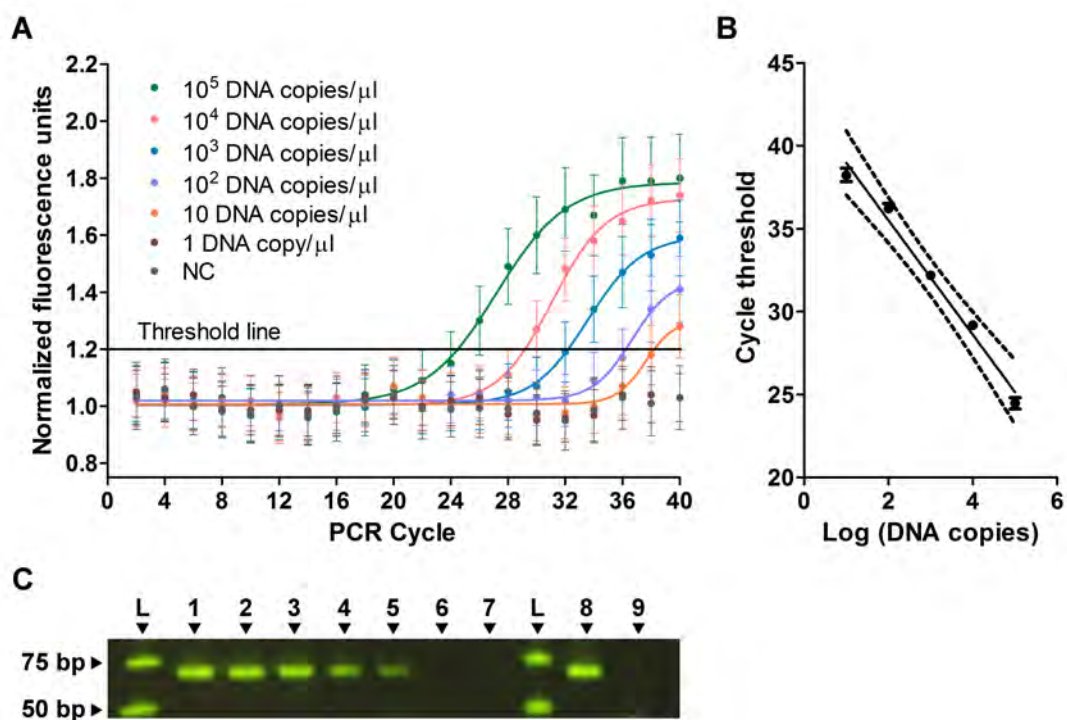
Figure 4.41: *E. coli* O157:H7 25 min residence time on-chip qPCR results.[67] A) On-chip qPCR optical detection data for serially diluted DNA template. Each data curve was normalized with its average baseline from cycles 4 to 16. Template concentrations begin at 10^5 DNA copies/μl and are reduced by one order of magnitude until the final trial of 1 DNA copy/μl. Also included is the negative control (0 DNA copies/μl). B) On-chip qPCR efficiency graph representing the cycle threshold versus the initial template concentrations in a logarithmic scale. Dotted lines represent 95 % confidence interval. The slope is 3.45$\pm$0.25 which correspond to a PCR efficiency of 95$\pm$5 %. C) Gel electrophoresis of on-chip amplicons (69 bp) with varying levels of template as shown in (A). Lane 1 has an initial template of 10^5 DNA copies/μl and template concentrations are reduced by one order of magnitude until the final trial of 1 DNA copy/μl in Lane 6 and the negative control (0 DNA copies/μl) in Lane 7. Off-chip PCR results are shown in Lane 8 (10^4 DNA copies/μl) and Lane 9 (0 DNA copies/μl) for comparison.

geted a similar length amplicon (85 bp versus 69 bp for *C. trachomatis* and *E. coli* O157:H7, respectively), the similarity in results may indicate that the conditions were optimized for this amplicon range. Assays targeting longer amplicons could require more residence time to achieve similar optimal detection while shorter amplicons would be predicted to require less residence time. Short amplicons are limited by the requirement for specificity (shorter amplicons are less specific) and room on the template for two primers and a probe. Sensitivity can also be increased by monitoring multi-copy, rather than single copy genes.

4.5.2 RT-PCR Chip

The function of the RT-PCR chip was assessed with Ebola virus (EBOV). An *in vitro* transcribed fragment of the L gene, one of the best conserved and most genetically stable EBOV gene, was targeted.[68,69] L gene codes for the RNA-dependent RNA polymerase (RdRp), which are highly conserved in RNA-viruses with no DNA stage.[68] Assays targeting well-conserved genomic regions have higher possibilities to be valid for different outbreaks with evolved EBOV variants.

For the characterization of the RT-PCR chip, two one-step RT-qPCR master mixes, a 'commercial' and a 'custom' mix, were tested at various flow rates. Both contain the same reverse transcriptase enzyme but different DNA-polymerases. To determine the influence of the flow rate and the sensitivity for each master mix, off-chip and on-chip experiments were performed. In the case of the off-chip experiments, the steps of the thermal profile protocol recommended by the manufacturer were modified and performed more rapidly. For both master mixes, the protocol recommended by the manufacturer is referenced as 'slow' (see Table 4.4). The 'rapid' protocol was selected based on the protocol recommended for Affymetrix VeriQuest® Fast qPCR Probe, which contains the DNA-polymerase used in the 'custom' mix (see Table 4.4). Additionally, for the 'commercial' mix, a 'mid' speed protocol was performed varying only the reverse transcription time respect to the 'slow' protocol. Figure 4.42 shows the performance of each master mix with the different thermal profile protocols for the same initial template concentrations (10^5 and 10^2 RNA copies/μl).
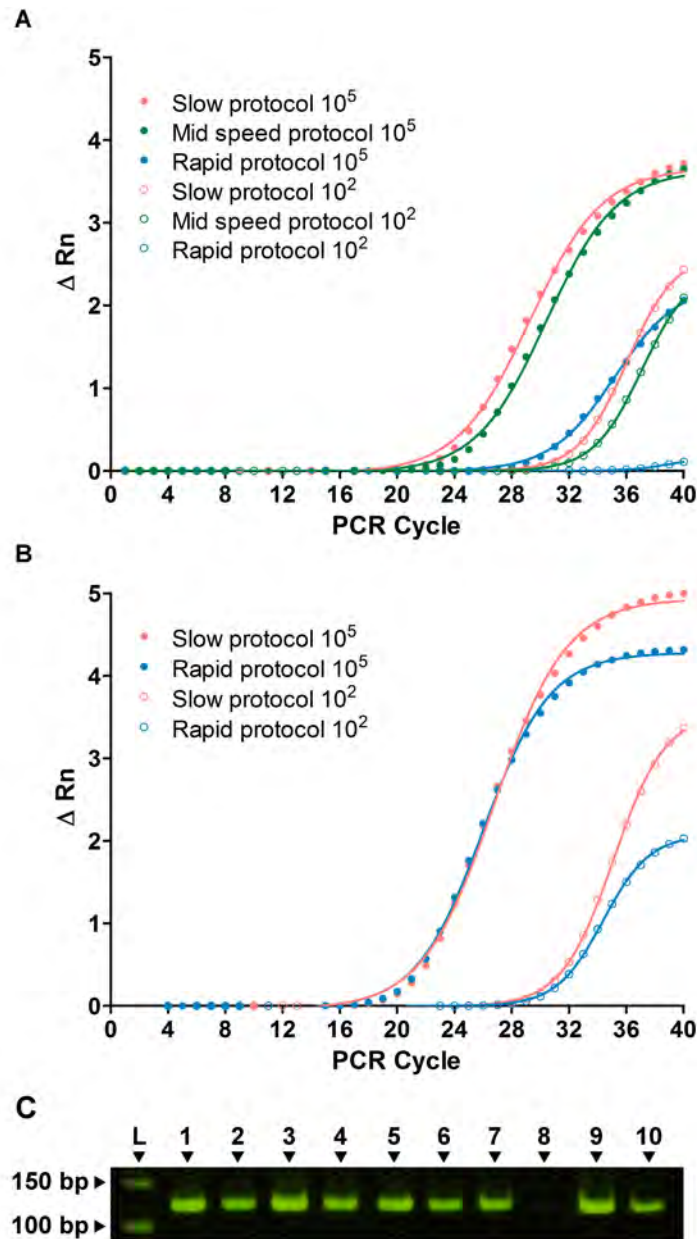
Figure 4.42: EBOV off-chip qPCR results. A) Off-chip RT-qPCR optical detection data performed using the 'commercial' one-step RT-qPCR master mix. Data were normalized by the internal thermocycler software. Template concentrations were 10^5 and 10^2 RNA copies/μl. 'Slow', 'mid', and 'rapid' thermal profile protocols were performed (information about the protocols can be found in Table 4.4). B) Off-chip RT-qPCR optical detection data performed using the 'custom' one-step RT-qPCR master mix. Data were normalized by the internal thermocycler software. Template concentrations were 10^5 and 10^2 RNA copies/μl. 'slow' and 'rapid' thermal profile protocols were performed (information about the protocols can be found in Table 4.4). C) Gel electrophoresis of off-chip amplicons (120 bp). Amplicons in Lane 1 ('slow', 10^5 RNA copies/μl), 2 ('slow', 10^2 RNA copies/μl), 5 ('mid', 10^5 RNA copies/μl), 6 ('mid', 10^2 RNA copies/μl), 7 ('rapid', 10^5 RNA copies/μl), 8 ('rapid', 10^2 RNA copies/μl) correspond to off-chip RT-qPCR runs presented in Figure A with the 'commercial' mix. Amplicons in Lane 3 ('slow', 10^5 RNA copies/μl), 4 ('slow', 10^2 RNA copies/μl), 9 ('rapid', 10^5 RNA copies/μl), and 10 ('rapid', 10^2 RNA copies/μl) correspond to off-chip RT-qPCR runs presented in Figure B with the 'custom' mix.

155

From the results shown in Figure 4.42 A, the 'commercial' master mix does not lose efficacy by reducing the RT time from 15 to 5 minutes (from the recommended 'slow' protocol to the 'mid' speed protocol). However, reducing the thermal cycling time increases the C_T values: from 24.7 and 33.2 ('slow' protocol) to 30.3 and undetermined ('rapid' protocol) for 10^5 and 10^2 RNA copies/μl respectively. This suggests that the standard DNA-polymerase contained in the mix does not achieve full amplification of the cDNA target at such high thermal cycling speed. In the case of the 'custom' mix, the 'slow' and 'rapid' protocols are equally effective (Figure 4.42 B). The C_T values are the same as those obtained with the 'commercial' mix, using the 'slow' and 'mid' protocols. These results indicate that the DNA-polymerase contained in the 'custom' mix functions well at rapid thermal cycling speed. Overall, the 'custom' mix allows for faster RT-PCR runs than the 'commercial' mix for the same sensitivity. Gel electrophoresis results (Figure 4.42 C) confirm the optical data shown in Figure 4.42 A and B.

Next, on-chip experiments were performed varying the residence time inside the chip. The same initial template concentration, 10^6 RNA copies/μl, was used for all the residence time experiments. The optical data for the 'commercial' mix, and 'custom' mix are presented in Figure 4.43 A and B respectively. In Figure 4.43 C, a gel electrophoresis including the on-chip RT-qPCR amplicons is shown.

Comparing the amplification curves for 50 min residence time for the two master mixes, the C_T for the 'commercial' and 'custom' mixes are identical. When decreasing the residence time to 40 min, the C_T for the 'custom' mix does not vary respect to the C_T at 50 min residence time; however, in the case of the 'commercial' mix, the C_T increases considerably. For the 'custom' mix at 50 and 40 min residence time, the DNA-polymerase enzyme performs a full amplification of the cDNA created by the RT-enzyme. However, for 'commercial' mix, the C_T shift can be attributed to insufficient time for the DNA polymerase to achieve full amplification (given that the RT-enzyme is the same in both mixes). Thus, for the 'commercial' mix, probably the best tradeoff between rapidity and sensitivity is 50 min residence time. These results confirm off-chip results: the 'commercial' mix is unable to perform as well as the 'custom' mix in terms of rapid thermal cycling.
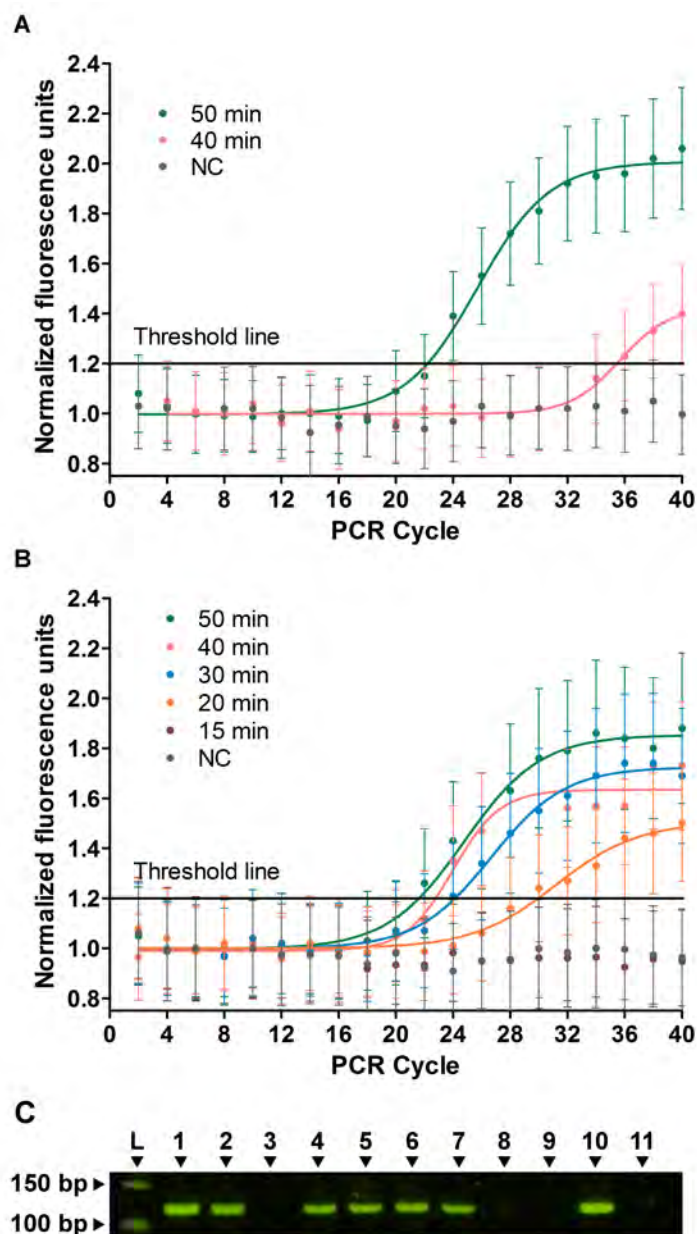
Figure 4.43: EBOV on-chip qPCR results with 10^6 RNA copies/μl initial template concentration. Each data curve was normalized with its average baseline from cycles 4 to 16. A) On-chip qPCR optical detection data for different on-chip residence time using the 'commercial' one-step RT-qPCR master mix. Independent trials were run for 50 and 40 minutes total on-chip residence times as indicated. Additionally, a negative control (0 RNA copies/μl) was run for 50 minute residence time. B) On-chip qPCR optical detection data for different on-chip residence time using the 'custom' one-step qRT-qPCR master mix. Independent trials were run for 50, 40, 30, 20, and 15 minutes total on-chip residence times as indicated. Additionally, a negative control (0 RNA copies/μl) was run for 50 minute residence time. C) Gel electrophoresis of on-chip amplicons (120 bp). Amplicons in Lanes 1 (50 min), 2 (40 min), and 3 (negative control) correspond to on-chip PCR runs presented in Figure A. Amplicons in Lanes 4 (50 min), 5 (40 min), 6 (30 min), 7 (20 min), 8 (15 min), and 9 (negative control) correspond to on-chip PCR runs presented in Figure B. Off-chip PCR for 80 min with 10^4 RNA copies/μl (Lane 10) and 0 RNA copies/μl (Lane 11) are shown for comparison purposes.

Based on both off-chip and on-chip results, for our application the most promising enzymatic combination appeared to be the 'custom' master mix. To further explore the maximum speed at which amplification occurs and determine the optimal flow-rate for the 'custom' mix, more experiments were performed at lower residence times. The C_T for 50 to 30 min residence time curves are very similar (see Figure 4.43 B), for 20 min residence time the C_T shifts to the right by approximately 6 cycles, and for 15 min residence time no amplification was optically detected on-chip. Thus, in the case of the 'custom' mix, 30 min residence time is probably the best compromise of sensitivity and speed. Gel electrophoresis results (Figure 4.43 C) confirm the optical data.

Although the 'custom' mix is the most promising master mix, due to its limited availability, we performed tests to determine the level of detection of the assay using the 'commercial' mix which could be more quickly translated to the market. LOD experiments were conducted at 50 min residence time to achieve full polymerization of all targets. LOD experiments were done with serially diluted EBOV RNA ranging from 10^6 to 1 RNA copies/μl by factors of 10. On-chip RT-qPCR results are presented in Figure 4.44.

The LOD for our on-chip RT-qPCR system using the 'commercial' mix and EBOV as target was 10 RNA copies/μl. As previously commented, it should be noted that for low template concentrations, such as 100 and especially 10 RNA copies/μl, fluctuations in the optical signal were observed due to stochastic sampling. When comparing with 80 min-long off-chip RT-qPCR using a commercial machine, the LOD was 10 RNA copies/μl. It is remarkable that our on-chip RT-qPCR was performed faster than off-chip. Additionally, as previously mentioned regarding the PCR chip, the optical measures on-chip were taken from only approximately 50 nl. The PCR efficiency was 99$\pm$6 % as shown if Figure 4.44. This PCR efficiency is comparable to the efficiencies obtained with off-chip commercial thermocyclers; a 3.3 threshold cycle shift is observed for 10 fold dilutions of initial template. For comparison, off-chip LOD results with the same master mix are presented in Appendix E (Figure E.3). Gel electrophoresis of on-chip amplicons confirmed the results observed optically. For 100 RNA copies/μl, no band could be distinguished by gel electrophoresis (Figure 4.44 C Lane 5) although amplification
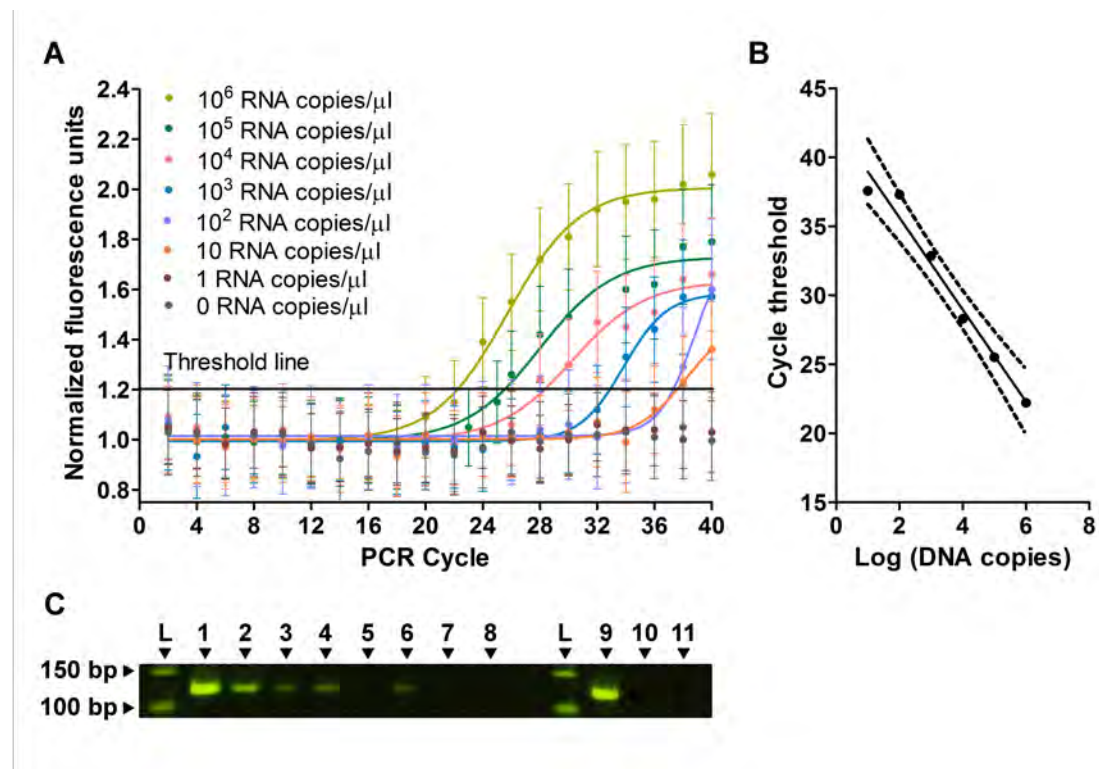
Figure 4.44: EBOV 50 min residence time on-chip RT-qPCR results performed using the 'commercial' one-step RT-qPCR master mix. A) On-chip qPCR optical detection data for serially diluted RNA template. Each data curve was normalized with its average baseline from cycles 4 to 16. Template concentrations begin at 10^6 RNA copies/μl and are reduced by one order of magnitude until the final trial of 1 RNA copy/L. Also included is the negative control (0 RNA copies/μl). B) On-chip qPCR efficiency graph representing the cycle threshold versus the initial template concentrations in a logarithmic scale. Dotted lines represent 95 % confidence interval. The slope is 3.34±0.28 which correspond to a PCR efficiency of 99±6 %. C) Gel electrophoresis of on-chip amplicons (120 bp) with varying levels of template as shown in (A). Lane 1 has an initial template of 10^6 RNA copies/μl and template concentrations are reduced by one order of magnitude until the final trial of 1 RNA copy/L in Lane 7 and the negative control (0 RNA copies/μl) in Lane 8. Off-chip PCR results for 80 min are shown in Lane 9 (10^4 RNA copies/μl), Lane 10 (0 RNA copies/μl), and Lane 11 (10^4 RNA copies/μl and master mix without RT-enzyme) for comparison.

was optically measured; probably the amplicons obtained were under the limit of detection of gel electrophoresis technique. For 10 RNA copies/μl (Figure 4.44 C Lane 6) a faint band could be detected, confirming the limit of detection measured optically on-chip for 50 min residence time using the 'commercial' master mix.

Given the equivalent sensitivity obtained for both 'commercial' and 'custom' mixes for 50 min and 30 min residence times respectively, we believe that a limit of detection of 10 RNA copies/μl is likely to be achieved for 30 min residence time using the 'custom' made master mix.

Along section 4.5, we demonstrated successful performance of both PCR and RT-PCR chips. Both bacterial and viral targets were amplified and detected in real-time with high sensitivity and rapidity.

4.6 Discussion

4.6.1 Comparison with other devices

In this chapter we presented a real-time, quantitative, and continuous-flow PCR and RT-PCR systems for DNA and RNA-based pathogen detection. Our PCR device provides quantitative results with high sensitivity and efficiency: 10 copies/μl were amplified within 20–25 min for both bacterial pathogens with PCR efficiencies between 90–100 %. RT-qPCR with a viral pathogen was performed faster (30 min) than conventional benchtop thermocyclers, with the same sensitivity (10 RNA copy/μl) and efficiencies between 90–110 %. Faster PCRs and RT-PCRs were possible (10 min and 20 min respectively) although the sensitivity was reduced.

In relationship to other designs and approaches, very few publications describe devices that combine quantitative detection and continuous-flow PCR. Frey et al. have reported amplification in 3 min residence with an initial template concentration of $2.2 \cdot 10^8$ molecules, which is more than 4 orders of magnitude more of template DNA than we have used in our speed tests.[37] Furutani et al. reported 8 min PCR with 4 copies/μl as input DNA.[29]

To the best of our knowledge, no continuous-flow RT-PCR systems that use conventional microfluidics and allow real-time detection have been reported in the

literature. On the one hand, some real-time RT-PCR systems reported use digital microfluidic technology, which through modifications in the electrical field, transport droplets with PCR reagents through different stations of the chip.[70,71] These assays are very similar to traditional benchtop thermocycler but with smaller volumes; they differ considerably from conventional microfluidics.[71,72] On the other hand, several platforms were reported which rely on conventional microfluidics to perform RT-PCR but present end-point detection either on-line[38,39,73] and off-line.[40,41] Few of these platforms report the sensitivity and maximum flow rate at which amplification is still observed. Li et al. reported a sensitivity of $6.4 \cdot 10^4$ copies/μl achieved in approximately 1 h RT-PCR;[73] Yamanaka et al. stated a limit of detection of $5.36 \cdot 10^3$ copies/μl completed in 15 min.[38] Other reported RT-PCR speeds are 100–120 min[40] and 73 min[41] (calculated from the published data). To the best of our knowledge, the continuous-flow RT-PCR system based on conventional microfluidics reported by Yamanaka et al. is the only one that reported faster amplification than ours (by 5 min); however, the sensitivity reported is lower and importantly only end-point detection was performed.[38] Additionally, we believe that this is the first time that the PCR efficiency is reported for continuous-flow PCR and RT-PCR.

It also worth mentioning the emerging isothermal techniques for RNA amplification. In contrast with PCR, isothermal systems do not require thermal cycling facilitating and reducing the costs of their designs, usually based in static chamber format.[74] There are a wide variety of isothermal techniques which differ in terms of complexity, reaction speed (usually from 30–50 min)[75], sensitivity, specificity, incubation temperatures, etc.; making comparison with PCR challenging.[76] When comparing isothermal techniques to PCR, the main drawback of isothermal techniques is that they are not quantitative, which limits their use in applications that require quantifying the target such as in viral load determinations.[77] Additionally, isothermal techniques require complex assay optimization (difficult primer design and buffer optimization, requirement of multiple enzymes, etc.).[78]

Regarding chip characteristics, our chip has the lowest channel depth (50 μm) and overall thickness (410 μm) compared to other published chip designs.[38–41] In terms of chip manufacturing, most designs use injection molding which is less

precise and more expensive than flat or roll-to-roll embossing. No articles were found that reported prototype or chip cost.[29,30,37] From the outset, we constrained our biological assay by the demands of large-scale manufacturing methods. Microfluidic channel designs including the aspect ratio and dimensions of features were selected to be compatible with ultra-precision machine manufacture of the chip molds and ultimate UV embossing. Optimizing the assay within these parameters is critical for ultimate translation of any device to the market. As an example of this process, the channel depth of our device is a mere 50 μm, which is an appropriate depth for the structure to be produced on a roll-to-roll ultra-violet embossing process according to companies in this sector[63,64] and a private communication from Dr. Xin Li from Microsharp Innovation. This means that only 50 nl of sample are monitored within the optical field of view at any time, which had the potential to make detection difficult. However, the shallow channel design was necessary for high-fidelity embossing of features in the rapid roll-to-roll manufacturing process and so we directed our energies into optimizing our optical system and assay rather than just make deeper channels. Many prototypes of POC devices developed without much regard for final production constraints fail to make the translation to the market. The demonstration of a holistic approach as described here underscores the ability to meet or exceed all the biological goals of the assay while paving the way for industrial scale production. Some of the next steps and future challenges include decreasing the size of the surrounding instrumentation and include sample pre-treatment to make the system more compact and easier to operate as POC device, through a standard product development process. Consequently, costs of the surrounding instrumentation would be sharply reduced and portability and ease of use increased. We provide here this system as an example of optimizing the biological task within the constraints and context of large-scale manufacturing methods.

With respect to the mobile PCR and RT-PCR POC landscape, currently an increasing number of suppliers of portable, low-cost, quantitative PCR and RT-PCR systems are entering the market. Prices range from \$3,000–\$25,000 and most provide results from 40–60 minutes. Cobas® Liat (Roche), q16 (PrimerDesign), and GeneXpertOmni (Cepheid) are just a few of these devices. All are based on

static chamber models that optimize the heat transfer and portability of standard thermal cycler design.

Regarding POC tests for *Chlamydia trachomatis*, most of the test currently available in the market rely in immunoassays and few are nucleic acid based. Some examples of antigen-based devices are Clearview® Chlamydia (Alere), ACON Chlamydia Rapid Test Device (Acon), Chlamydia Rapid Test (Diagnostics for the Real World). Although these tests can be performed rapidly with high specificity (about 99 %), their poor sensitivity (between 20–60 % in most cases), limit their applicability.[79,80] Consequently, nucleic acid based test continue to be the gold standard for *C. trachomatis* diagnosis. Some of the previously mentioned manufacturers, such as Cepheid and Roche, commercialize specific tests for *C. trachomatis* and report high sensitivity (90–100 %) and specificity (99–100 %), although as previously mentioned, the times to results are approximately 1 h.[79] The few, if any, POC devices available in the market that combine high sensitivity, specificity, and rapidity converts these test into a high research priority.[81]

A similar scenario exists for POC diagnostic tests for diarrheal causative pathogens. Some of the previously mentioned manufacturers, such as PrimerDesign, commercialize tests for *E. coli* O157:H7. We believe that more tests will be available in market soon due to high importance of the identification of the responsible pathogens to administer a correct treatment and importantly, to avoid the rise of antibiotic resistant pathogens.

After the 2014–2015 Ebola outbreak, numerous suppliers (including the previous mentioned ones) developed assays for Ebola virus detection. Some examples of commercialized assays are FilmArray Biothreat-E (bioMérieux), RealStar® Filovirus Screen RT-PCR kit 1.0 (Altona Diagnostics), and DoD EZ1 Real-time RT-PCR Assay (USA Department of Defense).[82] The time-to-result for most of the commercialized EBOV assays is 40–60 min. The usual genes targeted in these assays encode for RNA-dependent RNA polymerase (L), nucleoprotein (NP), glycoprotein (GP), and matrix protein (VP24); with the L gene being one of the best genetically conserved and the most likely to be valid for future outbreaks.[68,69,82–85] Blood plasma is the most common sample used. Typical EBOV viral load in blood for acutely ill infected patients ranges between 10^6–10^3 RNA copies/μl and then

decreases during the recovering phase until approximately 1 RNA copy/μl,[86,87] which is the reported lowest limit of detection of viral RNA in plasma on RT-PCR assays.[87] Most suppliers of Ebola assays reported sensitivities ranging from 10–10^3 copies/test.

We believe that our continuous-flow device, with its high sensitivity, PCR efficiency, low price (we anticipate a price of \$2,000),[67] portability, and rapidity is in good position to enter this competitive market. It would not only allow diagnosis but also monitoring the coarse of the diseases. Additionally, the fact that our platform is open and versatile would facilitate its adaptation to the diagnosis of new bacterial and RNA viral threats such as Zika or chikungunya viruses.

We consider that the characteristics of our system make it ideal to be exploited in developing countries. The few medical device industries in developing countries together with the fact that industries in high-resource settings typical have little interest in investing in proper need assessment for low-resource countries that promise a low return on investment, contribute to the lack of appropriate devices in poor nations. By contributing to better disease diagnosis in developing countries and as a consequence to better health of their population, poverty is reduced, economic productivity improved and inequalities between rich and poor countries are decreased.

4.7 Concluding Remarks

During this chapter we presented a real-time, quantitative, and continuous-flow PCR and RT-PCR systems for DNA and RNA-based pathogen detection demonstrating a holistic approach for POC device design. The development of these systems respond to health research priorities and fulfills several of the medical device prioritization criteria (criteria 1, 5, 6, 8). These devices will help to reduce the burden of infectious diseases (criterion 1), and since infectious diseases are more prevalent in resource-limited settings, these devices will also contribute to reduce the inequalities around the world (criterion 8). The few devices with similar characteristics in the market, even though the individual technologies required to conform the system are well developed, increase the priority of our research (crite-

ria 5 and 6). Additionally, considering the pathogens selected to demonstrate the function the system –*Chlamydia trachomatis*, *E. coli* O157:H7, and EBOV– criteria 2 and 4, which consider the expected impact of a new test and the availability, expense, and toxicity of a treatment respectively, are also fulfilled.

We described the development and the improvements made in the PCR and RT-PCR systems regarding the chip, surrounding instrumentation, and PCR reagents. More specifically, the chip was improved in terms of materials, chip production, bonding, and dimensions to achieve a faster and more economic chip production, and less reagent consumption. The surrounding instrumentation was improved regarding the microfluidic connections, optical system, and data acquisition in order to allow real-time detection with high sensitivity, accurately, and consistently. Biological reagents were tested in terms of primers/probe, polymerases, and chip channel passivation to increase the specificity and speed of the enzymatic reaction and avoid attachment to the channel walls and thus loss of reagents or nucleic acids.

The function of the PCR chip was demonstrated with two infectious bacteria, *C. trachomatis* and *E. coli* O157:H7, for which rapid diagnosis would be crucial for reducing patient morbidity. Successful amplification was obtained for 20 min residence time with high sensitivity (10 copies/μl) and PCR efficiencies between 90 and 100 % for both pathogens. Faster PCRs were possible although sensitivity was reduced.

The performance of our RT-PCR system was tested with EBOV. Two one-step master mixes with different DNA-polymerases were tested and the limit of detection was determined. Our system performs RT-qPCR faster, with the same sensitivity (10 RNA copy/μl) and efficiency (90–110 %) compared to conventional benchtop thermocyclers. Depending on the master mix used, amplification with high sensitivity was achieved in 30 to 50 min. Faster amplifications were possible (20 min) with lower sensitivities. Thus, our system achieves faster amplification than most commercial RT-qPCR platforms and commercialized Ebolavirus detection assays which typically require 40–60 min.

These successful results with *C. trachomatis*, *E. coli*, and EBOV make our system promising to be used with other DNA and RNA pathogens such as Zika

or chikungunya viruses. The portability, versatility, rapidity, sensitivity, and low-cost of our POC diagnostic device make it ideal for remote settings with low medical infrastructure and for outbreak control in which rapid identification of the causative pathogen is key to avoid the spread of the infection, and it might save many lives and aid to reduce inequalities around world.

Bibliography

1. Mabey, D. C. W., Solomon, A. W. & Foster, A. Trachoma. *Lancet* **362,** 223–9. ISSN: 1474-547X (2003).

2. Patel, A. L. *et al.* Prevalence of Chlamydia infection among women visiting a gynaecology outpatient department: evaluation of an in-house PCR assay for detection of Chlamydia trachomatis. *Annals of clinical microbiology and antimicrobials* **9,** 24. ISSN: 1476-0711 (2010).

3. Manavi, K. A review on infection with Chlamydia trachomatis. *Best Practice & Research Clinical Obstetrics & Gynaecology* **20,** 941–951. ISSN: 15216934 (2006).

4. Baud, D. *et al.* Role of Chlamydia trachomatis in miscarriage. *Emerging Infectious Diseases* **17,** 1630–1635. ISSN: 10806040 (2011).

5. World Health Organization. *Prevention of Blindness and Visual Impairment: Trachoma* 2016. <http://www.who.int/blindness/causes/trachoma/en/> (2016).

6. Clerc, O & Greub, G. Routine use of point-of-care tests: usefulness and application in clinical microbiology. *Clinical Microbiology and Infection* **16,** 1054–1061. ISSN: 1198743X (2010).

7. Nguyen, Y & Sperandio, V. Enterohemorrhagic E. coli (EHEC) pathogenesis. *Frontiers in Cellular and Infection Microbiology* **2,** 1–7. ISSN: 2235-2988 (2012).

8. Tarr, P. I., Gordon, C. a. & Chandler, W. L. Shiga-toxin-producing Escherichia coli and haemolytic uraemic syndrome. *Lancet* **365,** 1073–86. ISSN: 1474-547X (2005).

9. Lanata, C. F. *et al.* Global causes of diarrheal disease mortality in children <5 years of age: a systematic review. *PloS one* **8** (ed Sestak, K.) e72788. ISSN: 1932-6203 (2013).

10. Walker, C. L. F., Aryee, M. J., Boschi-Pinto, C. & Black, R. E. Estimating diarrhea mortality among young children in low and middle income countries. *PloS one* **7,** e29151. ISSN: 1932-6203 (2012).

11. World Health Organization. *Cause-specific mortality estimates for 2000-2012* 2014. <http://www.who.int/healthinfo/global_burden_disease/estimates/en/index1.html> (2016).

12. Bissonnette, L & Bergeron, M. Diagnosing infectionscurrent and anticipated technologies for point-of-care diagnostics and home-based testing. *Clinical Microbiology and Infection* **16,** 1044–1053. ISSN: 1198743X (2010).

13. Goldwater, P. N. & Bettelheim, K. a. Treatment of enterohemorrhagic Escherichia coli (EHEC) infection and hemolytic uremic syndrome (HUS). *BMC Medicine* **10,** 12. ISSN: 1741-7015 (2012).

14. World Health Organization. *Ebola virus disease Fact sheet N103* 2016. <http://www.who.int/mediacentre/factsheets/fs103/en/> (2016).

15. Centers for Disease Control and Prevention. *About Ebola Virus Disease* 2016. <http://www.cdc.gov/vhf/ebola/about.html> (2016).

16. Kucharski, A. J. & Edmunds, W. J. Case fatality rate for Ebola virus disease in West Africa. *The Lancet* **384,** 1260. ISSN: 1474547X (2014).

17. Park, S., Zhang, Y., Lin, S., Wang, T.-H. & Yang, S. Advances in microfluidic PCR for point-of-care infectious disease diagnostics. *Biotechnology Advances* **29,** 830–839 (2012).

18. Lee, T. M. H. & Hsing, I. M. DNA-based bioanalytical microsystems for handheld device applications. *Analytica Chimica Acta* **556,** 26–37. ISSN: 00032670 (2006).

19. Mullis, K. *et al.* Specific enzymatic amplification of DNA in vitro: the polymerase chain reaction. 1986. *Biotechnology (Reading, Mass.)* **24,** 17–27. ISSN: 0740-7378 (1992).

20. Zhang, C., Xu, J., Ma, W. & Zheng, W. PCR microfluidic devices for DNA amplification. *Biotechnology Advances* **24,** 243–284. ISSN: 07349750 (2006).

21. Northrup, M., Ching, M., White, R. & Watson, R. *DNA Amplification in a Microfabricated Reaction Chamber* in *Proceedings of the Seventh International Conference on Solid-State Sensors and Actuators (Transducers 93)* (IEEE Proceedings, Yokohama, Japan, 1993), 924–926.

22. Kopp, M. U., Mello, A. J. & Manz, A. Chemical amplification: continuous-flow PCR on a chip. *Science* **280,** 1046–8. ISSN: 0036-8075 (1998).

23. Zhang, C. & Xing, D. Miniaturized PCR chips for nucleic acid amplification and analysis: Latest advances and future trends. *Nucleic Acids Research* **35,** 4223–4237. ISSN: 03051048 (2007).

24. Heid, C. a., Stevens, J, Livak, K. J. & Williams, P. M. Real time quantitative PCR. *Genome research* **6,** 986–994. ISSN: 1088-9051 (1996).

25. Mackay, I. Real-time PCR in the microbiology laboratory. *Clinical Microbiology and Infection* **10,** 190–212. ISSN: 1198743X (2004).

26. Benson, D. A., Karsch-Mizrachi, I., Lipman, D. J., Ostell, J. & Wheeler, D. L. GenBank. *Nucleic Acids Research* **33,** 34–38. ISSN: 03051048 (2005).

27. Obeid, P. J., Christopoulos, T. K., Crabtree, H. J. & Backhouse, C. J. Microfabricated device for DNA and RNA amplification by continuous-flow polymerase chain reaction and reverse transcription-polymerase chain reaction with cycle number selection. *Analytical Chemistry* **75,** 288–295. ISSN: 00032700 (2003).

28. Fukuba, T., Yamamoto, T., Naganuma, T. & Fujii, T. Microfabricated flow-through device for DNA amplification - Towards in situ gene analysis. *Chemical Engineering Journal* **101,** 151–156. ISSN: 13858947 (2004).

29. Furutani, S *et al.* Rapid and highly sensitive detection by a real-time polymerase chain reaction using a chip coated with its reagents. *Analytical Sciences* **30,** 569–74 (2014).

30. Tachibana, H. *et al.* On-chip quantitative detection of pathogen genes by autonomous microfluidic PCR platform. *Biosensors and Bioelectronics* **74,** 725–730. ISSN: 09565663 (2015).

31. Park, N., Kim, S. & Hahn, J. H. Cylindrical Compact Thermal-Cycling Device for Continuous-Flow Polymerase Chain Reaction. *Analytical Chemistry* **75,** 6029–6033. ISSN: 00032700 (2003).

32. Curcio, M. & Roeraade, J. Continuous segmented-flow polymerase chain reaction for high-throughput miniaturized DNA amplification. *Analytical chemistry* **75,** 1–7. ISSN: 0003-2700 (2003).

33. West, J *et al.* Application of magnetohydrodynamic actuation to continuous flow chemistry. *Lab Chip* **2,** 224–230. ISSN: 1473-0197 (2002).

34. Liu, J., Enzelberger, M. & Quake, S. A nanoliter rotary device for polymerase chain reaction. *Electrophoresis* **23,** 1531–1536. ISSN: 01730835 (2002).

35. Chiou, J., Matsudaira, P., Sonin, A. & Ehrlich, D. A closed-cycle capillary polymerase chain reaction machine. *Analytical Chemistry* **73,** 2018–2021. ISSN: 00032700 (2001).

36. Belgrader, P. *et al.* A reusable flow-through polymerase chain reaction instrument for the continuous monitoring of infectious biological agents. *Analytical Chemistry* **75,** 3446–3450. ISSN: 00032700 (2003).

37. Frey, O., Bonneick, S., Hierlemann, A. & Lichtenberg, J. Autonomous microfluidic multi-channel chip for real-time PCR with integrated liquid handling. *Biomedical Microdevices* **9,** 711–718. ISSN: 1387-2176 (2007).

38. Yamanaka, K. *et al.* Rapid detection for primary screening of influenza A virus: microfluidic RT-PCR chip and electrochemical DNA sensor. *The Analyst* **136,** 2064–2068. ISSN: 0003-2654 (2011).

39. Obeid, P. J. & Christopoulos, T. K. Continuous-flow DNA and RNA amplification chip combined with laser-induced fluorescence detection. *Analytica Chimica Acta* **494,** 1–9. ISSN: 00032670 (2003).

40. Hartung, R. *et al.* Application of an asymmetric helical tube reactor for fast identification of gene transcripts of pathogenic viruses by micro flow-through PCR. *Biomedical Microdevices* **11,** 685–692. ISSN: 1387-2176 (2009).

41. Felbel, J. *et al.* Technical Concept of a Flow-through Microreactor for In-situ RT-PCR. *Engineering in Life Sciences* **8,** 68–72. ISSN: 16180240 (2008).

42. Li, Y., Zhang, C. & Xing, D. Integrated microfluidic reverse transcription-polymerase chain reaction for rapid detection of food- or waterborne pathogenic rotavirus. *Analytical Biochemistry* **415,** 87–96. ISSN: 00032697 (2011).

43. Ren, K., Zhou, J. & Wu, H. Materials for microfluidic chip fabrication. *Accounts of Chemical Research* **46,** 2396–2406. ISSN: 00014842 (2013).

44. Ren, K., Chen, Y. & Wu, H. New materials for microfluidics in biology. *Current Opinion in Biotechnology* **25,** 78–85. ISSN: 09581669 (2014).

45. Worgull, M. *Hot Embossing: Theory and Technology of Microreplication* (ed Ramsden, J.) ISBN: 9780815515791 (Elsevier, 2009).

46. Shan, X. C. *et al. Process study on roll-to-roll ultraviolet (UV) embossing* in *2010 12th Electronics Packaging Technology Conference* (2010), 231–235. ISBN: 978-1-4244-8560-4. doi:10.1109/EPTC.2010.5702638.

47. Becker, H. & Heim, U. Hot embossing as a method for the fabrication of polymer high aspect ratio structures. *Sensors and Actuators* **83,** 130–135. ISSN: 09244247 (2000).

48. He, Y., Fu, J.-Z. & Chen, Z.-C. Research on optimization of the hot embossing process. *Journal of Micromechanics and Microengineering* **17,** 2420–2425. ISSN: 0960-1317 (2007).

49. Lee, H. S., Kim, D. S. & Kwon, T. H. UV nano embossing for polymer nano structures with non-transparent mold insert. *Microsystem Technologies* **13,** 593–599. ISSN: 0946-7076 (2006).

50. Brecher, C., Baum, C. & Bastuck, T. *Comparison of roll-to-roll replication approaches for microfluidic and optical functions in lab-on-a-chip diagnostic devices* in *Proc. SPIE 9320, Microfluidics, BioMEMS, and Medical Microsys-*

tems XIII (eds Gray, B. L. & Becker, H.) **9320** (2015), 932008. doi:10.1117/12.2077592.

51. Nezuka, O., Yao, D. & Kim, B. H. Replication of Microstructures by Roll-to-Roll UV-Curing Embossing. *Polymer-Plastics Technology and Engineering* **47,** 865–873. ISSN: 0360-2559 (2008).

52. Becker, H & Gärtner, C. Polymer microfabrication methods for microfluidic analytical applications. *Electrophoresis* **21,** 12–26. ISSN: 0173-0835 (2000).

53. Do, J. & Ahn, C. H. A polymer lab-on-a-chip for magnetic immunoassay with on-chip sampling and detection capabilities. *Lab on a chip* **8,** 542–549. ISSN: 1473-0197 (2008).

54. Nunes, P. S., Ohlsson, P. D., Ordeig, O. & Kutter, J. P. Cyclic olefin polymers: Emerging materials for lab-on-a-chip applications. *Microfluidics and Nanofluidics* **9,** 145–161. ISSN: 16134982 (2010).

55. Bhattacharyya, A. & Klapperich, C. M. Thermoplastic microfluidic device for on-chip purification of nucleic acids for disposable diagnostics. *Analytical Chemistry* **78,** 788–792. ISSN: 00032700 (2006).

56. Wallow, T. I. *et al.* Low-distortion, high-strength bonding of thermoplastic microfluidic devices employing case-II diffusion-mediated permeant activation. *Lab on a chip* **7,** 1825–31. ISSN: 1473-0197 (2007).

57. Paul, D., Pallandre, A., Miserere, S., Weber, J. & Viovy, J. L. Lamination-based rapid prototyping of microfluidic devices using flexible thermoplastic substrates. *Electrophoresis* **28,** 1115–1122. ISSN: 01730835 (2007).

58. Kettner, P, Pelzer, L, Glinsner, T, Farrens, S & Lee, D. New results on plasma activated bonding of imprinted polymer features for bio MEMS applications. *Journal of Physics: Conference Series* **34,** 65–71. ISSN: 1742-6588 (2006).

59. Kricka, L. J. & Wilding, P. Microchip PCR. *Analytical and Bioanalytical Chemistry* **377,** 820–825. ISSN: 1618-2642 (2003).

60. Jeyachandran, Y. L., Mielczarski, E, Rai, B & Mielczarski, J. A. Quantitative and Qualitative Evaluation of Adsorption/Desorption of Bovine Serum Albumin on Hydrophilic and Hydrophobic Surfaces. *Langmuir* **25,** 11614–11620. ISSN: 0743-7463 (2009).

61. Duque, L. *et al.* Reactions of Plasma-Polymerised Pentafluorophenyl Methacrylate with Simple Amines. *Plasma Processes and Polymers* **7,** 915–925. ISSN: 16128850 (2010).

62. Sauer-Budge, A. F. *et al.* Low cost and manufacturable complete microTAS for detecting bacteria. *Lab on a chip* **9,** 2803–2810. ISSN: 1473-0197 (2009).

63. Epigem Ltd. *UV embossing* 2016. <http://epigem.co.uk/technology/uv-embossing> (2016).

64. SVG Optronics Co. Ltd. *R2R UV nanoimprinting* 2016. <http://www.svgoptronics.com> (2016).

65. Ganser, P. *Optimization of polymer fabrication techniques for the production of Lab-on-a-Chip devices* PhD thesis (RWTH Aachen University, 2014), 163.

66. Zeon Chemicals. *Zeonex: The Gold Standard of High-Purity Plastic* 2016. <http://www.zeonex.com/pharmaceuticals.aspx> (2006).

67. Fernández-Carballo, B. L. *et al.* Low-cost, real-time, continuous flow PCR system for pathogen detection. *Biomedical Microdevices* **18,** 34. ISSN: 1387-2176 (2016).

68. Jun, S. R. *et al.* Ebolavirus comparative genomics. *FEMS Microbiology Reviews* **39,** 764–778. ISSN: 15746976 (2015).

69. Silva, R. M., Pratas, D., Castro, L., Pinho, A. J. & Ferreira, P. J.S. G. Three minimal sequences found in Ebola virus genomes and absent from human DNA. *Bioinformatics* **31,** 2421–2425. ISSN: 14602059 (2015).

70. Prakash, R. *et al.* Multiplex, Quantitative, Reverse Transcription PCR Detection of Influenza Viruses Using Droplet Microfluidic Technology. *Micromachines* **6,** 63–79. ISSN: 2072-666X (2014).

71. Kaler, K. & Prakash, R. Droplet Microfluidics for Chip-Based Diagnostics. *Sensors* **14,** 23283–23306. ISSN: 1424-8220 (2014).

72. Beer, N. R. *et al.* On-Chip Single-Copy Real-Time Reverse-Transcription PCR in Isolated Picoliter Droplets. *Analytical Chemistry* **80,** 1854–1858. ISSN: 0003-2700 (2008).

73. Li, Y., Zhang, C. & Xing, D. Fast identification of foodborne pathogenic viruses using continuous-flow reverse transcription-PCR with fluorescence detection. *Microfluidics and Nanofluidics* **10,** 367–380. ISSN: 16134982 (2011).

74. Asiello, P. J. & Baeumner, A. J. Miniaturized isothermal nucleic acid amplification, a review. *Lab on a chip* **11,** 1420–1430. ISSN: 1473-0197 (2011).

75. Ahmad, F. & Hashsham, S. a. Miniaturized nucleic acid amplification systems for rapid and point-of-care diagnostics: A review. *Analytica Chimica Acta* **733,** 1–15. ISSN: 00032670 (2012).

76. Niemz, A., Ferguson, T. M. & Boyle, D. S. Point-of-care nucleic acid testing for infectious diseases. *Trends in biotechnology* **29,** 240–50. ISSN: 1879-3096 (2011).

77. Tang, Y.-W. & Ou, C.-Y. Past, present and future molecular diagnosis and characterization of human immunodeficiency virus infections. *Emerging Microbes & Infections* **1,** e19. ISSN: 2222-1751 (2012).

78. Yan, L. *et al.* Isothermal amplified detection of DNA and RNA. *Molecular bioSystems* **10,** 970–1003. ISSN: 1742-2051 (2014).

79. Herbst De Cortina, S., Bristow, C. C., Joseph Davey, D. & Klausner, J. D. A Systematic Review of Point of Care Testing for Chlamydia trachomatis, Neisseria gonorrhoeae, and Trichomonas vaginalis. *Infectious Diseases in Obstetrics and Gynecology* **2016.** ISSN: 10980997. doi:10.1155/2016/4386127 (2016).

80. Van der Helm, J. J. *et al.* Point-of-care test for detection of urogenital chlamydia in women shows low sensitivity. a performance evaluation study in two clinics in suriname. *PLoS ONE* **7,** 1–7. ISSN: 19326203 (2012).

81. Mohd Hanafiah, K., Garcia, M. & Anderson, D. Point-of-care testing and the control of infectious diseases. *Biomarkers in medicine* **7,** 333–47. ISSN: 1752-0371 (2013).

82. Foundation for Innovative New Diagnostics. *Situational review of Ebola diagnostics and opportunities for rapid improvement* tech. rep. (Geneva, 2014).

83. Towner, J. S., Sealy, T. K., Ksiazek, T. G. & Nichol, S. T. HighThroughput Molecular Detection of Hemorrhagic Fever Virus Threats with Applications for Outbreak Settings. *The Journal of Infectious Diseases* **196,** S205–S212. ISSN: 0022-1899 (2007).

84. Trombley, A. R. *et al.* Comprehensive panel of real-time TaqMan polymerase chain reaction assays for detection and absolute quantification of filoviruses, arenaviruses, and New World hantaviruses. *The American journal of tropical medicine and hygiene* **82,** 954–60. ISSN: 1476-1645 (2010).

85. Weidmann, M., Mühlberger, E. & Hufert, F. T. Rapid detection protocol for filoviruses. *Journal of Clinical Virology* **30,** 94–99. ISSN: 13866532 (2004).

86. Towner, J. S. *et al.* Rapid Diagnosis of Ebola Hemorrhagic Fever by Reverse Transcription-PCR in an Outbreak Setting and Assessment of Patient Viral Load as a Predictor of Outcome Rapid Diagnosis of Ebola Hemorrhagic Fever by Reverse Transcription-PCR in an Outbreak Setting an. *Journal of Virology* **78,** 4330–4341. ISSN: 0022-538X (2004).

87. Kreuels, B. *et al.* A Case of Severe Ebola Virus Infection Complicated by Gram-Negative Septicemia. *New England Journal of Medicine* **371,** 2394–2401. ISSN: 0028-4793 (2014).

Chapter 5

Conclusions

- A holistic approach for Point-of-care (POC) device development, which considers the context, the end-users, the prevalent diseases, and the end goal of production and implementation of the device, was applied to the development of POC diagnostic devices appropriate for low-resource countries.

- Prioritization criteria for POC device development were developed. The criteria for prioritization considered the impact of a new test on the burden of disease, the availability and expense of disease treatments, the technological investment to develop a new device, and the bioethical principles giving particular attention to the principle of justice.

- A paper chemical dipstick assay was developed which responds to the prioritization criteria and fulfills the holistic approach for POC device development. This low-cost diagnostic assay allows detecting biomarkers present in biological fluids and was fully produced with domestic inkjet printers and simple ink preparation recipes.

- The fabrication technique for dipstick assays was tested for the detection of iodine deficiency. Chemical inks were successfully prepared by adjusting the physico-chemical properties of the chemical solutions to make them resemble those of commercial inks and by performing corrosion inhibition studies in case of potentially corrosive inks. Chemical inks were effectively printed on paper, and iodine in the same concentrations present in the urine was detected (20–300 μgI/L). Semi-quantification of the iodine concentration was

possible and differences between deficient, adequate, and excessive iodine intake groups were unambiguously discriminated.

- A nucleic acid test was developed which responds to the prioritization criteria and fulfills the holistic approach for POC device development. Low-cost, continuous-flow, real-time, POC PCR and RT-PCR systems for quantitative detection of DNA and RNA-based pathogens were developed. Both systems were built around disposable microfluidic chips designed to be produced industrially by roll-to-roll embossing methods. The improvement of the system in terms of the chip, surrounding instrumentation, and reagents for nucleic acid amplification was described. More specifically, the improvements included: (1) the chip in terms of materials, chip production, bonding, and dimensions to achieve a faster and more economic chip production with lower reagent consumption; (2) the surrounding instrumentation including the microfluidic connections, optical system, and data acquisition in order to allow real-time detection with high sensitivity, accurately, and consistently; and (3) the biological reagents in terms of primers/probes, polymerases, and chip channel passivation to increase the specificity and speed of the enzymatic reaction and avoid loss of reagents or nucleic acids to the channel walls.

- The qPCR and RT-qPCR systems were characterized with two infectious bacteria and one viral target: *Chlamydia trachomatis*, *Escherichia coli O157:-H7*, and Ebola virus (EBOV). Our PCR device provided quantitative results with high sensitivity and efficiency: 10 DNA copies/μl were amplified within 20–25 min for both bacterial pathogens with PCR efficiencies between 90–100 %. RT-qPCR with EBOV was performed faster (30 min) than conventional benchtop thermocyclers, with the same sensitivity (10 RNA copy/μl) and efficiencies between 90–110 %. Faster PCRs and RT-PCRs were possible (10 min and 20 min respectively) although the sensitivity was reduced.

- Both POC diagnostic assays developed during this thesis are very versatile and can be applied to a wide variety of biomarkers and infectious pathogens. They are simple, inexpensive, rapid, sensitive, user-friendly and are appro-

priate to be used at health clinics in low-resource settings. Both POC assays presented here have the potential to save many lives and help to reduce worldwide inequalities.

Publications

Research publications from this PhD thesis

<u>Fernández-Carballo BL</u>, McGuiness I, McBeth C, Kalashnikov M, Borrós S, Sharon A, Sauer-Budge AF. Low-cost, real-time, continuous flow PCR system for pathogen detection. *Biomedical Microdevices* **18**, 34. ISSN: 1387-2176 (2016).

<u>Fernández-Carballo BL</u>, Comellas-del-Castillo A, Borrós S. Paper dipsticks for disease diagnosis produced with domestic inkjet printers. *International Health.* Manuscript submitted for publication on January 2017.

<u>Fernández-Carballo BL</u>, McBeth C, McGuiness I, Kalashnikov M, Baum C, Borrós S, Sharon A, Sauer-Budge AF. Point-of-care continuous flow RT-qPCR system for RNA virus identification. *Lab on a Chip.* Manuscript submitted for publication on February 2017.

<u>Fernández-Carballo BL</u>, Florensa A, Borrós S. Prioritization criteria for the development of diagnostic medical devices. In preparation.

Research awards from this PhD thesis

Honorable Mention in Good practices in university cooperation for development (Aristos Campus 2015) by Ramón Llull, Deusto, and Comillas universities. July 2016.

Honorable Mention in Good practices in university cooperation for development (Aristos Campus 2015) by Ramón Llull, Deusto, and Comillas universities. July 2013.

Appendix A

Current diagnosis methods used for the detection of various infectious diseases

Table A.1: Current diagnosis methods used for the detection of various infectious diseases. Adapted from Mabey et al.[1]

Disease	Diagnostic test
Acute respiratory infections	Blood/sputum culture
Diarrohoeal diseases	Microscopy
	Stool culture
Malaria	Blood film
	Antigen detection (dipstick)
	Antibody detection
HIV	Serology (antibody detection)
	CD4+ cell counts and viral load
Tuberculosis	Sputum microscopy (and culture)
	Tuberculin skin test
Visceral leishmaniasis	DAT serological field test
	Microscopy of spleen or bone marrow
	Culture of spleen or bone marrow
African trypanosomiasis	CATT serological field test
	Blood/CSF microcopy and examination
Onchocerciasis	Skin-snip microscopy
Syphilis	Serology (antibody detection)
Gonorrhea	Microscopy
	Culture
Leprosy	Skin smears
Lymphatic filariasis	Blood film
	Antigen detection
Schistosomiasis	Microscopy of stool/urine
Chagas' disease	Serology (antibody detection)
Dengue	Serology (antibody detection)

DAT: Direct agglutination test; CATT: Card agglutination trypanosomiasis test.

Bibliography

1. Mabey, D., Peeling, R. W., Ustianowski, A. & Perkins, M. D. Diagnostics for the developing world. *Nature reviews. Microbiology* **2,** 231–40. ISSN: 1740-1526 (2004).

Appendix B

Inkjet printed antibodies preliminary experiments

Table B.1: Reagents, equipment and software for conducting prelimiary experiments regarding inkjet printed antibodies.

Name	Reference	Vendor
Reagents		
'Capture' ab		
Rabbit anti-ferritin	Ab7332	Abcam
'Detection' ab		
Goat anti-rabbit Alexa Fluor® 488	Ab150077	Abcam
Nitrocellulose membrane	High-Flow™Plus 135	Merck Millipore
Equipment		
Desktop printer	SX420W	Seiko Epson
Drop Shape Analysis System	DSA100	KRÜSS GmbH

The methodology and main results obtained regarding printing antibodies on nitrocellulose paper are described as follows. An antibody ink was prepared containing a low concentration of 'capture' antibody to reduce the cost of the test. 2 μg/ml of 'capture' antibody in phosphate-buffered saline (PBS) was prepared. PBS has very similar viscosity and surface tension compared to water. The viscosity of the solution was not modified since, as previously stated, viscosities in the range of water present good jetting performance without adjustments. Regarding surface tension, Tween-20 was selected to adjust the surface tension instead of

Triton X-100 because the later could compromise the folding stability of the antibody. Different concentrations of Tween-20 were tested (0.05 %, 0.1 %, 1 %, 2 %, and 10 %(v/v)) and in all cases the superficial tension achieved was 38–40 mN/m. Given the insignificant differences in surface tension reached with the different concentrations of surfactant tested, 0.05 %(v/v) Tween-20 was selected and added to the antibody solution.

Once the ink solution was prepared, it was introduced into a refillable cartridge which was previously blocked with blocking buffer (1 % BSA in PBS) for 4 h and then washed with PBS. The antibody ink was printed on nitrocellulose paper. Since the concentration of antibody ink was low and to ensure that enough 'capture' antibody was deposited, the same area of nitrocellulose was printed several times (approximately 20 times). Afterwards, printed nitrocellulose paper was blocked with 0.05 %(w/w) Tween-20 in blocking buffer for 30 min and then dried out for 3 h.

To test the functionality of the printed antibody, a 0.2 μg/ml in blocking buffer:PBS 1:1 secondary antibody conjugated to Alexa Fluor® was used. One side of nitrocellulose paper was immersed into the 'detection' antibody, which flowed through the nitrocellulose paper through to the other end, where an absorbent pad was placed. When the fluid with 'detection' antibody reached the test line, where 'capture' antibody was immobilized, the 'detection' antibody bound. The rest of the fluid was collected at the absorbent pad. In Figure B.1, the disposition of membrane and the components of the assay are shown. By observing the nitrocellulose paper under a microscope fluorescence filter set, the test line was detected which confirmed the functionality of the printed antibody. In this case, 'IQS' was printed with 'capture' antibody ink and in Figure B.2, fluorescence detail pictures of the letter 'Q' are shown.
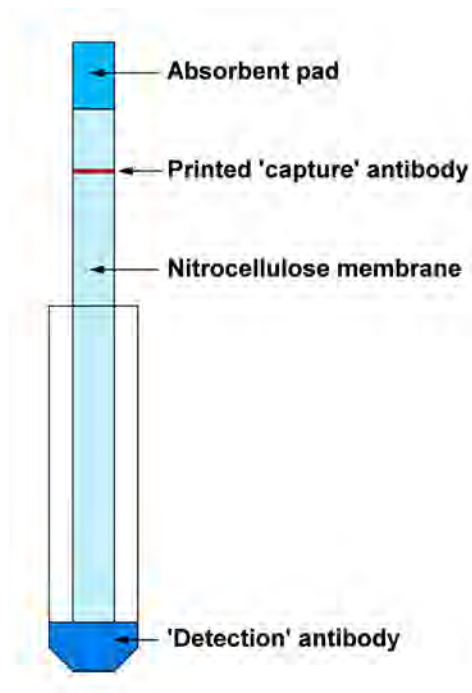
Figure B.1: Schematic drawing of the disposition of the nitrocellulose membrane and other components of the assay.
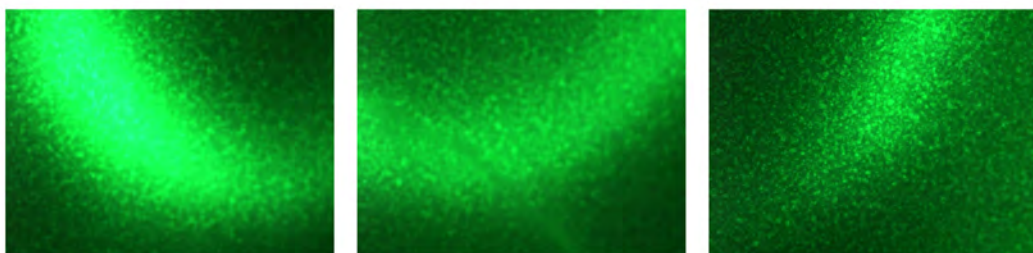

Figure B.2: Fluorescence picture detail of the test line of an immunoassay printed with 'capture' antibody and detected with a fluorescent-labeled 'detection' antibody. 'IQS' was printed as capture line and details of the letter 'Q' are shown in the pictures.

Appendix C

Application oriented advantages and disadvantages of the different materials for lab-on-a-chip microfluidic devices

Table C.1: Main application oriented advantages and disadvantages of the different materials for lab-on-a-chip (LOAC) microfluidic devices.[1–3]

Advantages	Disadvantages
Glass/silicon	
High thermal stability and conductivity	Expensive manufacture
High optical transparency	High materials cost
High chemical inertness	Impermeability to gases
High solvent compatibility	High brittleness
Good mechanical strength	
Elastomers (silicon-based elastomers: PDMS)	
Enable low-cost prototyping	Time consuming manufacture
High optical transparency	Inappropriate for mass production
Good chemical inertness	Low melting point
Good gas permeability	Low solvent compatibility
High elasticity	
Thermoplastics	
Rapid and inexpensive microfabrication	May exhibit autofluorescence
Excellent for commercial production	May absorb water
Can be reshaped multiple times	May absorb light in the UV range
Broad variety of types	May adsorb proteins
Medium-high optical transparency	Expensive for prototypic use
Medium-high thermostability	Barely permeable to gases
Medium-high solvent compatibility	
Good mechanical resistance	
Lightweight and disposable	
Thermosets	
High optical transparency	Expensive manufacture
High thermostability	Cannot be reshaped once cured
High solvent compatibility	
High strength	
Hydrogels	
Good for cell-culture research	Low optical transparency
Biocompatible	Low thermostability
High gas permeability	
Paper	
Simple and economical manufacture	Inability to perform in continuous flow
Inexpensive and easy to use	Restricted to low temperature
	Sensitivity is usually unsatisfactory
	Low optical transparency

Bibliography

1. Ren, K., Zhou, J. & Wu, H. Materials for microfluidic chip fabrication. *Accounts of Chemical Research* **46,** 2396–2406. ISSN: 00014842 (2013).

2. Ren, K., Chen, Y. & Wu, H. New materials for microfluidics in biology. *Current Opinion in Biotechnology* **25,** 78–85. ISSN: 09581669 (2014).

3. Nunes, P. S., Ohlsson, P. D., Ordeig, O. & Kutter, J. P. Cyclic olefin polymers: Emerging materials for lab-on-a-chip applications. *Microfluidics and Nanofluidics* **9,** 145–161. ISSN: 16134982 (2010).

Appendix D

Relevant physical properties for on-chip qPCR assays for the main thermoplastic materials for microfluidic applications

Table D.1: Relevant physical properties for on-chip qPCR assays for the main thermoplastic materials for microfluidic applications (PMMA, PC, COC/COP). PDMS and glass physical properties are also presented for comparison.[1–5]

Propertiy	Glass	PDMS	PMMA	PC	COP/COC
General					
A_w [% in 24 h]	-	>1	0.1–0.5	0.04–0.15	<0.01
T_g [°C]	560–1215	-120	110	148	70–180
T_{hd} [°C]	-	200	90	125	140/170
k [W m^{-1} K^{-1}]	0.27–5.1	0.15	0.19–0.22	0.19–0.23	0.12–0.15
α [10^{-6} K^{-1}]	3.3	310	59–101	70	60–70
Optical					
τ_L [%]	92	-	92	88	92
λ_u [nm]	160–3500	220–1580	430–1600	380–1550	280–1650

A_w = water absorption; T_g = glass transition temperature; T_{hd} = Heat distortion temperature; k = thermal conductivity; α = thermal expansion coefficient; τ_L = light transmittance; λ_u = usable transmission range.

Bibliography

1. Nunes, P. S., Ohlsson, P. D., Ordeig, O. & Kutter, J. P. Cyclic olefin polymers: Emerging materials for lab-on-a-chip applications. *Microfluidics and Nanofluidics* **9,** 145–161. ISSN: 16134982 (2010).

2. Zeon Corporation. *New high-performance thermoplastics for next-generation* 2014. <http://www.zeonex.com/applications_medical.asp> (2014).

3. CiDRA Precision Services. *Materials* 2016. <http://www.cidraprecisionservices.com/life-sciences-materials.html> (2016).

4. Lötters, J. C., Olthuis, W, Veltink, P. H. & Bergveld, P. The mechanical properties of the rubber elastic polymer polydimethylsiloxane for sensor applications. *Journal of Micromechanics and Microengineering* **7,** 145–147. ISSN: 0960-1317 (1997).

5. Ganser, P. *Optimization of polymer fabrication techniques for the production of Lab-on-a-Chip devices* PhD thesis (RWTH Aachen University, 2014), 163.

Appendix E

Off-chip limit of detection qPCR amplification results for *C. trachomatis*, *E. coli* O157:H7, and Ebola virus
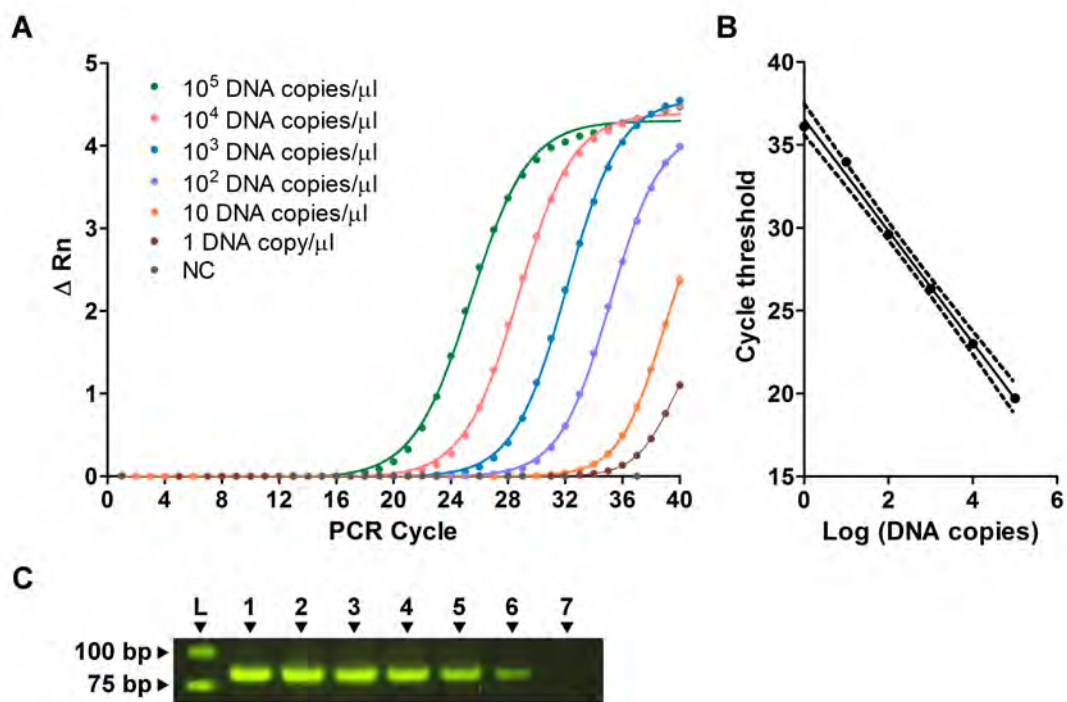
Figure E.1: *C. trachomatis* off-chip qPCR results.[1] A) Off-chip qPCR optical detection data for serially diluted DNA template. Data were normalized by the internal thermocycler software. Template concentrations begin at 10^5 DNA copies/μl and are reduced by one order of magnitude until the final trial of 1 DNA copy/μl. Also included is the negative control (0 DNA copies/μl). B) Off-chip qPCR efficiency graph representing the cycle threshold versus the initial template concentrations in a logarithmic scale. Dotted lines represent 95 % confidence interval. The slope is 3.38$\pm$0.11 which corresponds to a PCR efficiency of 98$\pm$2 %. C) Gel electrophoresis of off-chip amplicons (85 bp) with varying levels of template as shown in (A). Lane 1 has an initial template of 10^5 DNA copies/μl and template concentrations are reduced by one order of magnitude until the final trial of 1 DNA copy/μl in Lane 6 and the negative control (0 DNA copies/μl) in Lane 7.
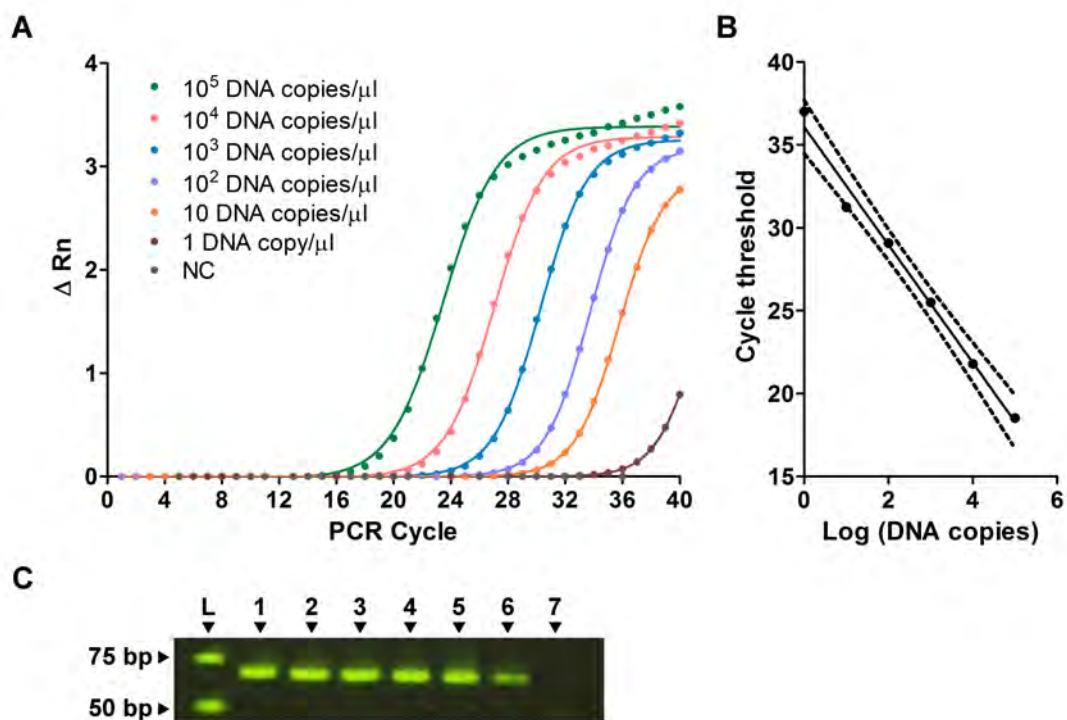
Figure E.2: *E. coli* O157:H7 off-chip qPCR results.[1] A) Off-chip qPCR optical detection data for serially diluted DNA template. Data were normalized by the internal thermocycler software. Template concentrations begin at 10^5 DNA copies/μl and are reduced by one order of magnitude until the final trial of 1 DNA copy/μl. Also included is the negative control (0 DNA copies/μl). B) Off-chip qPCR efficiency graph representing the cycle threshold versus the initial template concentrations in a logarithmic scale. Dotted lines represent 95 % confidence interval. The slope is 3.56$\pm$0.19 which corresponds to a PCR efficiency of 91$\pm$3 %. C) Gel electrophoresis of off-chip amplicons (69 bp) with varying levels of template as shown in (A). Lane 1 has an initial template of 10^5 DNA copies/μl and template concentrations are reduced by one order of magnitude until the final trial of 1 DNA copy/μl in Lane 6 and the negative control (0 DNA copies/μl) in Lane 7.
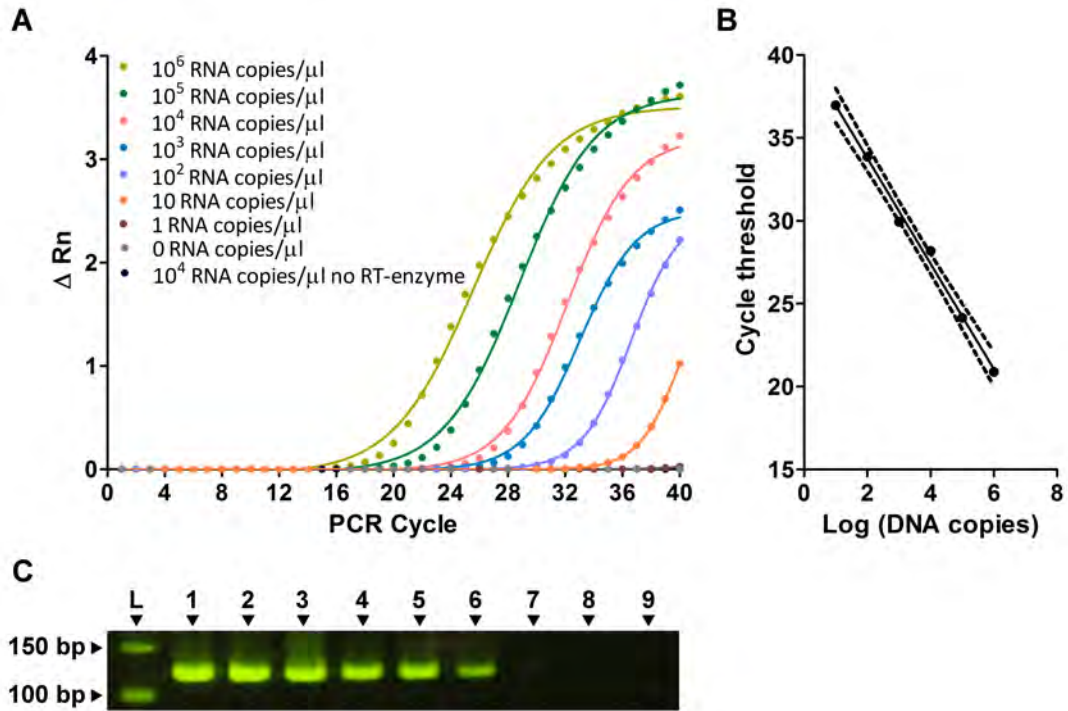
Figure E.3: EBOV 80 minutes off-chip qPCR results performed using the 'commercial' one-step qRT-PCR master mix. A) Off-chip RT-qPCR optical detection data for serially diluted RNA template. Data were normalized by the internal thermocycler software. Template concentrations begin at 10^6 RNA copies/μl and are reduced by one order of magnitude until the final trial of 1 RNA copy/μl. Also included is a negative control with 0 RNA copies/μl and a negative control with 10^4 RNA copies/μl and no RT-enzyme. B) Off-chip qPCR efficiency graph representing the cycle threshold versus the initial template concentrations in a logarithmic scale. Dotted lines represent 95 % confidence interval. The slope is 3.18±0.12 which corresponds to a PCR efficiency of 106±3 %. C) Gel electrophoresis of off-chip amplicons (120 bp) with varying levels of template as shown in (A). Lane 1 has an initial template of 10^6 RNA copies/μl and template concentrations are reduced by one order of magnitude until the final trial of 1 RNA copy/μl in Lane 7. Two negative controls with 0 RNA copies/μl and 10^4 RNA copies/μl and master mix without RT-enzyme are included in Lanes 8 and 9 respectively.

Bibliography

1. Fernández-Carballo, B. L. *et al.* Low-cost, real-time, continuous flow PCR system for pathogen detection. *Biomedical Microdevices* **18,** 34. ISSN: 1387-2176 (2016).